FDL-TDR-64-149
PART II

HYPERSONIC DYNAMIC STABILITY

PART II. CONICAL BODY EXPERIMENTAL PROGRAM

R. B. HOBBS, JR.

GENERAL ELECTRIC COMPANY

Distribution of this document is unlimited

FOREWORD

The information released in this report has been generated in support of studies on the Hypersonic Dynamic Stability Characteristics of lifting and non-lifting re-entry vehicles. These studies were conducted by the General Electric Co., Re-entry Systems Dept., for the Control Criteria Branch of the Air Force Flight Dynamics Laboratory, Research and Technology Division. The program was sponsored under Air Force Contract No. AF 33(657)-11411, Project No 8219, and Task No. 821902. Mr. J. E. Jenkins is the Project Engineer on the contract. The author, Mr. R. B. Hobbs, Jr., is an engineer in experimental and design aerodynamics, Systems Technology Section, Re-entry Systems Dept., General Electric Co. The project supervisor was Mr. L. A. Marshall. The experimental program covered in this report was started in May 1963 and was completed in October 1965.

The author gratefully acknowledges the assistance and cooperation of the Dynamics Section, Supersonic Branch, von Karman Gas Dynamics Facility, of the Arnold Engineering and Development Center, and the Hypervelocity Section, Wind Tunnel Laboratories, Vought Aeronautics Division, of Ling-Temco-Vought, Inc. The author expresses particular appreciation to Mr. L. K. Ward and Mr. A. E. Hodapp of AEDC and Mr. C. J. Stalmach and Mr. J. L. Lindsey of Ling-Temco-Vought, all of whom made significant contributions to the experimental programs.

This technical report has been reviewed and is approved.

C. B. Westbrook

C. B. WESTBROOK
Chief, Control Criteria Branch
Flight Control Division
AF Flight Dynamics Laboratory

ABSTRACT

Wind Tunnel Tests were conducted in the AEDC Tunnel C at M = 10 and in the Ling Temco Vought Hypervelocity Tunnel at M = 14 and 20 to obtain experimental data on the hypersonic dynamic stability characteristics of a 10-degree half-angle cone. These data were generated to support dynamic stability studies and to evaluate the effects of many geometric and environmental variables, which influence the oscillatory motion of re-entry vehicles.

The state-of-the-art of experimental ground testing in hypersonic dynamic stability is reviewed in detail with respect to simulation and data measuring capabilities. Data correlations were obtained to compare facilities and to evaluate the degree of consistency of results using different techniques in measuring and reducing the data. The confidence level for the data is established by means of these correlations, and conclusive interpretations of the data for application in flight estimates can only be made when the significance of these correlations are fully realized. The data correlations do bring out definite inconsistencies in test results and demonstrate the more obvious shortcomings of ground test simulation in this type of experiment research.

Test results indicate that the 10-degree cone configuration is dynamically stable over the entire scope of matrix variables covered in this experimental program. Dynamic instabilities observed in flight remain unconfirmed by these ground test results. Logically, these instabilities are induced by some other influence, such as ablation, and require more advanced, sophisticated studies to define the causes and effects in entirety. Although the experimental program left much to be defined, it has yielded a considerable amount of valuable information which presents a solid foundation for the more advanced work in the future. Most ground test facilities are striving to improve their capabilities to handle the more sophisticated approaches. Three-degree-of-freedom dynamic stability testing is in the design phase, and mass addition testing has been attempted with encouraging results.

The data obtained in this program demonstrates that dynamic damping can be predicted for the effects of many dependent and independent variables. Specifically, geometric variables such as nose bluntness, cone angle, and center of gravity location can be predicted with a good degree of accuracy using the flow field analyses developed under this program. In many instances Newtonian theory gave an adequate prediction of the significant trends. Reynolds number effects are in general consistent, but the data demonstrate trends which are not adequately predicted by theory.

As a result of the conclusions formed from this experimental program, recommendations are expressed as to the nature of the next generation of experimental research, the facility capabilities which will be required, and the improvements in testing techniques which must be accomplished to provide adequate ground test data.

TABLE OF CONTENTS

TABLE OF CONTENTS (Continued)

TABLE OF CONTENTS (Continued)

LIST OF ILLUSTRATIONS

LIST OF ILLUSTRATIONS (Continued)

LIST OF TABLES

SYMBOLS

α	- angle of attack, deg.
$\dot{\alpha}$	- rate of change in angle of attack, rad/sec.
C_m	- pitching moment coefficient, m/q_∞ SL.
C_{m_α}	- pitching moment coefficient slope, per deg.
C_{m_θ}	- restoring moment derivative, per rad.
C_{m_q}	- partial derivative of C_m with respect to pitching velocity, $\partial C_m / \partial \left(\frac{qL}{2V}\right)$
$C_{m_{\dot{\alpha}}}$	- partial derivative of C_m with respect to rate of change in α, $\partial C_m / \partial \left(\frac{\dot{\alpha}L}{2V}\right)$
$C_{m_q} + C_{m_{\dot{\alpha}}}$	- dynamic damping derivatives in pitch, per rad.
D	- model base diameter, in.
f	- model oscillation frequency, cps.
I	- model mass moment of inertia, ft-lbs-sec^2
K	- mechanical spring constant, ft-lbs./deg.
L	- reference length (model length), in.
M	- Mach Number
M_θ	- restoring moment term, ft.-lbs./rad.
$M_{\dot{\theta}}$	- damping moment term, ft.-lbs.-sec./rad.
m	- pitching moment, ft-lbs.
N	- Number of oscillation cycles, $\omega t/2\pi$
p_∞	- free stream static pressure, psia
P_o	- free stream total pressure, psi
q_∞	- free stream dynamic pressure, psi
q	- pitching velocity, rad/sec.
R_e	- free stream Reynolds Number, per ft.
R_{e_L}	- Reynolds Number based on model axial length.
R_B	- model base radius, in.
R_N	- model nose radius, in.
R_N/R_B	- model bluntness ratio

S	- reference area (model base area), $in.^2$
T_∞	- free stream static temperature, °R
T_o	- free stream total temperature, °R
T_w	- model wall temperature, °R
t	- time, sec.
V_∞	- free stream velocity, ft./sec.
X	- axial length measured from nose, in.
$X_{c.g.}$	- center of gravity location, (pivot location)
$X_{c.p.}$	- center of pressure location, in. from nose
ω	- oscillation frequency, rad/sec.
θ_c	- cone half angle, deg.
θ	- angular displacement (amplitude), rad.
$\dot{\theta}$	- angular velocity, rad/sec.
$\ddot{\theta}$	- angular acceleration, $rad./sec^2$.
$\omega L/2V$	- reduced frequency parameter
δ	- boundary layer/shock layer thickness, in.
δ/D	- B.L./S.L thickness ratio

1. INTRODUCTION

A wind tunnel ground test program was generated to provide experimental data in support of theoretical studies of the hypersonic dynamic stability characteristics of advanced re-entry systems. Also, a secondary purpose was to evaluate the effects of principal geometric and environmental variables in an effort to determine the cause of dynamic instabilities, frequently observed in flight test data but not predicted by theory.

Through the first decade of coping with the many facets of the re-entry problem, the dynamic stability of a vehicle was not given much consideration. The oscillatory motion of a vehicle during re-entry didn't have much effect on the gross performance of a flight. Static stability characteristics as well as spin stabilization prevented any significant effects of dynamic instabilities on long range objectives of a program. The more important problems came first, and the state-of-the-art in the analysis of causes and effects of dynamic instabilities slipped behind the other technologies.

As the design of re-entry vehicles became more advanced, the importance of a greater technological understanding of hypersonic dynamic stability increased significantly. Initial requirements were generated through structural design problems which were associated with the increased lateral loads associated with dynamic instabilities during re-entry. More sophisticated requirements are concerned with the "circular error probability" or impact accuracy, the radar detection specifications, and the effects on advanced control problems.

Considerable interest has been generated in advancing the technologies in dynamic stability. Joint efforts under the sponsorship of the U.S. Air Force have been accomplished in which industrial contractors have cooperated with each other in an effort to establish a rapid advancement in the state-of-the-art. A special committee of the Supersonic Tunnel Association was formed by various facilities to generate testing techniques and to provide adequate testing capabilities, specifically for dynamic stability testing.

Projecting an awareness of all the problems associated with both flight and ground test simulation of dynamic stability is a major objective in the preparation of this report. Much of the information expressed is derived from experience and from an exhaustive survey of available literature and can be used as a guide in the familiarization of the present state-of-the-art in hypersonic dynamic stability simulation.

Manuscript released by author, February 9, 1966 for publication as an ASD Technical Documentary Report.

2. TEST FACILITIES

2.1 INTRODUCTION

From the original list of five proposed facilities to carry out this experimental program as expressed in Reference 1, only two were eventually utilized. Because of budget limitations and delays in the development of capabilities, the program was was abbreviated to testing in just AEDC Tunnel C and the Ling-Temco-Vought Hypervelocity tunnel. Unfortunately, the additional data that would have been generated in these other facilities could have contributed significantly to the overall scope of the study.

The specific facilities were chosen to perform these tasks primarily because of their established capabilities, and their interest in extending prior capabilities to meet the needs of the program. Free flight ground testing was not considered for this program because of insufficient data accuracy at hypersonic speeds.

Other facilities, in addition to those used, which provide advanced hypersonic capabilities and which should be definitely considered for advanced work are; the AEDC Tunnel B (M = 8), the AEDC Tunnel F (M = 20), the FluiDyne 20-inch Tunnel (M = 7, 10, 12, 14, and 16), the ARL 20-inch Hypersonic Tunnel (M = 10-15), the NASA-Ames 3.5-foot Tunnel (M = 8, 10, 12), and the JPL 21-inch Tunnel (M = 8, 10).

2.2 FACILITY DESCRIPTIONS

The AEDC Tunnel C is a continuous flow, closed-circuit, hypersonic wind tunnel with a 50-inch diameter test section. An axisymmetric contoured nozzle expands the flow to M = 10 in the test section at a total temperature of about 1900°R. Total pressures up to about 1800 psi provide a Reynolds number range from about 0.3×10^6 per foot to a maximum of about 2.2×10^6 per foot for continuous operation. An injection and retraction system allows model installation, inspection, or cooling without interrupting the tunnel operation. The entire model support and sector is retracted into a vacuum tank which is sealed off from the tunnel for access. For model injection, the tank is evacuated to tunnel free stream static pressure. For dynamic stability tests, this injection and retraction system is used very effectively for balance and model cooling after each run. This facility is part of the Arnold Engineering Development Center, which provides services to all agencies of the Federal Government and to industry for research and development work. The facility is operated by a private concern, ARO, Inc., under contract to the United States Air Force, and is located on the Arnold Air Force Station reservation, Tullahoma, Tennessee. Additional information may be obtained from Reference 2.

The Ling-Temco-Vought Hypervelocity wind tunnel is an arc-driven hypersonic blow down facility with a 13.5-inch diameter test section. Interchangeable throats

and a conical nozzle provide a Mach number range from about 14 to about 21. A vacuum chamber and a diffuser downstream provided durations of uniform flow up to a maximum of about 100 milliseconds. Improvements to the facility have subsequently extended the duration of uniform test time to 250 milliseconds. Arc chamber total pressures are obtained up to 22,000 psi with a maximum energy discharge density of 11,000 joules per cubic inch. The Reynolds number range varies between about 0.1×10^6 and 1.5×10^6 per foot, and the flow medium used for these tests was nitrogen. All arc discharge tunnels have a certain amount of flow contamination due to high electrical currents, temperatures and pressures. This facility maintains a relatively low level of contamination due to (1) the rapid discharge of electrical energy, (2) low levels of electrical energy, (3) a choice of least corrosive design materials, (4) the design of arc discharge components, and (5) the use of nitrogen as the test gas as opposed to air. Additional tunnel information may be obtained from Reference 3. This facility is privately owned and operated by the Vought Aeronautics Division, Ling-Temco-Vought, Inc., and is a part of their Wind Tunnel Laboratories located in Grand Prairie, Texas.

2.3 FACILITY COMPARISONS - DATA CORRELATIONS

Table 1 shows the comparison of significant flow properties in the Ling-Temco-Vought hypervelocity tunnel and the AEDC Tunnel C. The free stream conditions of Reynolds number per foot, static pressure, and dynamic pressure are quite similar. However, Mach number, velocity, total temperature, and total pressure are significantly higher in the Ling-Temco-Vought facility. The higher temperatures also cause significantly lower flow densities than obtained in Tunnel C, and although free stream Reynolds numbers compare relatively well, the flow densities and velocities are significantly different. Simulated altitudes for a typical flight vehicle are presented in Table 1, based on the free stream Reynolds number for a specific model length and the free stream Mach number. Free stream temperature, density, and pressure are not considered directly as simulation parameters. The difference in altitude simulation is, therefore, contributed primarily to model size and Mach number differences.

TABLE 1
COMPARISON OF FACILITY FLOW PROPERTIES

Flow Properties	LTV-HVWT	AEDC Tunnel C
Mach No. Range	14-21	10
Reynolds No. Range	0.1×10^6-1.5×10^6/ft	0.3×10^6-$2 \times 2 \times 10^6$/ft
Flow Velocity, V_∞	6000-11,500 fps	4400-4700 fps
Static Pressure, p_∞	0.0015-0.0150 psia	0.0041-0.0370 psia
Altitude (based on R_{e_L})	120,000-190,000 ft	65,000-110,000 ft
Dynamic Pressure, q_∞	0.3 - 3.0 psia	0.3 - 2.7 psia

Flow Properties	LTV-HVWT	AEDC Tunnel C
Total Pressure, P_o	6000-22,000 psi	200-2000 psi
Total Temperature, T_o	2700-8100°R	1700-1900°R
Flow Medium	Nitrogen	Air
Flow Duration	40-100 milliseconds	Continuous

Nitrogen is used as the flow medium in the Ling-Temco-Vought facility instead of air so that the real gas effects of dissociation are not present at the high temperatures.

Table 2 shows the comparison of testing techniques, test apparatus, and resulting test conditions utilized in each of the facilities. The major consideration in comparing the facilities and in making a data correlation is the difference in frequency. Because of the extremely short duration of uniform flow in the Ling-Temco-Vought facility, the frequency must be large so that a sufficient number of cycles may be obtained to analyze the amplitude decay. Although the frequency differs by almost two orders of magnitude between the two facilities, the reduced frequency parameter, $\omega L/2V$, which is commonly used in dynamic stability as a simulation parameter, is in relatively good agreement and the two facilities bracket flight simulation in this respect. Other distinct differences between facilities are the model scaling, which is dependent upon the size of the tunnel test section, and the testing techniques, which are associated directly with balance and model design. In each case, the facilities are seeking the optimum performance capability from their test apparatus with basically the same theoretical approach.

A measure of the performance of these facilities is made by means of data correlations. Ideally, additional facilities with overlapping capabilities would be used to make a more valid correlation. A correlation of data using both a free oscillation and a forced oscillation technique was obtained in the AEDC Tunnel C. Discrepancies were obtained, which indicate the performance of each technique. This correlation is discussed in detail in Section 6. A data correlation for the facilities can be roughly interpreted in Figure 39. The major differences between the two sets of data are frequency and Reynolds number. All data indicate a consistent trend with increased frequency and decreased Reynolds number. A slight frequency effect has been observed in all the data, however, the differences in dynamic damping as measured in each facility can be interpreted entirely as viscous effects, as derived in Reference 4, making frequency an insignificant variable. Correlations of tunnel C data alone appear also to support this conclusion.

A general interpretation for a facility correlation is that the two sets of data show good agreement, well within the data accuracy, when considering viscous effects.

TABLE 2
COMPARISON OF FACILITY TESTING

Comparison		LTV-HVWT	AEDC Tunnel C
Test Techniques		Free Oscillation	Forced Oscillation Free Oscillation
Balance Pivot		Cruciform Flexure	Cross-Flexure Gas Bearing
Pivot Location(s)		0.549 L	0.50, 0.55, 0.60 L * 0.60 L **
Balance Spring Constant		21.675 ft-lb/rad	144-1079 ft-lb/rad * approximately 1.0×10^{-4} ft-lb/rad **
Model:	Length	5.52 inches	28.35 inches
	Diameter	1.974 inches	10 inches
	Inertia	17.196×10^6 (ft-lb-sec^2)	0.031-0.28 ft-lb-sec^2 * 0.22-0.47 ft-lb-sec^2 **
Initial Oscillation Amplitude		$\pm$2 degrees	$\pm$ 2 degrees * $\pm 8^o$ and Higher **
Oscillation Frequency		180 cps	2 to 11 cps * 1 to 3 cps **
Reduced Frequency Parameter, $\omega L/2V$		0.032-0.043	0.0091-0.0190 * 0.0012-0.0048 **
Angle of Attack Range		0 degrees to 8 degrees	0 degrees to 10 degrees * 0^o **

* Cross-flexure
** Gas bearing

2.4 FACILITY ADVANTAGES AND DISADVANTAGES

When considering the requirements for ground test simulation, every facility has some advantages and disadvantages. The primary disadvantage of a hot shot facility is the required frequency level and the resulting requirement of relatively high structural damping. A secondary disadvantage is the transient flow conditions, accompanying the decay in reservoir pressure. Both of these effects can be minimized through proper design. Some advantages of a Hot Shot type facility are high Mach number conditions without significant temperature effects and extremely light weight models (low inertia). The fact that the short time duration eliminates the temperature problems associated with high Mach number flow, is a very important consideration. Balance calibrations and minimum model mass moments of inertia would be greatly compromised if temperature effects were significant. If, in fact, frequency is an insignificant variable in hypersonic flow, continued improvement in balance design, model moments of inertia and flow properties in Hot Shot facilities would dictate a direction toward testing in this type facility instead of the hybrid facilities.

At this time, the AEDC Tunnel C appears to be an ideal hypersonic facility for dynamic stability testing. Although this facility is temporarily limited to a relatively low hypersonic Mach number (10), experience gained in extending the capabilities has been beneficial in coping with the problems associated with temperature and with balance design and calibration. The disadvantages of this facility are relatively insignificant, and the scope of their testing capabilities appears to be continually expanding with the simulation requirements.

3. ENVIRONMENTAL SIMULATION

3.1 INTRODUCTION

In obtaining ground test data, it is very important to know exactly what flight conditions should be duplicated and to what degree these conditions are simulated. In the particular case of hypersonic dynamic stability there are many environmental conditions which may, directly or indirectly, influence the oscillatory motion of a vehicle re-entering the earth's atmosphere. In order to properly evaluate the data, the extent of environmental simulation must be defined in entirety, by demonstrating how well the more significant variables are duplicated and by pointing out the significant areas where flight simulation is not provided in the ground test facility. Obviously, there are compromises which must be accepted until the state-of-the-art is advanced to the point where the duplications and extrapolations of the significant variables are possible, and the less important variables are neglected.

3.2 STATE-OF-THE-ART FLIGHT SIMULATION

The question initially arises as to what are the significant variables which should be considered for flight simulation in a ground test facility. This is best answered through a physical interpretation of the vehicle motion experienced in flight. As a vehicle follows its prescribed trajectory and approaches the outermost fringes of the earth's atmosphere, the body is oriented at some angle of attack with reference to the trajectory path. As the vehicle enters the atmosphere, this angle of attack will tend to converge to the natural aerodynamic trim angle of attack as the aerodynamic forces build up. The rate of convergence is dependent on several factors. The vehicle spin rate and mass moment of inertia in spin can influence the convergence so that an effective angle of attack is maintained well into the re-entry portion of flight. An aerodynamic restoring moment imposed on a spinning vehicle induces a spiraling motion, often referred to as coning. An effective angle of attack is maintained during this coning motion, and because the motion is not planar, the rate of angular convergence is partially dependent on the moment of inertia in spin and not entirely on the aerodynamic restoring moment.

Damping (positive or negative) affects the rate of angular convergence. As observed in flight, dynamic instabilities cannot only cause a "hang up" in the angular convergence, but can also cause a significant divergence, and it is this divergence which requires a complete investigation of dynamic stability characteristics during re-entry.

Flight test data indicate that the divergence is experienced at specific altitudes, which would suggest that the induced instabilities are caused by the effects of environmental variables. From this interpretation of vehicle motion during re-entry, a logical guess of the most significant variables can be made. The angle of attack and amplitude of oscillation are variables which logically require investigation based on experience. The frequency of oscillation is a variable which is a function of the aerodynamic restoring moment and the vehicle mass moment of inertia. Other variables such as Mach number, velocity, Reynolds number, and many other associated boundary layer conditions are considered to have possible effect on dynamic oscillation decay.

The state-of-the-art in environmental simulation of these flight variables is outlined in the following pages. A great deal of work would be required in ground test facilities to develop capabilities to encompass simulation with respect to all the variables. The only acceptable answer to the problem is to evaluate the effects of the variables independently, and, by means of scaling parameters and extrapolations of the data to flight conditions, determine the over-all stability characteristics. Facility operators are building blowdown tunnels, continuous flow tunnels, hot shot tunnels, ballistic ranges, and hybrid tunnels in an effort to provide various aspects of environmental simulation. No facilities have been able to match all the conditions of hypersonic flight to date.

3.3 SIMULATION PARAMETERS

3.3.1 Altitude — Mach Number — Velocity

Mach number is the ratio of velocity to speed of sound, where the speed of sound is a function of the ambient temperature. In compressible fluid flow, Mach number is unmistakably the most important parameter. However, at hypersonic speeds, Mach number effects presumably approach an asymtotic value. In dynamic stability, free stream velocity is a significant parameter, and by simulating Mach number in a hypersonic wind tunnel, an assumption of velocity simulation is erroneous, because of the significant differences in ambient temperature. For hypersonic dynamic stability, there is still a question as to the relative importance of Mach number and velocity simulation. This question is discussed further in Section 9.

The concept of altitude simulation in a wind tunnel is also in question and should be clarified. Altitude simulation is usually specified as density or pressure altitude, corresponding to the standard atmospheric altitude for a particular density or pressure. These two conditions could and usually do represent a different altitude simulation because of the static temperature of the flow. Ideally, the Reynolds number, which retains the required similarity for density, pressure, and temperature, should be used as the significant altitude simulation parameter together with Mach number in a wind tunnel.

Environmental simulation of altitude under the above conditions in terms of Reynold's number is usually difficult to attain as discussed in Section 3. 3. 2 on Reynold's number simulation. Velocity simulation is generally difficult to obtain in a wind tunnel because of the extremely low static temperatures in a wind tunnel. For a given Mach number, the flight velocities are considerably higher than those obtained in a wind tunnel because the speed of sound is considerably higher in flight. Mach number is the basic simulation parameter in a ground test facility, and wind tunnels are designed and built specifically for Mach number simulation, if for no other reason. As Mach number requirements were extended, facilities were built to meet the demand. The evolution was accomplished initially by gradually increasing the total temperatures to prevent liquefaction of the expanded flow until maximum temperature levels were approached. Then Mach number capabilities were extended further with the extremely high instantaneous pressure and temperature levels of arc discharge facilities. The result has been that the facilities are readily available for Mach number simulation, but simultaneously they compromise many other considerations of simulation.

3.3.2 Reynolds Number

The Reynolds number is a non-dimensional parameter for fluid flow which satisfies the condition of similarity in a ratio of inertia force to friction force. The unit Reynolds number per foot for the free stream flow characteristics in a wind tunnel matches that obtained in flight relatively well in most facilities, and if it were possible to use a full scale model in a wind tunnel, Reynolds number simulation would be attained. Generally, this is not the case, and in considering model scaling, Reynolds numbers are nominally an order of magnitude lower in the wind tunnel. Low Reynolds number conditions, associated with the higher altitude portion of flight, can usually be simulated relatively well in a wind tunnel either by reducing model scale or by going to lower pressure, higher temperature, or both.

3. 3. 3 Frequency — Reduced Frequency

The environmental simulation of frequency is a function of several considerations depending on the testing technique and the test apparatus. For example, in the specific case utilized in this program, the frequency obtained with the free oscillation, gas bearing technique is dependent primarily on the aerodynamic moment and the model mass moment of inertia. In the case of testing in a hot shot type facility, the frequency is dictated by available test time and regulated by the design of the balance structural stiffness.

An interpretation of the frequency simulation for a scaled model is generally represented by the reduced frequency parameter which relates size, frequency and velocity. In most cases of experimental work to date in hypersonic dynamic stability, this parameter has been designated a variable to obtain frequency effects. In general, reduced frequencies obtained in ground test facilities simulate reduced frequencies in flight fairly well, and an exact reduced frequency match could probably be obtained through balance and model design specifications. The procedure is not recommended, however, because of additional fabrication expenses.

3.3.4 Scaling Effects

The effects of model scaling in ground test simulation has been discussed in Section 3.3.2 for Reynolds number simulation and in Section 3.3.3 for frequency simulation. Both considerations imply scaling effects are important in dynamic stability simulation. Other considerations, such as the effects of boundary layer thickness and proportionment relative to size, the effects of entropy gradients in the flow field relative to size, and the effects of boundary layer momentum thickness relative to size, might all have significant implications in dynamic stability characteristics.

In order to evaluate scaling effects in general (inclusive of Reynolds number, frequency, etc.), it becomes necessary to accurately define other influences on the data which vary with model scaling, (i.e., support interference effects and balance calibration considerations). Data are being generated in an effort to define scaling effects, but with the present state-of-the-art it is anticipated that no scaling effects will be discernible other than those attributed to Reynolds number and frequency.

3.3.5 Oscillation Amplitude

Ground test simulation of oscillation amplitude does not present a significant problem in the present state-of-the-art. Physical limitations of amplitude for specific configurations are encountered in model-sting interference. However, high amplitudes can be obtained for these configurations on transverse rod supports or by means of free flight testing.

Flight simulation of oscillation amplitude in ground test facilities is at present limited to one degree of freedom motion (amplitude variation in one plane). Planar amplitude effects on damping characteristics are generally used in trajectory simulations as being representative of six degrees of freedom motion. However, it is pointed out in Reference 5 that for a vehicle which is free to oscillate in combined pitch and yaw, the amplitude effects on pitch damping may be significantly different. Therefore it is desirable to provide two or three degrees of freedom to adequately define these effects on dynamic damping.

3. 3. 6 Angle of Attack

Angle of attack simulation is obtained readily in ground test facilities using sting mounted flexure balances; however, angle of attack limits are often dictated because of the static aerodynamic moment imposed on the balance. In the case of configurations with essentially linear damping characteristics, data obtained for small oscillations at angles of attack can be interpreted as data for large amplitude oscillations at zero angle of attack. Generally, the effective angles of attack demonstrated in flight are well within the capabilities of ground test simulation.

3. 4 NUMBER OF DEGREES OF FREEDOM

In considering ground test simulation of oscillatory motion of a re-entry vehicle, one of the most significant questions is whether a one-degree-of-freedom analysis of dynamic stability is representative of the six-degrees-of-freedom in flight. Free flight ballistic range tests have been made whereby the model has more than one degree of freedom; however, the data is consistent with data obtained from one degree of freedom tests.

For cases in which amplitude effects are significant and especially if the configuration is unstable with a limit cycle amplitude, it may be assumed that damping characteristics for three degrees of freedom will not be consistent with one degree of freedom characteristics. This assumption is expressed theoretically in Reference 5, as discussed previously in Section 3. 3. 5.

The state-of-the-art ground test simulation has progressed to the point that three degrees of freedom techniques are in the design phase. With the successful development of this capability, the effects of spin and coning motion can be simulated in ground test facilities. It may demonstrate identical stability characteristics as those obtained with one degree of freedom techniques, but a significant advancement will have been made in ground test simulation.

3. 5 VISCOUS INTERACTION EFFECTS

As discussed under 3. 3. 1 high Mach number simulation can be achieved in a blowdown or hot-shot tunnel only by going to very low temperature, low density flows. Under these conditions viscous interaction between the boundary layer and the inviscid flow becomes important. Flight conditions under which viscous interaction occurs are divided into weak and strong interaction regimes, identified by the parameter:

$$\chi \cong \frac{M_\infty^3}{\left(Re_L\right)_\infty^{1/2}}$$

For

weak interaction: $\bar{\chi} < 3$ approximately

strong interaction: $\bar{\chi} > 3$ approximately

as indicated by Lees and Probstein. Test data from several facilities indicates that on slender slightly blunted cones, viscous interaction decreases dynamic stability. In the weak interaction regime there is a small but observable decrease in stability, however with strong interaction ($\bar{\chi} > 10$) the loss in stability can be great enough to cause the cone to go unstable. The implications of this trend depends on the type of trajectory flown. On ballistic trajectories aerodynamic damping effects are negligible at the high altitudes at which strong interaction occurs. Thus wind tunnel dynamic damping data which includes strong interaction effects will not be applicable at the lower altitudes which are of interest, even though the Mach number is simulated. For shallow re-entry path angles the vehicle spends a relatively long time at high altitudes and here viscous interaction effects may become significant. Clearly, ground test data must be evaluated in terms of the anticipated full scale flight conditions to determine the degree of simulation achieved.

3.6 WALL TEMPERATURE — SURFACE PRESSURE

In most cases, wall temperature effects are not simulated in ground test facilities for dynamic stability, and test data indicate wall temperature effects alone can contribute a variation in surface pressure of about 10 percent. In general, the model wall temperatures are kept relatively cool in dynamic stability testing to protect the balances.

3.7 EFFECTS OF ABLATION

The capability of adequately simulating ablation in dynamic stability testing will be the most significant contribution to the state-of-the-art when it is perfected. Flight test data have demonstrated conclusively that the effects of ablative mass addition alter the dynamic stability during re-entry as expressed in Reference 6. Various ground test facilities have successfully tested models with subliming coatings and models with mass flow ejection from a porous wall into the boundary layer. Initial wind tunnel results confirm the flight data and indicate significant variations in damping as a result of mass addition to the boundary layer. A survey of available ground test data of mass addition effects on re-entry aerodynamics may be found in Reference 7. The ground test capabilities are being perfected to adequately simulate these conditions and should be available for the next generation of experimental research in dynamic stability.

3.8 EFFECTS OF BOUNDARY LAYER TRANSITION

A considerable amount of opinion has been voiced as to the nature of boundary layer transition in flight. Some flight data have demonstrated that transition from laminar to turbulent flow is instantaneous over the entire vehicle, while other data indicate transition begins at the aft end of the vehicle and moves forward. For the specific case of a sharp 10-degree cone, AEDC wind tunnel data, in the form of shadowgraph flow visualization, indicate without a doubt that in a hypersonic flow field boundary layer transition begins at the base of the model and moves forward. Transition occurs on this cone at zero angle of attack between a R_{eL} of about 1.0×10^6 and 4.0×10^6 with totally laminar flow at 1.0×10^6 and fully turbulent flow at 4.0×10^6.

Simulation of flight transition in wind tunnels is exceedingly difficult and wind tunnel data are often misleading. Adequate simulation would depend on the effects of ablation, wall temperature, model surface roughness and flow turbulence factors.

3.9 TRANSIENT FLOW PROPERTIES

In certain ground test facilities such as arc discharge tunnels and also some intermittent hypersonic blowdown tunnels, a gradual decay in the flow properties is experienced. The effect of time variations of the aerodynamic properties on dynamic stability characteristics has been analyzed in detail in Reference 8. It was found that as long as the ratio of V_∞/q_∞ remains relatively constant, the effects are not significant. In most cases any effects contributed to this condition are well within the accuracy of measuring the data.

4. TEST APPARATUS

4.1 INTRODUCTION

In most cases, the type of test apparatus used in a given facility is dictated by the characteristics of the facility. The types of test apparatus can vary significantly from facility to facility and, generally, the best equipment available is needed. Experience is very important in this respect, and continuous improvement of test apparatus is essential for the rapid advances and requirements placed on ground test simulation technology. The importance of a good working knowledge of the test equipment, its performance capabilities, and its flexibility in comparison with other types of apparatus cannot be underestimated.

The various techniques used in making dynamic stability measurements are classified basically as "captive" model or "free flight" model techniques. Specifically, "captive" model testing employs free or forced oscillation techniques with either gas bearing, ball bearing, or flexure type pivots. In "captive" model testing, either sting mounts or transverse mounts are usually employed for model support. Free flight techniques eliminate the effects of support interference and provide the additional degrees-of-freedom which are regarded as possibly significant in dynamic stability. Models are fired as projectiles in ballistic ranges and, more recently, in wind tunnels. In wind tunnels, models are fired at relatively low muzzle velocities into the flow so that the model velocity is about equal to that of the flow. Analysis of the motion is made from photographic records for measurements of dynamic oscillation decay.

Probably the most significant factor in providing valid measurements of dynamic stability characteristics in captive testing is the degree of accuracy with which balance calibrations can predict the level of structural damping. The importance of adequate balance design and calibration is discussed in detail in the following pages.

4.2 BALANCE DESIGN AND CALIBRATION

In designing an adequate dynamic stability balance, estimates must be made as to the range of model sizes, restoring moments, moments of inertia, and desired frequencies and amplitudes. The degree of structural damping for a particular balance is inherent in the specified material and in the design for the above conditions. The most important consideration in design is to provide a balance with the least amount of structural damping, because the accuracy of the data to be obtained with a particular balance is dependent on the largest possible ratio of aerodynamic damping to structural damping.

The material selection for balance fabrication is important because of its elastic properties, spring constant, etc., under specific conditions of temperature and stress. The molecular structure of most materials is such that the spring constant and, therefore, structural damping, is not consistent under conditions of high stress level. For this reason, small, high frequency balances are very difficult to design, and often calibrations of structural damping do not show the repeatability which is required to adequately determine the aerodynamic damping.

Other critical aspects of flexure balance design are any joints, sealants, welds, etc., which can absorb some of the energy and damp the motion. Improperly designed releasing mechanisms can result in large energy losses and compromise otherwise perfectly adequate balances.

Flexure balance calibrations are performed to evaluate the resultant spring constant of the flexure and to determine if the spring constant remains constant over the entire deflection range. If there is any variation in the spring constant, the structural damping increment in dynamic stability can not be properly evaluated. Balance calibrations for structural or tare damping are made for each particular test model so that calibration includes the effects of specific moments of inertia. The calibrations of tare damping are subtracted from the total damping obtained in tunnel tests to evaluate the aerodynamic damping contribution. Other considerations of balance calibrations with respect to tare damping are discussed in Sections 4.3 and 4.5.

In the case of gas bearing balances, calibrations are obtained to evaluate the load carrying capability and the tare damping characteristics. Techniques used in obtaining these calibrations are discussed in Reference 9.

4.3 STRUCTURAL DAMPING

4.3.1 Axial Force Effects

The consideration of a change in tare damping with a model axial load bearing on the balance pivot is discussed in Reference 10. A change is definitely indicated, which would imply that the structural damping is influenced by aerodynamic loads. In most cases, the change represented is relatively small and is neglected; however, if the aerodynamic damping is small relative to the structural damping, the small change in tare damping can produce a large effect on the measured magnitude of the aerodynamic damping. Similarly, other aerodynamic forces can affect the structural damping of a balance. The effect of loading on a gas bearing balance is shown in Reference 6, and indicates relatively little change especially in the mid-load range. The axial load carrying effects on tare damping are expected to vary for each type of balance design, and all balances should be calibrated to determine these effects.

4.3.2 Frequency Effects

The effects of oscillation frequency are also discussed in detail in References 6 and 7. The structural damping of a cross flexure balance decreases with increasing frequency, and sample data shows a significant change in the dynamic damping coefficient when frequency effects on tare damping are taken into account. Tare damping of a gas bearing also demonstrates very significant frequency effects, and in relatively low Reynolds number flow where the tare damping of a gas bearing becomes significant, a small change in frequency can affect the tare damping considerably. As in the case of flexure balances, the tare damping decreases with increased frequency.

4.3.3 Amplitude Effects

In specific incidents using flexure balances, the structural damping has been observed to vary with amplitude, or possibly with the stress level reached in the balance. A variation in tare damping was also observed after continuous use as if the properties of the material were changing, although calibrations of the balance spring constant do not seem to reflect this condition. Amplitude effects of this type were obtained for high frequency balances, and a redesign of flexure length and width seems to alleviate or eliminate the effects.

4.3.4 Vacuum Effects

In making tare damping calibrations, it has been conclusively demonstrated that the static pressure does affect tare damping. The variation in damping from atmospheric pressure to vacuum conditions appears to be linear; however, when obtaining damping calibrations in a vacuum, the repeatability of the measurements is not as good as at the higher pressures. Therefore, the recommended procedure in obtaining calibrations for near vacuum conditions would be to define the linear variation with pressure from atmosphere and fair through vacuum data.

4.4 CONTRIBUTIONS TO TOTAL DAMPING

The tare damping of different balances under different environmental conditions will have vastly different effects on the accuracy of aerodynamic damping. It should be realized that, for a particular balance, the tare damping is relatively constant, and for variations in free stream conditions, the aerodynamic damping varies considerably. Therefore, the percentage of aerodynamic damping with respect to the total damping can also vary tremendously. This consideration should be studied carefully for every balance range and Reynolds number variation, to determine the tolerances placed on the data and the resultant effects on the previously mentioned errors in tare damping. In the cases where aerodynamic damping is a small percentage of the total damping, the data is invalid unless the tare damping and associated errors in measuring tare damping are accurately determined.

The percentage of total damping contributed by aerodynamics can vary from as low as 5 percent to about 70 percent, and possibly higher under ideal conditions, for a flexure balance. For gas bearing balances, the percentage of total damping should range from at least 60 percent, depending on environmental conditions, up to essentially 100 percent. For gas bearing performance, any worse than that described above, the balance design should be critically evaluated.

4.5 FORCE AND MOMENT CROSS COUPLING

The effects of static forces and moments have already been discussed briefly in Section 4.3. The degree to which the forces affect the strain in the balance material is a necessary consideration in balance design. Most flexure balances utilize strain gage elements which measure the model angular deflection. Orientation of the strain gage elements as well as orientation of the flexure material to eliminate or significantly reduce the effects of static forces and moments is a very important criterion in design. These effects are especially significant at angle of attack.

4.6 SUPPORT SYSTEMS

4.6.1 Types - Advantages and Disadvantages

Basically, there are two general types of support systems; sting mount, which supports the model from the downstream end and through the base of the model, and the transverse or cross mount, which is usually a cylindrical rod supporting the model at either or both sides of the model. For dynamic stability testing, the sting mount is generally preferred. A sting mount is located downstream in the model wake and does not disrupt the aerodynamic flow field about the model. The disadvantages of a sting mount are the limitations on amplitude, due to sting-model interference at the base, and the possible alteration of base flow effects due to the presence of the sting.

The advantages of a transverse support are that large trim angles of attack and large amplitudes are possible, especially on a gas bearing balance. A disadvantage of this type of mount is rather obvious in that the rod does disrupt the flow field about the model; however, this disorder is in a plane perpendicular to the flow which is the critical contribution to pitch damping. The philosophy is that cross flow effects are not too significant, which in many cases could be an erroneous assumption. Also the induced deflections in the transverse support due to aerodynamic loads, which means a relatively rigid, short rod is required, and compromises must be made. Other significant disadvantages of a transverse support, which have been discovered through experience, are that high temperature and pressure induced on the rod can be fed into the model and balance interior. Both systems have some advantages and the choice depends on the specifications placed on the data to be measured.

4.6.2 Aerodynamic Interference Effects

One of the major tasks encompassed in this experimental program was to investigate the aerodynamic interference effects of the two common types of support systems. Using the identical model configuration and balance, data was obtained for both the transverse rod and the sting support systems at various environmental conditions. Using the transverse rod support system, a series of runs was also made with various dummy stings located in the base region of the model to evaluate the aerodynamic interference effects of sting support systems.

The results of these experimental studies on aerodynamic interference effects demonstrate that dynamic stability measurements may be significantly biased by the support systems. The effects of sting supports on aerodynamic damping are shown in Figure 1 as a function of sting to model diameter ratio. Sting effects are observed primarily at low Reynolds numbers and indicate as much as a 30% reduction in damping with a 0.18 diameter ratio. At higher Reynolds numbers and higher oscillation amplitudes, sting effect appears to be reduced.

A comparison of data for a sting mounted model and a transverse rod mounted model is shown in Figure 2. These results indicate that the aerodynamic interference from a transverse rod support has a pronounced effect on the damping derivatives throughout most of the Reynolds number range tested. As much as a 60% reduction in stability is observed at the onset of boundary layer transition, but it appears as if the effects are greatly reduced as the boundary layer becomes turbulent. The significant effect of transverse rod supports on experimental measurements of dynamic damping has also been observed for laminar flow conditions in Reference 11.

In general, studies indicate that aerodynamic interference from support systems definitely has a significant effect on damping measurements. It may also be inferred that much of the data discrepancies among facilities can be attributable to support interference effects. The data implies that sting effects are most pronounced at low Reynolds numbers and at small oscillation amplitudes, and that the effect is to reduce aerodynamic damping. Sting effects are discussed further in Section 7 with specific reference to the experimental results.

Additional data on sting support interference effects at supersonic Mach numbers and the corresponding effects on model base pressure may be found in Reference 12. More information on the effects of support interference on the model wake is found in Reference 13.

TRANSVERSE ROD - FREE OSCILLATION DATA

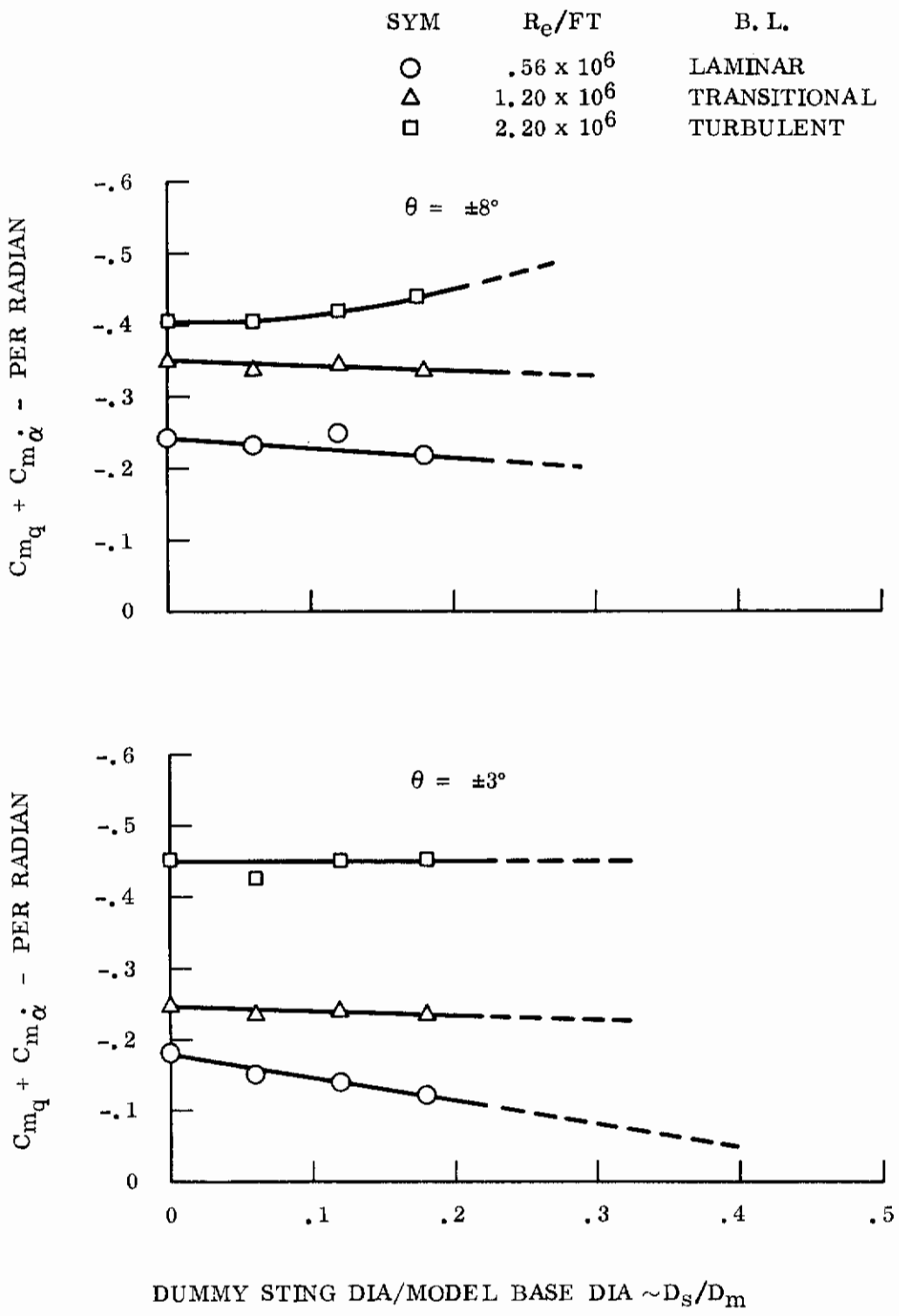

Figure 1. Sting Support Interference Effects

SYM	TEST TECHNIQUE	STING. DIA.
○	STING MOUNT. - FREE OSC.	1.8 IN. STING
□	STING MOUNT. - FORCED OSC.	1.8 IN. STING
▲	TRANS. ROD MOUNT. - FREE OSC.	1.8 IN. DUMMY STING

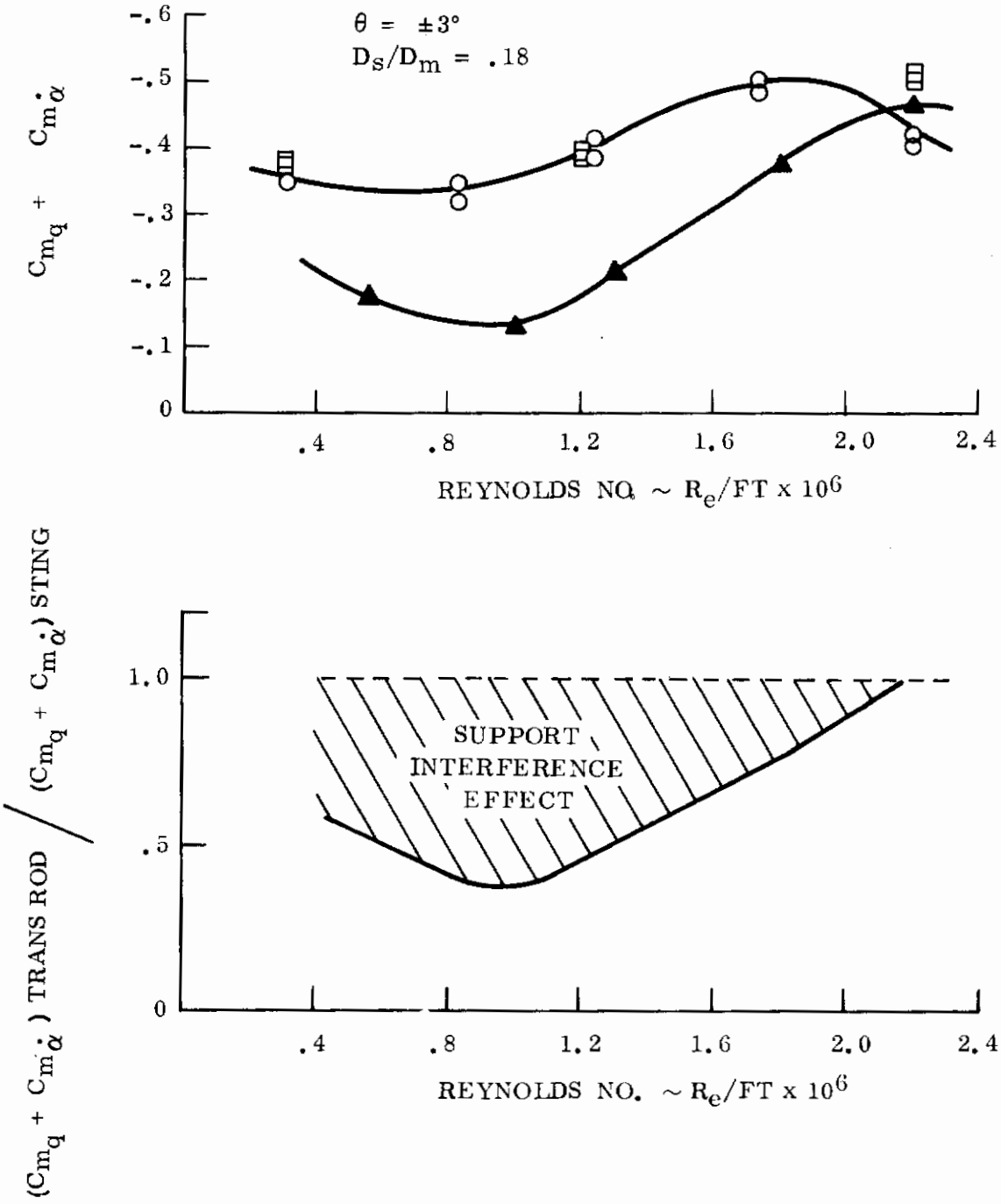

Figure 2. Transverse Support Interference Effects

4.6.3 Vibrational Interference Effects

In dynamic stability tests, unless adequate precautions are taken, a resonant vibration may be induced in the supporting system either as a result of model oscillation or tunnel or flow characteristics. The support system vibration can be fed into the model and picked up in the measuring of model data, which may completely invalidate the measurements. If the vibration frequency is significantly different from that of the model dynamics, the superimposed vibrations may be filtered out, but the effects are still present and it remains questionable whether the effects are significant.

These considerations must be taken into account, however, in the design of support equipment and in the proper reduction of the data.

4.6.4 Mechanical Interference Effects

Mechanical interference effects are usually prevented but, occasionally, limits are accidentally exceeded and possibly go unnoticed. Mechanical interference can limit model excursions or absorb torque. The latter effect would indicate a greater level of aerodynamic damping. Other possible mechanical interference problems may be induced by poor model-balance connections or poor balance-sting connections. As previously stated, these problems are usually prevented but can occur and go unnoticed. A grounding circuit to provide an indication of mechanical interference is occasionally used and is recommended for tests in which these problems might occur.

4.7 TEMPERATURE EFFECTS ON MEASURING DEVICES

In facilities where temperature variations are significant, extreme caution must be taken to assure that temperature does not affect data measurements. In the case of both flexure and gas bearing balances, balance temperatures should be accurately controlled by design and constantly monitored during a testing cycle. Adequate balance calibrations with respect to temperature variations must be provided to assure the validity of measurements over a given temperature range.

4.8 ON-RESONANCE FORCED OSCILLATION

In the case of free oscillation, the model oscillates at its natural frequency which is dictated by the moment of inertia and the aerodynamic and structural spring constants. In the case of forced oscillation, however, the mode of torque input can be off resonance. Data can be determined accurately in a case of off-resonance, but the data reduction becomes more complex and introduces the possibility of additional errors. For this

reason, an on-resonance condition is highly recommended in forced oscillation testing, especially at high mach numbers.

4.9 FLOW VISUALIZATION MEASUREMENTS

Good visual measurements of the flow field, in the form of Schlieren or shadowgraph photography, has always been a very beneficial aid to the aerodynamicist. In the case of dynamic stability, there are still many effects of oscillatory motion on the boundary layer and flow field which need to be defined, and visual aids can help considerably. Significant improvements can be made in this field and are recommended. Continuous Schlieren photography has been successfully obtained in the Ling-Temco-Vought facility to the extent of getting a variation in the boundary layer thickness with oscillation amplitude. Extending this type of capability in other facilities would be very advantageous and, in cases where radiation effects prevent adequate visualization, other methods should be investigated.

5. TEST MODELS

5.1 INTRODUCTION

The design and fabrication (or modification) of models were performed specifically under the cognizance of the respective facility project engineer so that complete harmony was maintained between model and facility hardware specifications. In all cases of model design, fabrications, and modification in this program, the work was subcontracted to experienced and well-qualified organizations. All aspects of model design and fabrication were completed with very satisfactory results.

In dynamic stability testing, sophisticated model designs are required to satisfy various specifications of the facilities and their particular test apparatus. In some cases, changes in the configuration are even dictated by these specifications. Special model design criteria are established in dynamic stability testing for conditions requiring static and sometimes dynamic balancing about the pivot point. These and other conditions relating to the test models used in this program are discussed in the following pages. Brief discussions of the selection of model configuration variables are also included.

5.2 CONFIGURATION APPLICATION

This report deals with an axially symmetrical configuration, which is a 10-degree, half angle cone, with variations in nose bluntness ratios from 0 to 0.30. The particular conical configuration is representative of advanced ballistic re-entry vehicles and represents a relatively simple configuration to analyze. It also happens to be the identical configuration selected by the Supersonic Tunnel Association (STA) to provide a standard facility correlation model.

5.3 DESCRIPTION OF TEST MODELS

The 10-degree cone model configuration used in the LTV Hypervelocity Wind Tunnel, Figures 3 and 4 was designed and fabricated by the facility and their associated departments in the Vought Aeronautics Division of Ling-Temco-Vought, Inc. The model was 5.52 inches in length with the pivot center of gravity located at 54.9 percent of the model length from the nose. The model base diameter was approximately two inches. The shell of the model was machined from magnesium bar stock to a wall thickness of approximately 0.015 inches. This shell was bonded to the balance ring and to the loading cylinder at the base of the model. The combined sections resulted in an extremely strong, light weight structure.

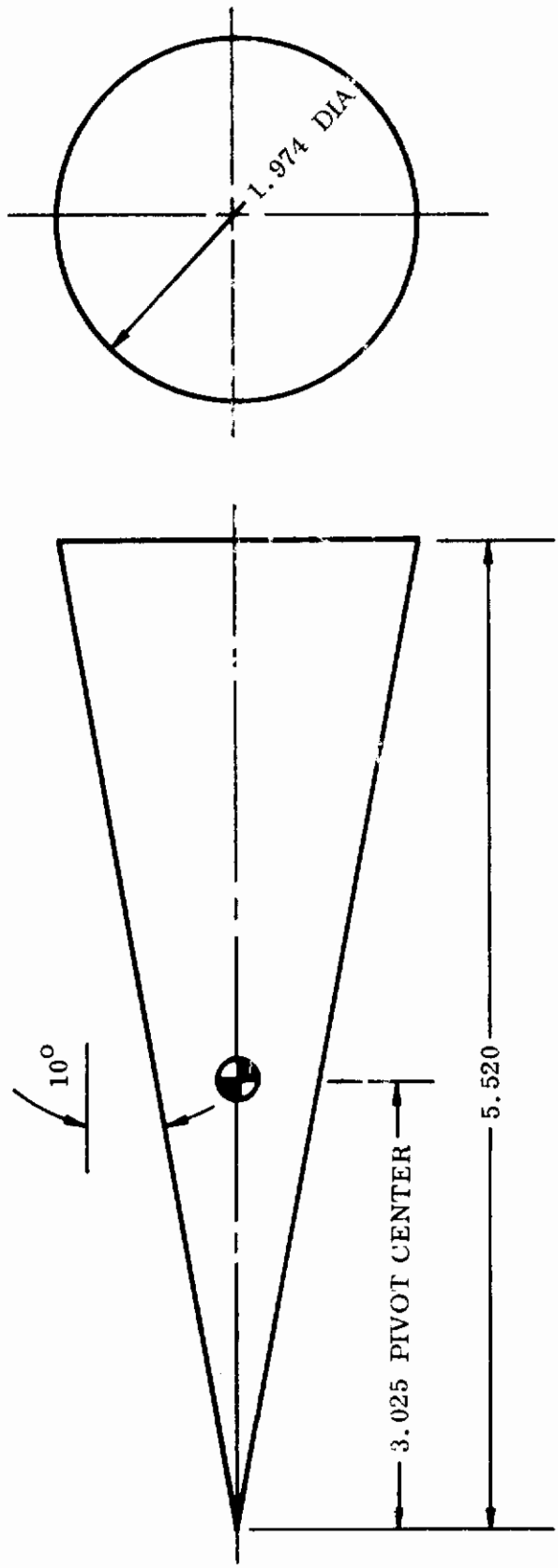

NOTE: ALL DIMENSIONS ARE IN INCHES

Figure 3. LTV Hypervelocity Wind Tunnel (10-Degree Cone Configuration)

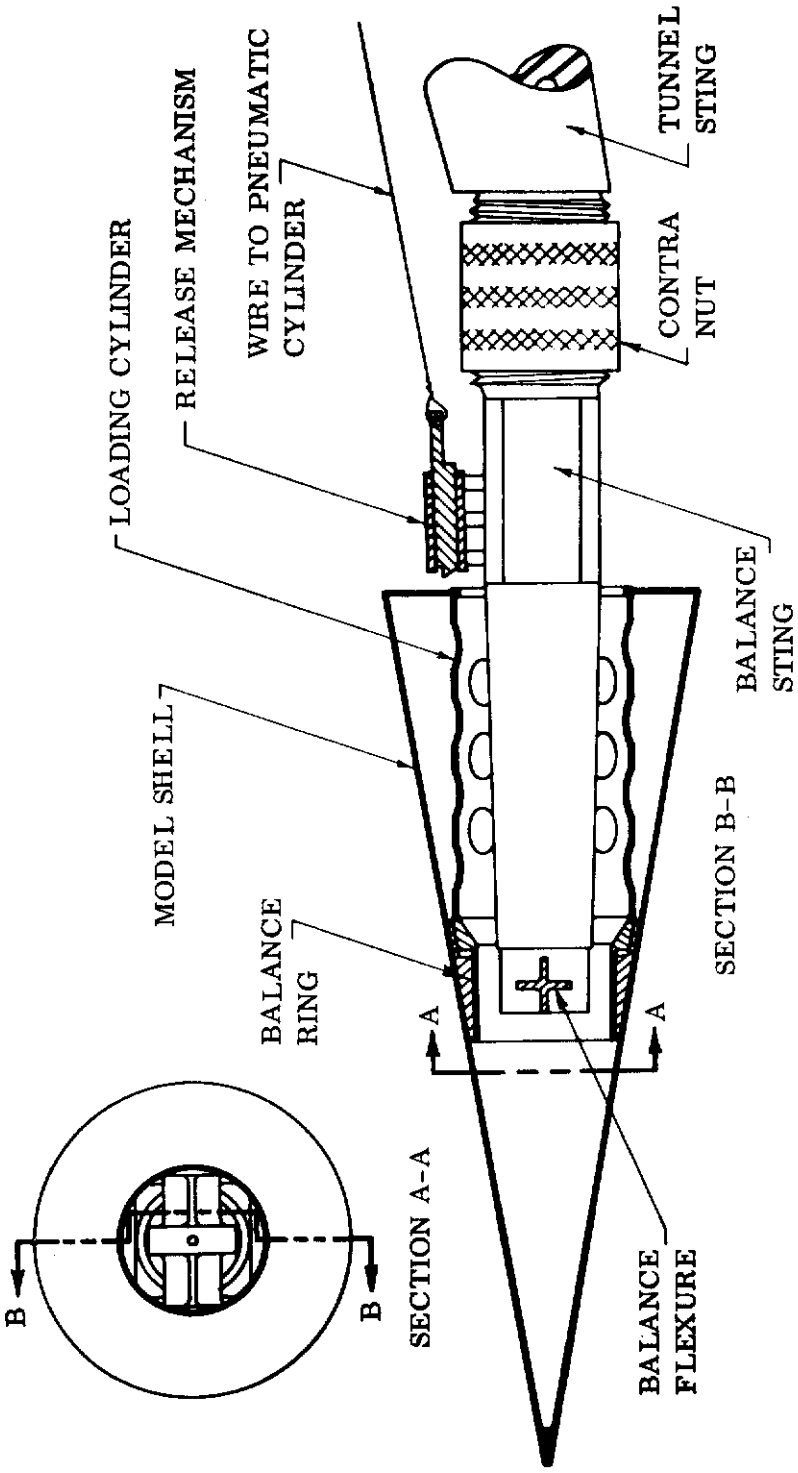

Figure 4. LTV Hypervelocity Wind Tunnel Dynamic Stability Model Construction and Installation Test 23 (10-Degree Cone Configuration)

The 10-degree half angle cone model utilized in the AEDC Tunnel C program, Figure 5, was fabricated of stainless steel by Micro Craft Inc., of Tullahoma, Tennessee, under subcontract from the General Electric Company. The model had interchangeable spherical noses for bluntness ratios of 0, 0.15 and 0.30 and adapters for variable pivot center locations of 50, 55, and 60 percent of the length for each bluntness. The model had a base diameter of about 10 inches and a conical length of 28.35 inches. Modifications were provided to enable model installation on the transverse rod support at the aft center of gravity location. The model had a 0.019-inch wall thickness to provide the minimum mass moment of inertia, and still maintain structural integrity against the loads and temperatures in the AEDC Tunnel C environment. Provisions were also included to add ballast at the nose and at the base of the model in order to adjust the static balance at each pivot center and to change the mass moment of inertia. Original design specifications had called for greater frequency range than was physically possible by adjusting the model moments of inertia. The limiting factors were a combination of maximum ballast and mass balancing, and the greatest frequency range was attained at the farthest aft pivot location, 60 percent L. Inasmuch as the frequency is inversely proportional to the square root of the moment of inertia, the frequency variation was very small for the free oscillation case. A large variation was obtained with the forced oscillation system by interchanging balances with flexures of different spring constants.

An additional 10-degree cone model was fabricated with a six-inch base diameter for the transverse rod support to investigate scaling and frequency effects on a small gas bearing balance in the AEDC Tunnel C. Unfortunately, balance problems were incurred during the tests which completely invalidated the results, and this portion of the experimental program was deleted.

5.4 SELECTION OF CONFIGURATION VARIABLES

5.4.1 Base Diameter

In most cases, the model base diameter and, therefore, the entire model scaling, is selected with respect to the size of the facility test section and to the capacity of the related test apparatus. The maximum model size was generally chosen in order to get the most aerodynamic contribution and, therefore, get the best performance out of the balances.

5.4.2 Center-of-Gravity-Locations

The specific center of gravity locations were selected primary because the range covers most typical values represented in flight vehicles. The 60-percent location was selected for the majority of the research work primarily in order to accommodate balance installations and static balancing requirements.

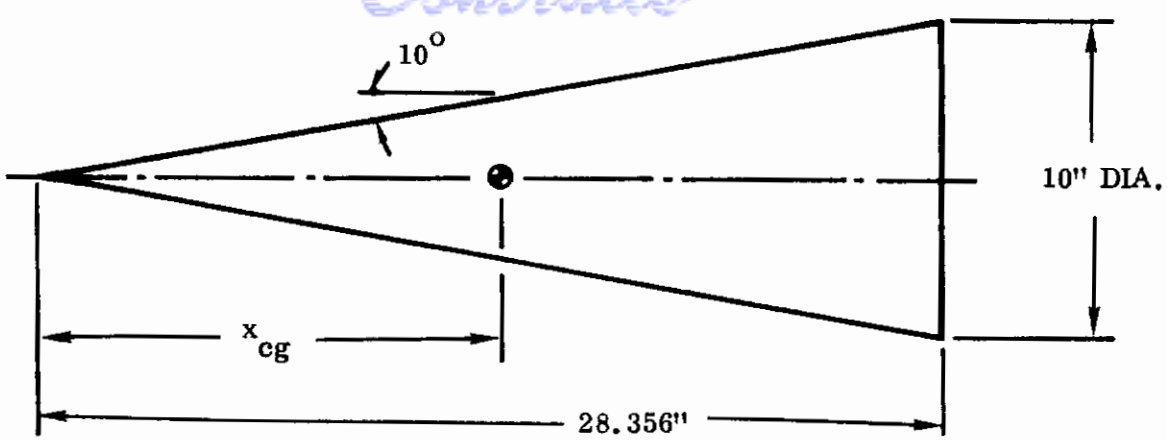

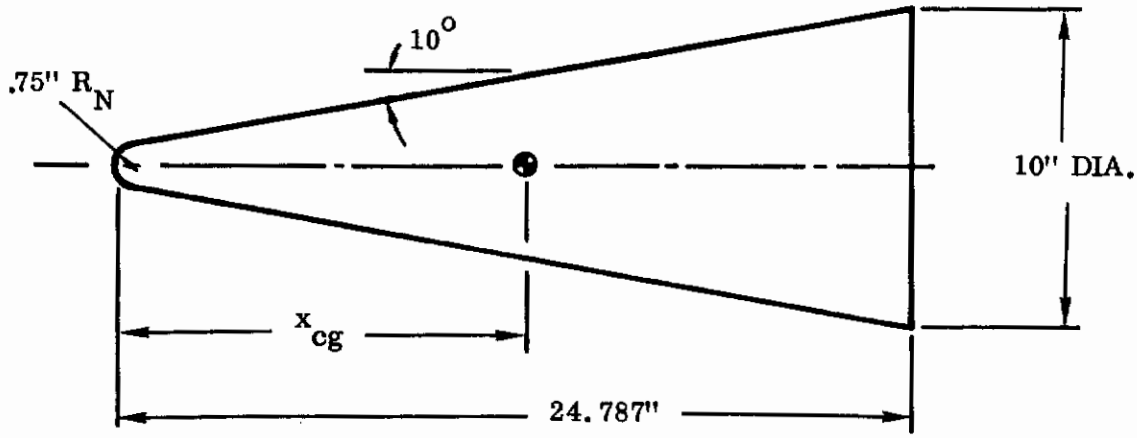

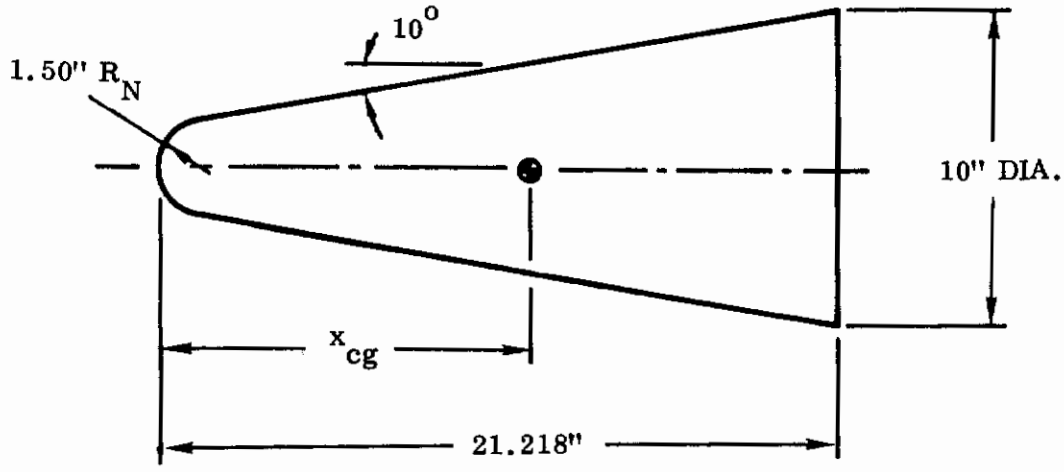

R_N/R_B	x_{cg} 50% L	55% L	60% L
0	14.178"	15.596"	17.014"
.15	12.389"	13.633"	14.882"
.30	10,609"	11.675"	12.731"

Figure 5. Model Configurations - AEDC Tunnel C

5.4.3 Nose Bluntness

The three nose bluntness ratios investigated cover a relatively large range and were selected to evaluate bluntness effects adequately without creating an over expanded program. The purpose was to evaluate a sharp cone and a blunt sphere cone and relate the variation between the two with an intermediate bluntness.

5.5 STATIC MASS BALANCING

5.5.1 Effects of Model Weight

Prior statements have implied that a minimum model weight is desired to obtain the most accurate data. Once the model is fabricated, weight usually must be added either in the nose or at the base to put the model in static equilibrium about the pivot. This is required so that the motion is not affected by any moment of inertia contributions due to mass eccentricity. If the weight and, therefore, the moment of inertia is kept to a minimum, the effect of aerodynamic damping on the model is easier to measure. In the case of high frequency oscillation on a flexure pivot, the structural damping represents the greater percentage of the total damping and will dictate the relative oscillation frequency. In that the damping derivatives to be derived from the test are directly proportional to the moment of inertia and to the measured aerodynamic damping, the level of aerodynamic damping is inversely proportional to the decrease in inertia. In the case of free oscillation on a gas bearing where the aerodynamic contribution is a high percentage of the total damping, the inertia must also be kept to a minimum. In this case, the purpose is to keep the frequency as high as possible to reduce tare damping, as discussed in Section 4.3.

5.5.2 Effects of Frequency

In all cases of dynamic oscillation, the frequency is determined by mass moment of inertia and viscous and mechanical restoring moments. The basic relationship is that the square of frequency varies directly with the sum of the viscous and mechanical restoring moments and inversely with the moment of inertia. For a given model shape and a given balance, then the frequency may be varied inversely with the square root of the moment of inertia. Rather large variations in moment of inertia are required to give a significant change in frequency.

5.6 DYNAMIC MASS BALANCING

The concept of dynamic mass balancing is neither as significant or as common as static balancing. Static balancing is mandatory while dynamic balancing is optional. The advantage of dynamic balancing is that it makes the model less susceptible to excitation by mechanical disturbances from the tunnel and support systems. In these particular tests, facility vibration was not transmitted to the model because of improved balance and sting design features. This type problem has been observed in previous experimental programs.

6. DATA REDUCTION

6.1 INTRODUCTION

Due to the nature of this type of an experimental study, the techniques used in obtaining, reducing, and presenting the data are extremely important. A realistic evaluation of the assumptions and errors involved in data measuring and data reduction is essential to the reliability of the information derived from the experimental program. In evaluating the data, the conservative approach, which is always justifiable in experimental verification, has been discarded in an effort to establish trends, correlations, and significant design criteria for perpetuating a growth in the understanding of dynamic stability. In this particular technological field, many aspects must apparently be derived from experimental research, and important contributions can only be made from a very thorough evaluation of the data and the techniques used to obtain the data.

The methods used in obtaining and reducing the data do vary slightly; however the underlying theory is basically the same and the results should be consistent. In the following pages, the techniques which were utilized in this program are described and discussed in detail. The discussion is directed primarily toward the analysis of one degree of freedom motion of "captive" models, and the application of these concepts in free flight is not necessarily justified.

6.2 DATA REDUCTION - FORCED OSCILLATION

6.2.1 Physical Interpretation of Technique

A forced oscillation technique basically relies on the measurement of the external torque input required to maintain an amplitude stabilized oscillation. Since the damping of the system is related directly to the energy dissipated per cycle, the damping can be defined by the energy required to compensate for the damping and maintain a constant amplitude of oscillation. In this case, the external force or moment is applied in resonance with the undamped natural frequency of the oscillating system.

6.2.2 Analytical Derivation of Technique

The basic equation of motion for an oscillating system with no external forces is:

$I\ddot{\theta} + D\dot{\theta} + K\theta = 0$, where I is the moment of inertia, D is the damping coefficient, K is the spring constant, and θ is the displacement, which in this case is amplitude. The one degree of freedom motion can be expressed also in terms of the externally applied force as follows:

$$I\ddot{\theta} - M_{\dot{\theta}}\dot{\theta} - M_{\theta}\theta = T \cos \omega t$$

For the specific case of steady oscillation, the inertia term, $I\ddot{\theta}$, and the restoring moment term, $M_{\theta}\theta$, are exactly balanced and the damping term, $M_{\dot{\theta}}\dot{\theta}$ becomes equal to the forcing term,

$$- M_{\dot{\theta}}\dot{\theta} = T \cos \omega t.$$

This equation reduces to the following form for resonance at the undamped natural frequency, and is evaluated at t = 0 seconds.

$$M_{\dot{\theta}}\theta_o = T/\omega \qquad\qquad M_{\dot{\theta}}\theta\omega = - T$$

The damping moment is therefore a function of the resultant torque input, amplitude, and frequency, all of which can be measured with a relatively high degree of accuracy. The aerodyanmic damping can then be evaluated from the difference between "wind-on" (total) damping and the "wind-off" (tare) damping.

6.2.3 Analysis of Assumptions

In forced oscillation testing the assumptions on which data reduction depends are:

1. Errors in torque input phasing are negligible.
2. Errors in amplitude stabilization are negligible.
3. Damping characteristics can be adequately subdivided into aerodynamic damping, structural damping, and environmentally induced structural damping.

The first assumption is simple and is considered valid. The forcing term is a function of the cosine of the phase angle, and therefore a very large phasing error would be required to create a significant change in the forcing term.

The validity of the second assumption relies on several factors, which include the level of torque input required, the turbulence of the flow in the tunnel, and the operator's ability to maintain amplitude stabilization while recording data. The torque input can be measured with a high degree of accuracy, but the assumption relies on matching the torque with the damping which varies from run to run. Therefore, error is induced by the flow characteristics in the tunnel and by the degree to which amplitude stabilization is not attained. These errors are not considered large, but are essentially indeterminate and could contribute to the overall accuracy of the data.

The validity of the third assumption appears to be the weak link in data reduction, however extensive calibrations and bench tests, etc., have been conducted to

define the various damping contributions. The assumption that "wind-on" damping less the "wind-off" damping (corrected for frequency effects) gives aerodynamic damping is a possible source of error. The integrated effects of frequency, aerodynamic loading, low pressure, temperature and model inertia on the balance readings are exceedingly difficult to determine for the "wind-on" condition. It should also be noted that some balance designs are more susceptible to these errors than others.

6.2.4 Aerodynamic Derivatives

The dynamic stability of a vehicle and the aerodynamic damping of oscillation are generally expressed in terms of derivatives. A derivative is basically defined as the local slope of the function describing the variation of a given reaction with a given translational or rotational coordinate or its time rate of change. Static derivatives are concerned with the variation of a given reaction with a displacement coordinate. Dynamic derivatives are concerned with the time derivative of a displacement coordinate. In the particular case of one degree of freedom oscillation about the pitch axis, the damping is expressed by the sum $C_{m_q} + C_{m_{\dot{\alpha}}}$. Generally, $C_{m_{\dot{\alpha}}}$ is significantly smaller than C_{m_q}, but the two damping components obtained in the wind tunnel are not separable.

6.2.5 Expression in Coefficient Form

The coefficient form of the aerodynamic damping moment is expressed in terms of the damping derivatives and is obtained from the following relationship.

$$C_{m_q} + C_{m_{\dot{\alpha}}} = M_{\dot{\theta}} \left[(2 V_\infty / q_\infty S L^2) \right]$$

which, in substituting for $M_{\dot{\theta}}$, becomes

$$C_{m_q} + C_{m_{\dot{\alpha}}} = - \frac{2 V_\infty}{q_\infty S L} \left[(T/\theta_\omega)_{Run} - (T/\theta_\omega)_{Tare} \right]$$

In this particular program, standard nomenclature has been designated to express C_{m_q} in terms of q L/2V, using base area and model length for reference.

6.2.6 Sources of Error

Possible sources of error in this particular technique are associated primarily with the evaluation of structural damping, as expressed in Section 4, and with the evaluation of the aerodynamic contribution to damping from "wind-on" and "wind-off" conditions.

In forced oscillation testing there are errors present in the data outputs which may or may not be totally compensated for in the final evaluation. Balance calibrations generally are made to account for the effects of axial and normal loading, frequency variations, amplitude variations, temperature variations and pressure on strain gage readings. Based on the calibrations, estimated maximum error in the data is presented in Figure 6 for the AEDC forced oscillation tests. Repeated data indicate these tolerances do not represent the total source of error in the measurements, and additional errors may be expected from general tunnel turbulence, amplitude stabilization, and from possible aerodynamic and mechanical interference effects. Many of these errors are unpredictable and indeterminate.

6.2.7 Tolerances Placed on Data

Tolerances placed on the data obtained using this technique are shown in Figure 6. These estimates were derived by the facility from an evaluation of changes in calibration factors in both bench and tunnel tests of structural damping characteristics and transducer measurements of model displacement and torque input. Resulting errors in either parameter were within ±1 percent of the maximum values of the range in which each parameter was measured.

Based on the repeatability and the correlations of the data, the total induced error in the data is expected to be considerably greater than the errors derived from calibration tests. Primary sources of these errors are most probably aerodynamic and mechanical interference effects as described in Section 4.6. In this respect, tolerances are functions of several variables which are not entirely definable at present, and it should be understood that these tolerances do exist in addition to those expressed for balance calibrations.

6.2.8 Limitations in Use of the Data

The use of wind tunnel data in predicting flight characteristics is essential to the aerodynamicist, especially in the case of hypersonic dynamic stability, which is influenced by many environmental variables. Wind tunnel results represent a consolidation of these variables, some of which simulate flight conditions and some of which do not. Hopefully, the aerodynamicist manipulates the data and extrapolates

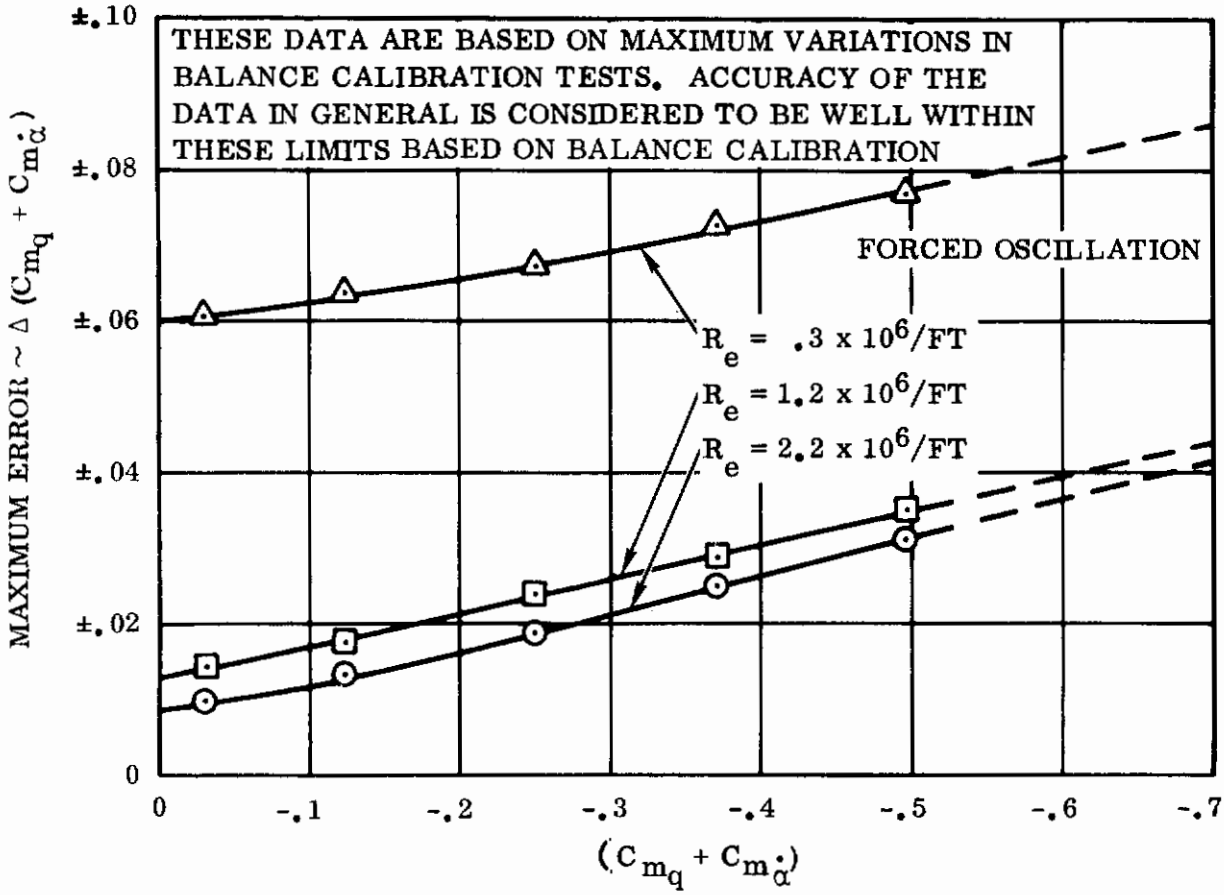

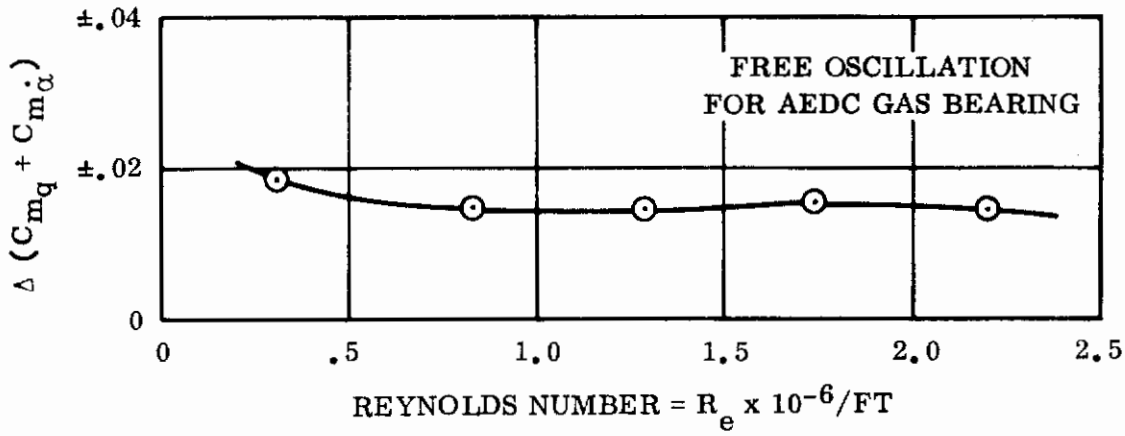

Figure 6. Estimated Maximum Error in $C_{m_q} + C_{m_{\dot{\alpha}}}$

the results to match the flight environment. In the specific case of hypersonic dynamic stability, available data indicate that a much greater technical understanding must be achieved before adequate predictions of flight characteristics may be generated from wind tunnel results. Wind tunnel results always suffer from a number of unknown effects, such as uncertainties in corrections to the data due to tare and interference effects. The most significant contributions of available wind tunnel data are not necessarily the level of damping, which may be grossly in error, but the trends in the data with many geometric and environmental variables. Any flight predictions based on experimental results with the present state-of-the-art should be clearly qualified as to the degree of simulation and the techniques used.

In the case of forced oscillation testing, results generated in the program provide some excellent data on the trends in damping characteristics with geometric variables such as nose bluntness and pivot location. Reynolds number effects are also considered excellent in a range which encompasses boundary layer transition from laminar to turbulent flow, however, trends in the data indicate that extrapolations are impossible with these data. Oscillation frequency effects as demonstrated by these data are possibly biased by alterations in testing apparatus. Also variations in the data with angle of attack appear to be biased either by the oscillation frequency or most probably by the balance stiffness on which frequency depends.

Therefore, the use of these results should be restricted to the effects of geometric variables and the effects of Reynolds number in the designated range. Also extrapolations of these trends would not be recommended without adequate supporting information. The angle of attack effects and frequency effects would require further verification if they should be used for performance predictions.

6.3 DATA REDUCTION - FREE OSCILLATION

6.3.1 Degree of Structural Damping

Probably the most important consideration in discussing free oscillation techniques is the degree of structural damping for a particular test. In the two cases of sting mounted free oscillation testing conducted on this program, the tare damping varied from essentially zero in the gas bearing tests, to as high as 75 percent of the total damping in the high frequency, flexure tests. As expressed in Section 4, the accuracy and reliability of the measurements is primarily a function of tare damping. When aerodynamic damping is a small portion of total damping, the measurement of a difference in an amplitude decay between "wind-on" and "wind-off" becomes exceedingly difficult. Under these circumstances, a quantitative evaluation of several repeat runs is essential to establish the consistency and reliability of the data.

6.3.2 Physical Interpretation of Technique

In direct contrast to the forced oscillation technique, the aerodynamic damping is determined from measurements of the rate of change in oscillation amplitude. No external energy is added to the system, and a combination of the aerodynamic and structure restoring moments cause a dissipation of the energy of the system in the form of amplitude decay. By evaluating the rate of amplitude decay contributed directly to aerodynamic forces, the dynamic damping may be determined.

6.3.3 Analytical Derivation of Technique

In the case of free oscillation, the analysis of damping is also derived from the basic equation of motion for an oscillating system.

$$I\ddot{\theta} + D\dot{\theta} + K\theta = 0$$

The roots of the characteristic equation for motion, in which D equals $-M_{\dot{\theta}}$ and K equals $-M_{\theta}$, are

$$\frac{M_{\dot{\theta}}}{2I} \pm i\sqrt{-\frac{M_{\theta}}{I} - \left(\frac{M_{\dot{\theta}}}{2I}\right)^2}$$

From this pair of complex roots, a solution of the equation can be written as follows, assuming max. amplitude at $t = 0$ to evaluate the arbitrary constants

$$\theta = \theta_o\, e^{(M_{\dot{\theta}}/2I)t} \cos\sqrt{-\frac{M_{\theta}}{I} - \left(\frac{M_{\dot{\theta}}}{2I}\right)^2} \cdot t$$

This solution demonstrates that for a freely oscillating body, the amplitude decay varies exponentially with time. The solution to the above equation for the damping term, $M_{\dot{\theta}}$ in terms of the amplitude ratio θ/θ_o when evaluated at maximum conditions, becomes

$$\ln(\theta_2/\theta_1) = (M_{\dot{\theta}}/2I)(t_2 - t_1)$$

but the change in time, $t_2 - t_1$, can be expressed as the number of cycles analyzed divided by the frequency of oscillation, $\Delta t = N/f$, therefore

$$\ln(\theta_2/\theta_1) = (M_{\dot{\theta}}/2I)(N/f)$$

which shows that the damping is determined directly from measurements of oscillation frequency, amplitude decay, and model mass moment of inertia.

$$M_{\dot{\theta}} = \frac{2If}{N}\ln(\theta_2/\theta_1)$$

The aerodynamic damping is determined from the difference obtained in $M_{\dot{\theta}}$ for "wind-on" and "wind-off" conditions. In the specific case of measurements with a gas bearing, the value of M_{θ} for wind off conditions is often insignificant in comparison with "wind-on" conditions and may be neglected.

The static aerodynamic moment can be derived also from an analysis of the frequency and the mass moment of inertia. Inasmuch as the spring constant term, M_{θ}, is essentially equal to $I\omega^2$, the aerodynamic contribution, m_{α}, may be determined from the difference in the squares of measured frequency from "wind-off" to "wind-on" conditions.

$$m_{\alpha} = I\left(\omega^2_{\text{Total}} - \omega^2_{\text{Tare}}\right)$$

6.3.4 Analysis of Assumptions

The preceding technique derivation is based on the assumptions that the system is statically stable and that the damping is less than critical. These assumptions imply that an oscillatory motion, either divergent or convergent, must be present. The assumption that the system is statically stable while pivoted at 50, 55, and 60% L, is supported by theory and experimental data and is considered valid. The assumption that damping is less than critical is imposed on the derivation by introducing imaginary parts in the roots of the characteristic equation and is confirmed experimentally by oscillatory motion. Neglecting any tare damping effects, it would appear that both these basic assumptions are valid.

6.3.5 Aerodynamic Derivatives

The significance of the aerodynamic derivatives in free oscillation testing would be the same as in forced oscillation testing, expressed in Section 6.2.4.

6.3.6 Expression in Coefficient Form

The expression of aerodynamic damping in coefficient form for free oscillation testing is basically identical to that for forced oscillation as shown in Section 6.2.5.

$$C_{m_q} + C_{m_{\dot{\alpha}}} = M_{\dot{\theta}}\left[2V_{\infty}/(q_{\infty} S L^2)\right]$$

The only difference lies in the expression of the damping moment, $M_{\dot{\theta}}$, which gives the following equation:

$$C_{m_q} + C_{m_{\dot{\alpha}}} = \frac{-4IV_{\infty}\omega}{q_{\infty} S L^2}\left[\left(\ln\frac{\theta_o}{\theta}\right)_{\text{RUN}} - \left(\ln\frac{\theta_o}{\theta}\right)_{\text{TARE}}\right]$$

As in the case of forced oscillation, coefficients are expressed in term of $q_\infty L/2V$, model base area, and model length.

6.3.7 Sources of Error

The sources of error incurred in free oscillation testing are derived from accuracies in measuring tare damping, peak amplitudes, model moments of inertia, and oscillation frequency. The errors involved in measuring tare damping are generally accounted for and were discussed in Section 4. Neglecting these effects of tare damping as a source of error, the accuracy in measurements of peak amplitudes is the primary concern. From these measurements, the amplitude ratio is determined and if the damping is small in the case of cones, this ratio approaches 1.0. Any small errors in the evaluation of this ratio are greatly magnified when taking the logarithm of a number approaching 1.0. . and therefore the data are very susceptible to amplitude measurement accuracies especially at small oscillation amplitudes or when the damping is nearly neutral.

Measurements of model moments of inertia and oscillation frequencies are determined in bench tests using a known structural spring constant. A possible source of error is the effect of oscillation frequency and loading on the calibration spring. If these effects are not adequately accounted for in calibrations of the spring constant, an error in the measured moments of inertia may be incurred. In general oscillation frequencies can be measured extremely accurately, and neglecting any significant loading effects the change in oscillation frequency from wind-off to wind-on conditions can be used to determine the average static moment derivative. If the static moment derivatives compare with known values, it may be assumed that mass moments of inertia have been adequately determined. Such a comparison for the AEDC Tunnel C data is shown in Figure 7, and Figure 8 for both the free and forced oscillation data.

6.3.8 Tolerances Placed on Data

Tolerances placed on the data obtained with gas bearing balances are shown in Figure 6. These estimates were derived by the facility from an evaluation of the changes in calibration factors in bench and tunnel tests. Calibrations of a variable reluctance angular transducer, which measures the angular displacement in the gas bearing balance and of tare damping were used to evaluate maximum deviations in an effort to estimate tolerances on the data. Tolerances placed on data obtained in the LTV hypervelocity tunnel are obtained by means of a statistical analysis for deviations from the mean of the quantitative results.

An example of the statistical analysis used in the Chance Vought data may be found in Reference 14. This analysis shows that for a given run, 60% of 18 data

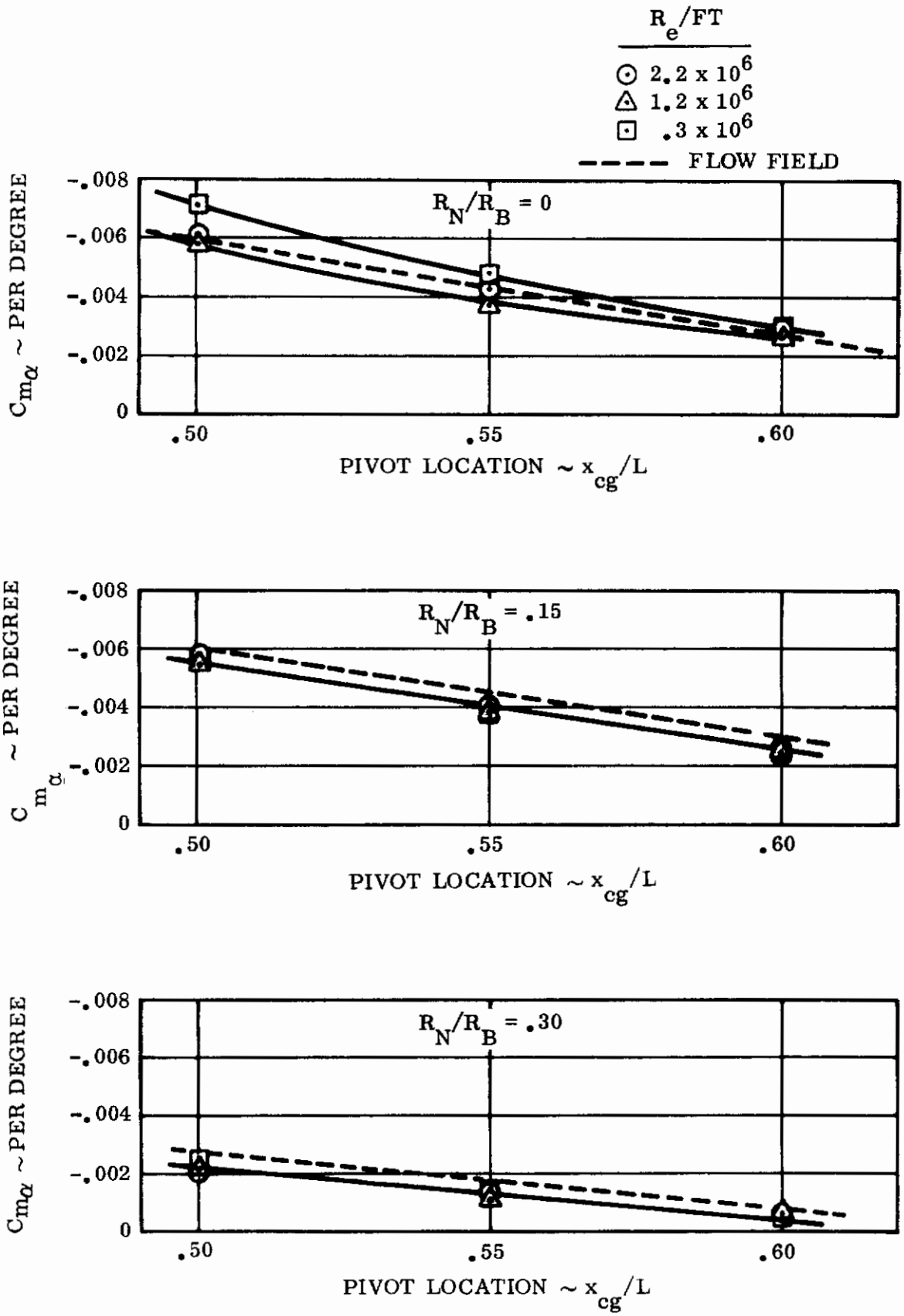

Figure 7. Pitching Moment Coefficient Slope vs Pivot (Center of Gravity) Location ($\alpha = 0^o$)

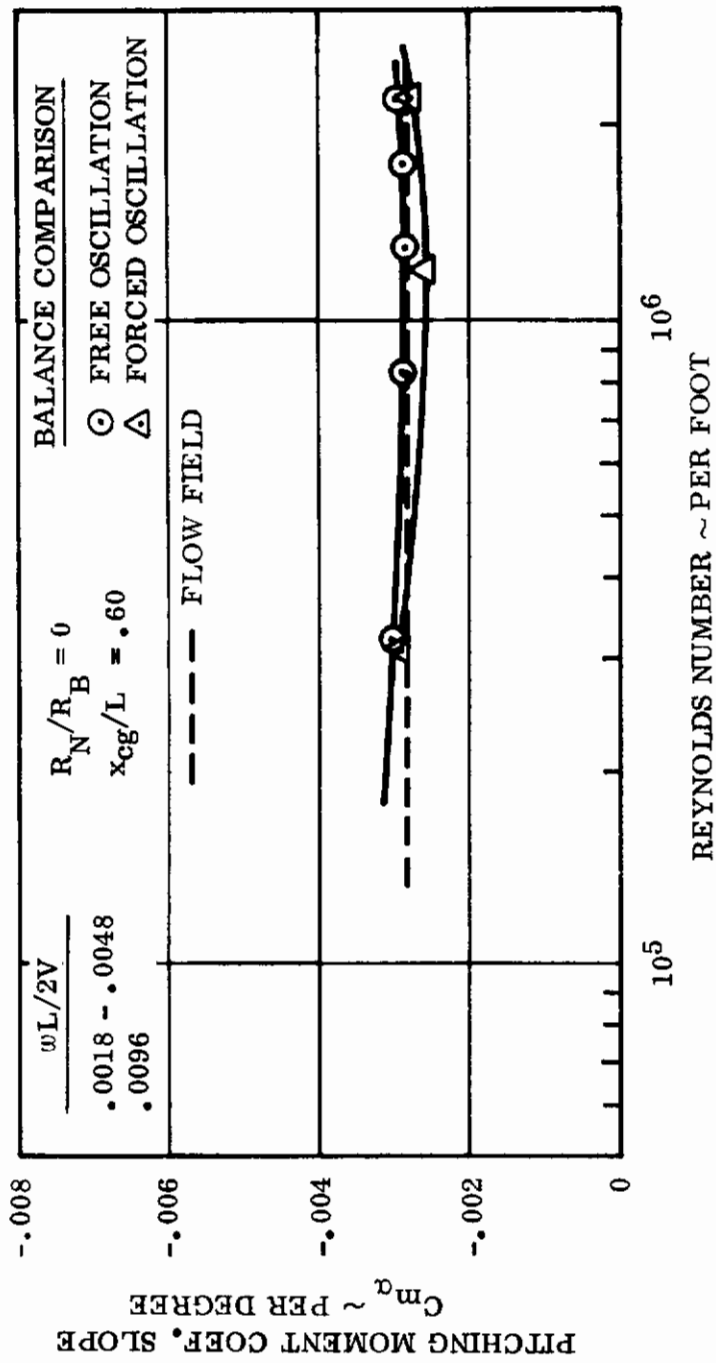

Figure 8. Pitching Moment Coefficient Slope vs Reynold's Number

points fall within a ±10% tolerance band, 70% within a ±20% tolerance band, and 100% fall with a ±50% tolerance band. These tolerances may be attributed primarily to the difficulty in measuring peak amplitudes and to perturbations in the amplitude decay due to tunnel flow characteristics. Additional unknown tolerances would also be required to account for induced errors involved in measuring structural damping; however, the significant problem in this type facility is measuring amplitude decay.

The AEDC free oscillation data show the characteristic damping over a much larger range of amplitude decay than is obtained in the LTV Hot Shot Facility. This permits a much more exact measurement of the amplitude ratio, especially if the amplitude decay may be attributed solely to aerodynamic damping. Assuming that frequency effects are negligible, which is not necessarily true, Figure 6 demonstrates that the results are repeatable within 10%. Reference 15 also demonstrates that the AEDC free oscillation data is highly repeatable using a transverse rod support. Tolerances placed on the data by calibration tests, from Figure 9, range from about 3% to 6%. Tolerances between 5% and 10% appear more reasonable, but are considered good.

6.3.9 Limitations in Use of Data

Most of the statements made on the limitations in the use of the data expressed in Section 6.2.8 for forced oscillation will also apply for free oscillation. Inasmuch as the forced oscillation technique was used to generate most of the data on the effects of both geometric and environmental variables, the primary objective of the free oscillation tests was to correlate the testing techniques and facilities. It is generally accepted that the level of aerodynamic damping is more accurately determined using a free oscillation gas-bearing-balance because of negligible structural damping. With essentially no structural damping, the aerodynamic moments are easier to measure and there is less probable error induced through tare calibrations.

Therefore, free oscillation data obtained from a system with negligible structural damping should represent the best available estimate for a level in damping. These results should be used as a measure of the other ground test capabilities, but should not be used for flight estimates without adequate qualification as to the degree of simulation.

6.4 TECHNIQUE COMPARISONS - DATA CORRELATIONS

In some cases, the AEDC free and forced oscillation techniques can be compared by means of correlations of the data when overlapping or nearly overlapping environmental conditions were obtained. Initial reaction to these correlations is that they should demonstrate conclusively any discrepancies between the two techniques. Overlapping variables include frequency and angular displacement.

$R_N/R_B = 0$

$X_{cg}/L = .60$

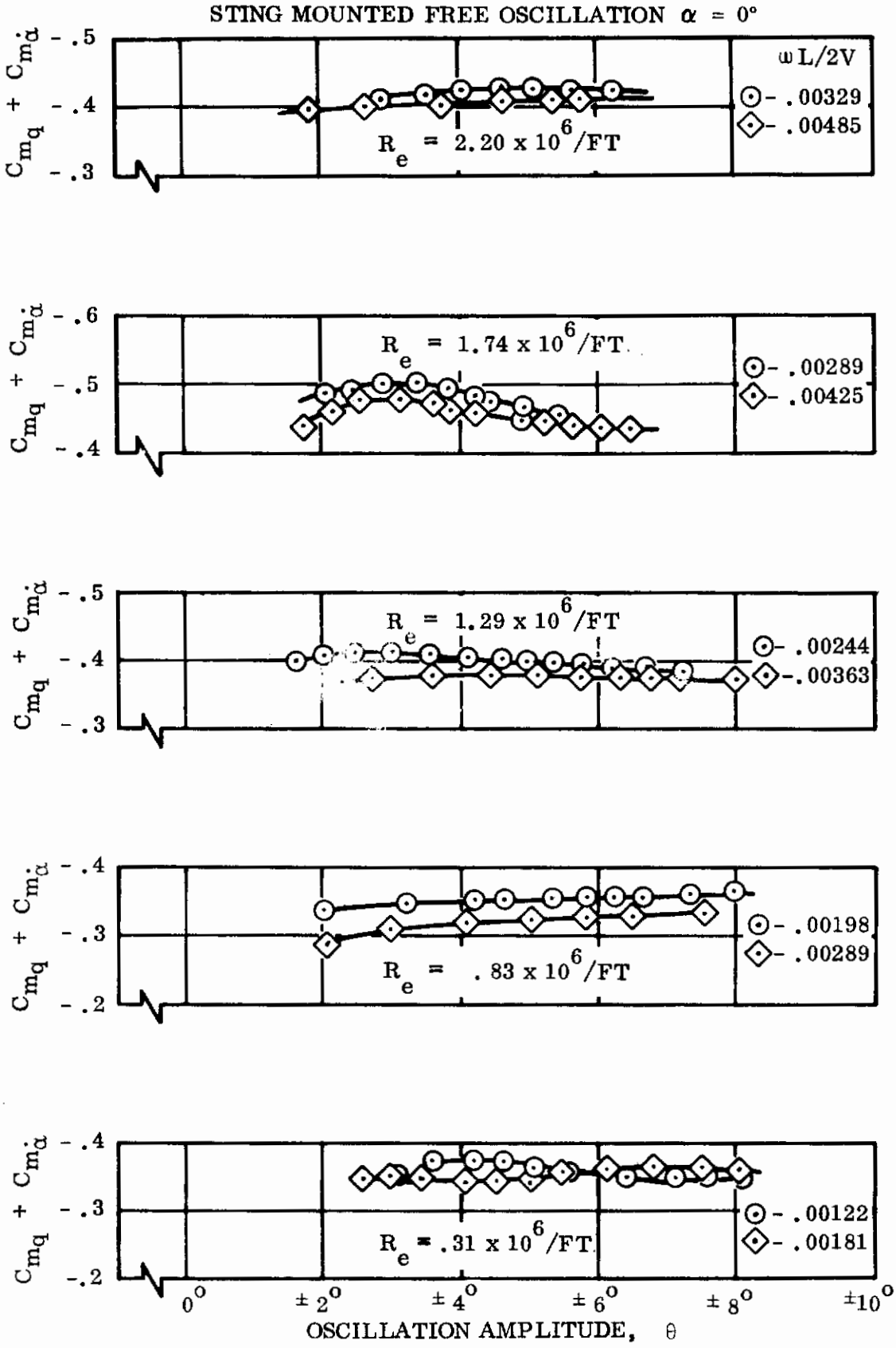

Figure 9. Pitch Damping Variation with Amplitude

Using an identical model configuration and the same flow conditions, a comparison is made for ±2° oscillations at zero angle of attack as a function of frequency. These correlations are shown in Figures 10, 11, and 12 for three flow conditions. The results show that for a sharp 10° cone pivoted at 60% L, there is not an adequate correlation in damping characteristics for the two techniques. A lack of repeatability in the forced oscillation data, as observed in Figures 10 and 11, implies that inconsistencies may be traced to balance problems incurred using this technique with high moments of inertia to reduce the oscillation frequency. It should also be noted that free oscillation data become increasingly more difficult to evaluate as the oscillation amplitude is reduced, and that at ±2°, the validity of the correlation may be questionable.

Another technique correlation is presented in terms of angular displacement or combined amplitude and angle of attack. This type of correlation depends on the linearity of aerodynamic characteristics, which, for a 10° sharp cone, should be valid. The results are shown in Figures 13 and 14, and are consistent with the frequency correlations, demonstrating slightly higher damping measurements with the forced oscillation technique. Most significant discrepancies are apparent at high Reynolds numbers, which implies that flexure balance problems may be induced under the relatively large aerodynamic loading conditions. Figure 15 shows a similar correlation for 10° sphere cone with bluntness ratio of 0.15. A greater discrepancy would be expected due to the non-linearity in aerodynamic characteristics, but the correlation is exceedingly better than that for the cone. With the higher bluntness ratio, normal loads and restoring moments are considerably less than those for the cone. Although aerodynamic loading and moment cross coupling effects were considered in balance calibrations, as discussed in Sections 4.2, 4.3 and 4.5, the results appear to indicate that these effects may be underestimated with cross-flexure balances.

In general, data correlations on technique comparisons are not good. The lack of correlation is sufficient to warrant a thorough evaluation of testing techniques as well as balance calibration techniques. Any advancements in the state of the art will rely heavily on the ability to evaluate the effects which bias data measurements and to compensate for them. Data correlations in terms of oscillation frequency and Reynolds number, the two major environmental variables, become meaningless when the accuracy of the measurements is biased by these same variables.

6.5 STANDARDIZED DATA PRESENTATION

The presentation of dynamic stability data has never been entirely consistent throughout experimental facilities, and efforts are being made to standardize the nomenclature by the STA. The misinterpretation of dynamic stability data is not unusual when the nomenclature varies from presentation to presentation. Universal adherence to standard methods of description and presentation in defining dynamic stability criteria will be very beneficial to progress.

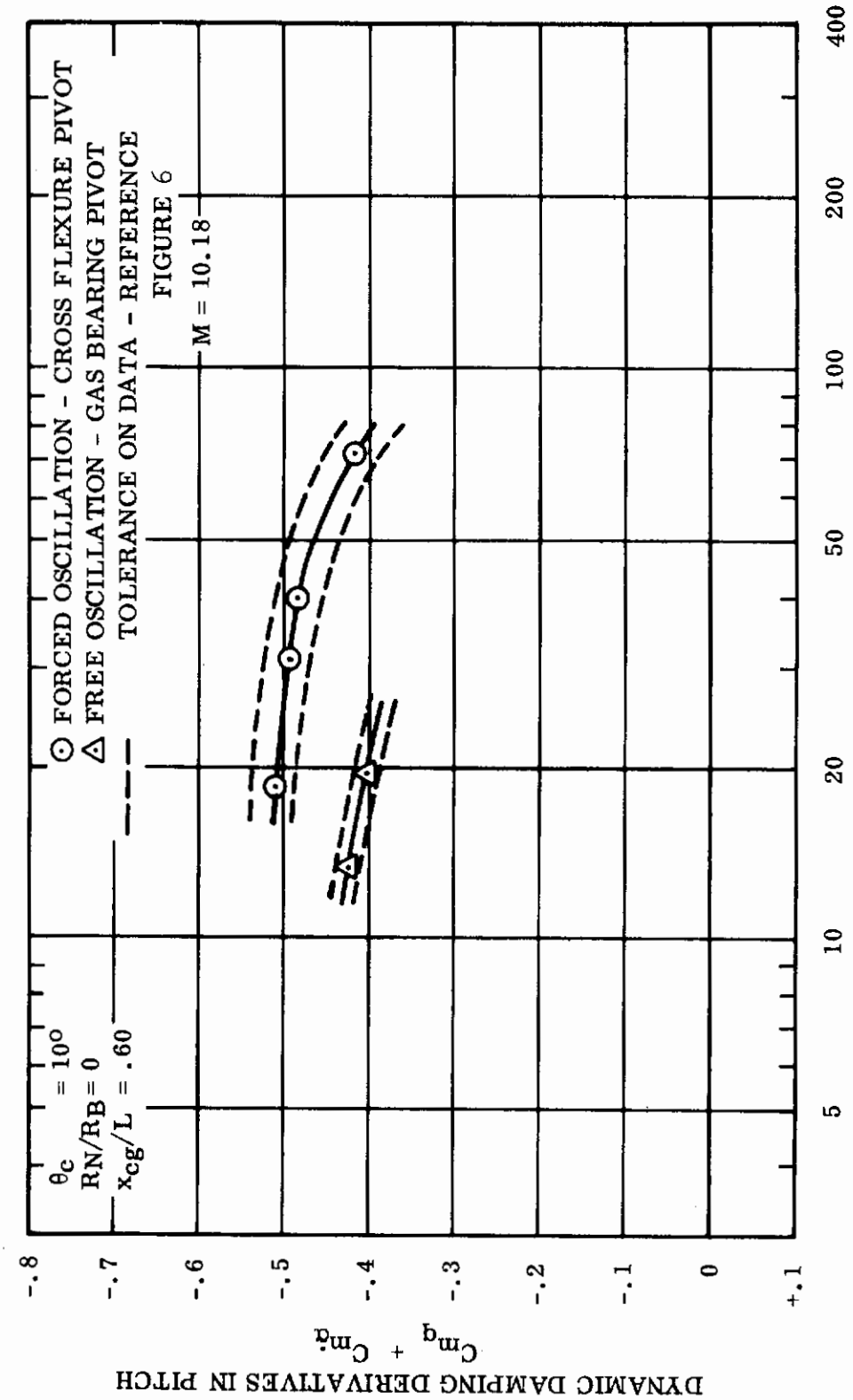

Figure 10. Comparison of AEDC Testing Techniques at $R_e = 2.2 \times 10^6$/ Foot

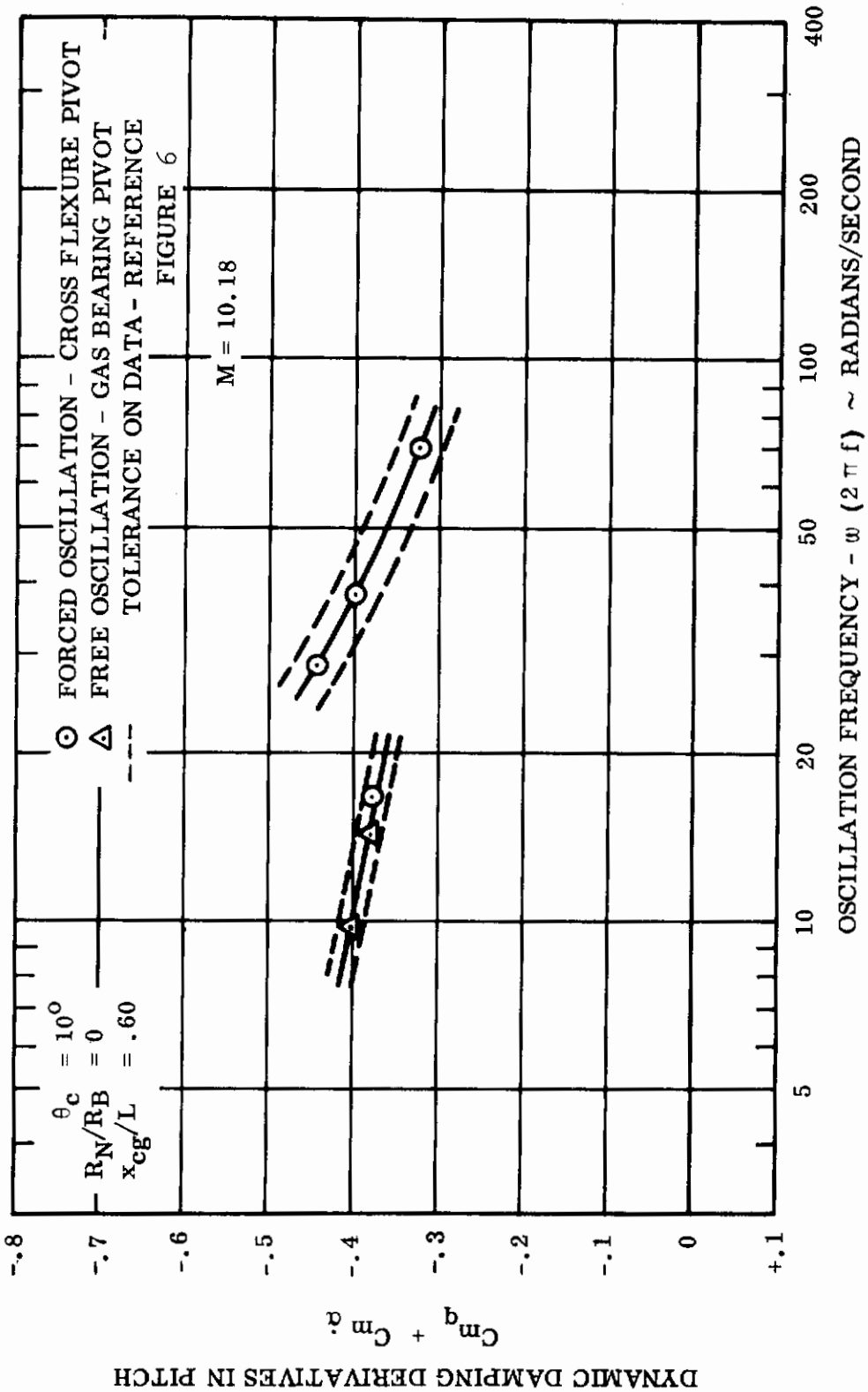

Figure 11. Comparison of AEDC Testing Techniques at $R_e = 1.2 \times 10^6$/Foot

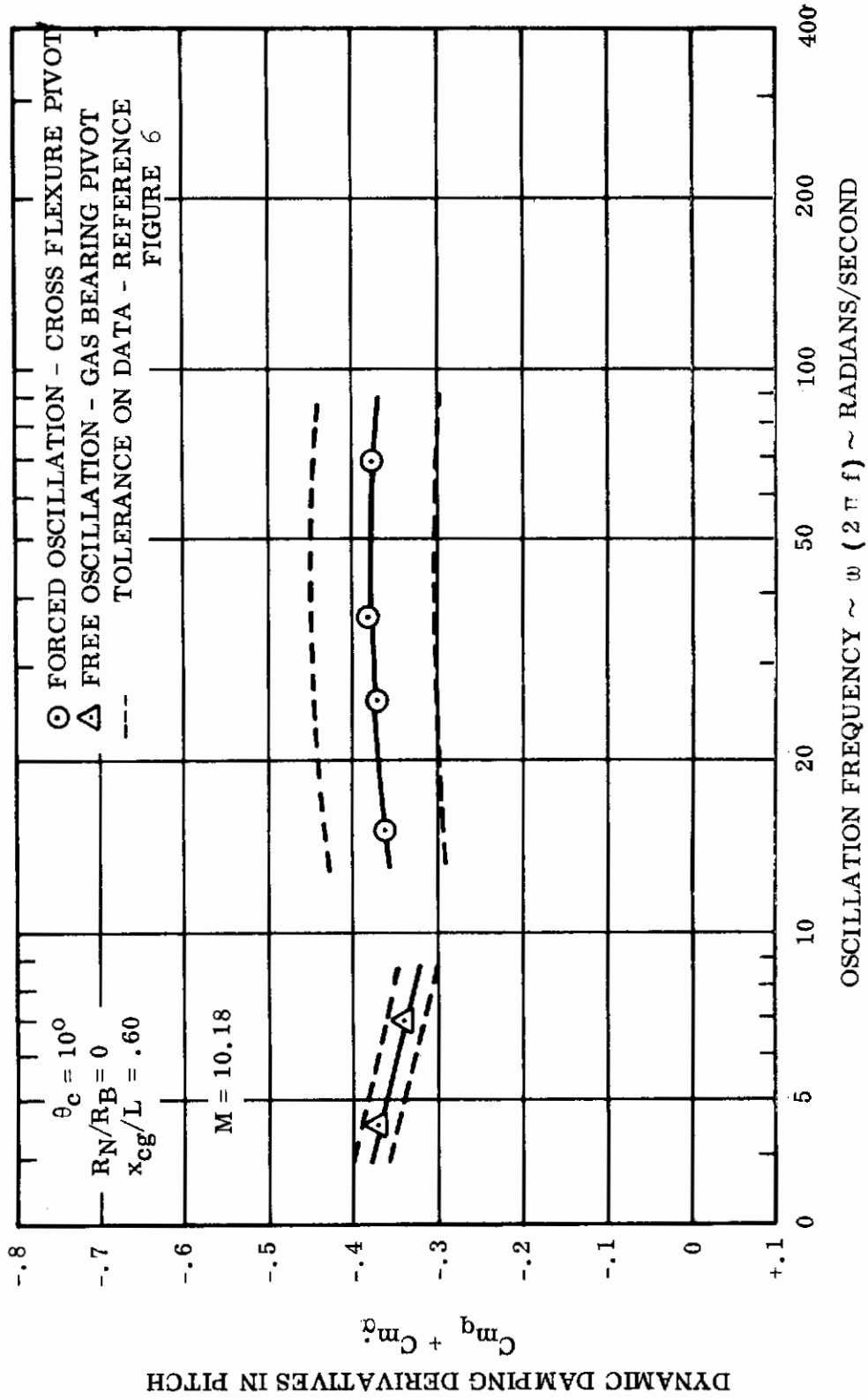

Figure 12. Comparison of AEDC Testing Techniques at $R_e = .3 \times 10^6$/ Foot

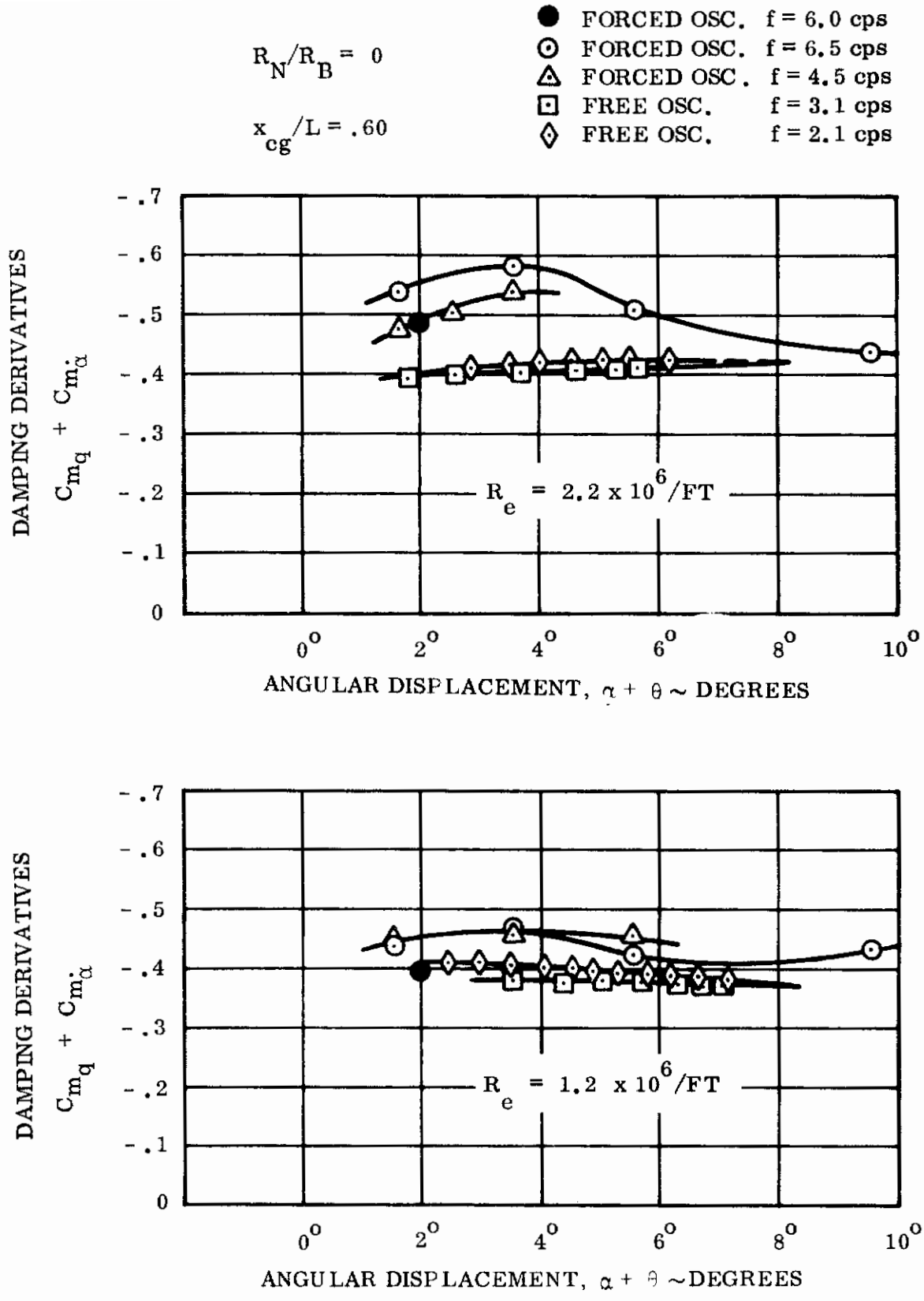

Figure 13. Amplitude/Angle of Attack Correlation

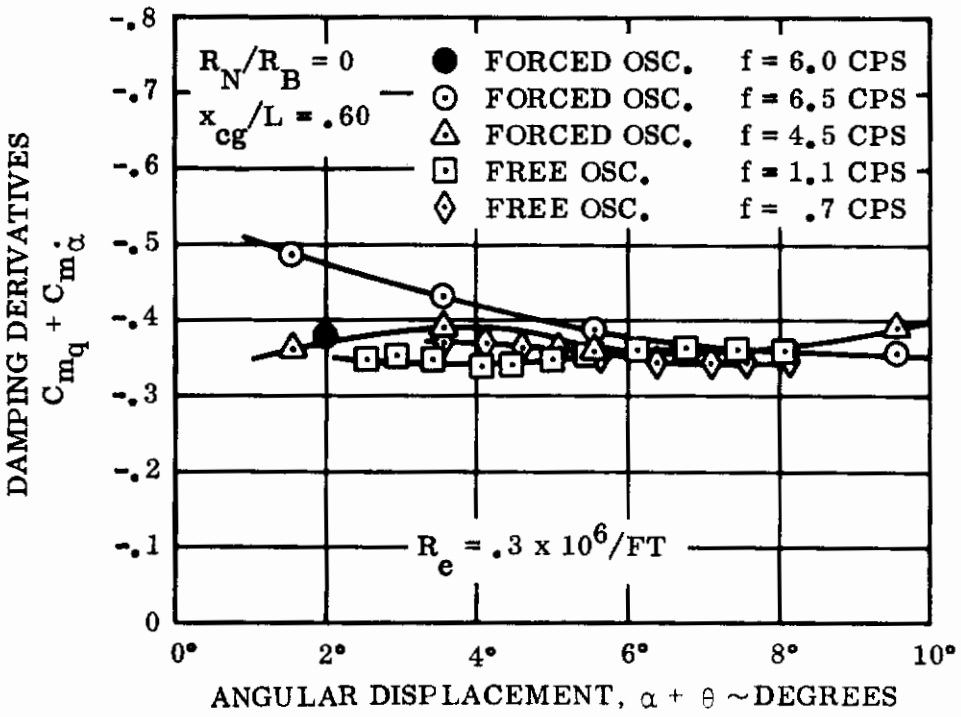

Figure 14. Amplitude/Angle of Attack Correlation

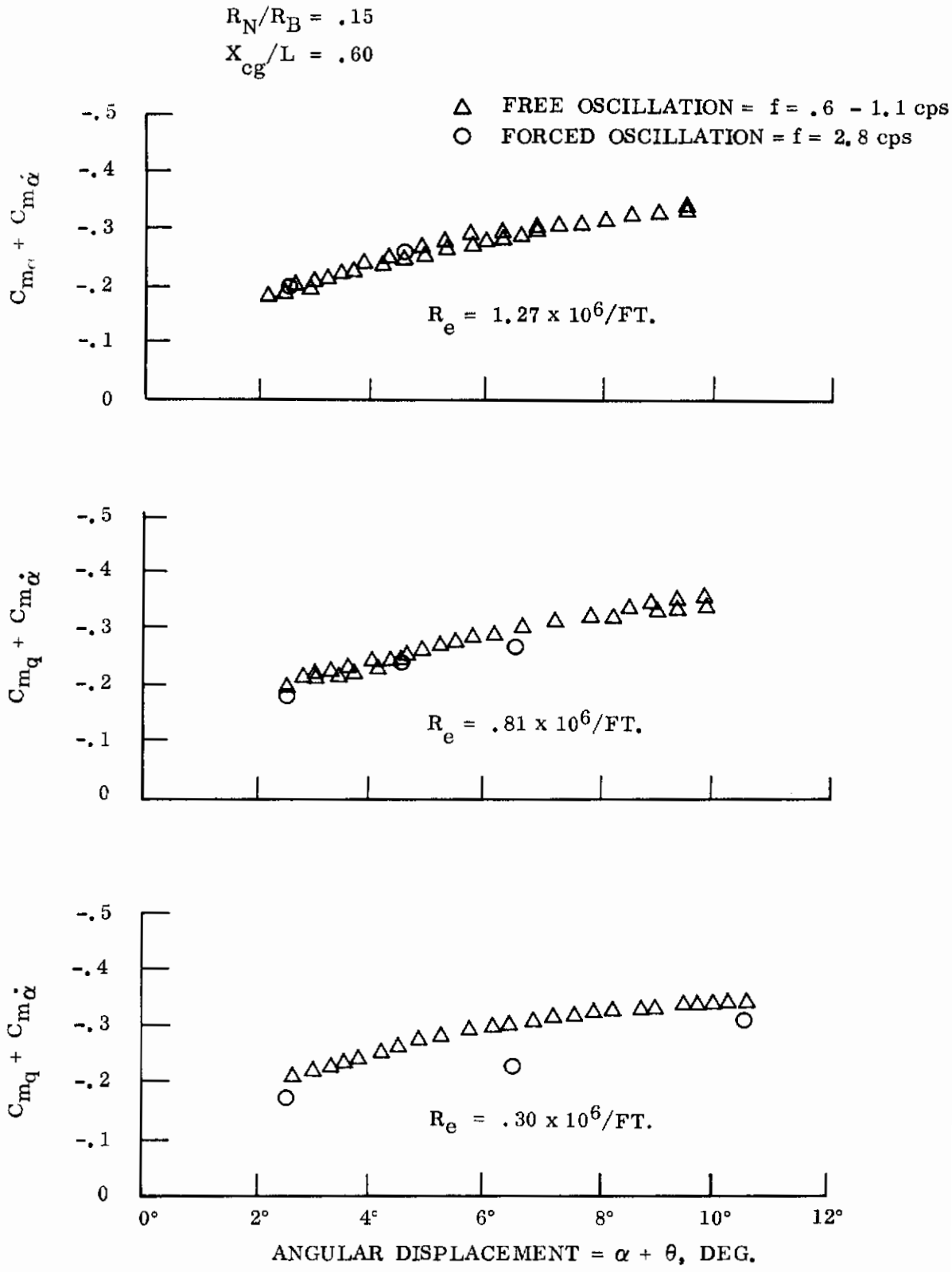

Figure 15. Amplitude/Angle of Attack Correlation

6.6 INTERPRETATION OF DATA

An interpretation of the data obtained in this program from the standpoint of data measurement and reduction is that, in general, the trends are significant; the absolute level of measured damping is questionable but within expected design tolerances; and effects of environmental variables can be investigated more thoroughly as capabilities are extended.

In the particular case of forced oscillation data, the level of damping appears to be questionable as a result of data correlations and repeatability, however the trends in the data appear to be consistent with other techniques and with theory. Analyses of data reduction techniques illustrate the susceptibility of data to errors incurred from measurement of tare damping. Other sources of error are also inferred in measuring damping data, which may or may not be significant depending on the requirements placed on interpretations of the results.

7. EXPERIMENTAL RESULTS

7.1 INTRODUCTION

The presentation of experimental data obtained on the 10-degree half-angle cone in support of this program is contained in the illustrations in this section. Data correlations which tend to demonstrate the significant trends and the comparisons between facility environments and techniques are attempted. The effects of geometric variables are explored primarily to evaluate the validity of theorectical estimates of dynamic damping relating a specific geometry to a general hypersonic flow field. The effects of environmental variables are explored to determine which parameters are significant in defining hypersonic dynamic stability and to provide a means of extrapolating the data to flight conditions. Each of these objectives represent significant contributions to technological understanding of hypersonic dynamic stability. The degree to which they are attained is expressed in Section 9.

7.2 DATA CORRELATIONS

Correlations of the data from this experimental program are discussed here. Correlations from other available data sources are discussed in Section 8, overall conclusions on these correlations are discussed in Section 9.

Attempts have been made to correlate the AEDC data and the LTV data without any significant results. Correlation parameters which have been investigated encompass variations in oscillation frequency, ω; reduced frequency; $\omega L/2V$; Mach number, M; and Reynolds number Re_L. Computer program analyses (GE Data Transformation and Multiple Regression Programs) could not produce an adequate correlation using these data and the appropriate simulation variables. Trends in the data indicate consistent variations with frequency and Reynolds number, which would imply a correlation, but these trends may be attributable to a bias in the data due to data measurement and reduction techniques as discussed in Section 6.4. Also, the effects of base pressure, sting interference, and wake expansion as discussed in Section 4.6 were not considered in the data correlations and could have a very significant effect on the results.

Typical examples of the more obvious correlations are shown in Figures 16 and 17. Figure 16 demonstrates the variations in damping characteristics with reduced frequency. The data obviously do not correlate as a function of reduced frequency alone, but the trends do imply a reduction in stability with increasing frequency. Also, this trend would appear consistent within the AEDC Tunnel C and LTV correlation. Lines faired through the data represent constant Reynolds numbers with varying frequency and suggest a viscous effect on damping. The damping derivatives are nondimensionalized by the theoretical flow field prediction so that Mach number and pivot

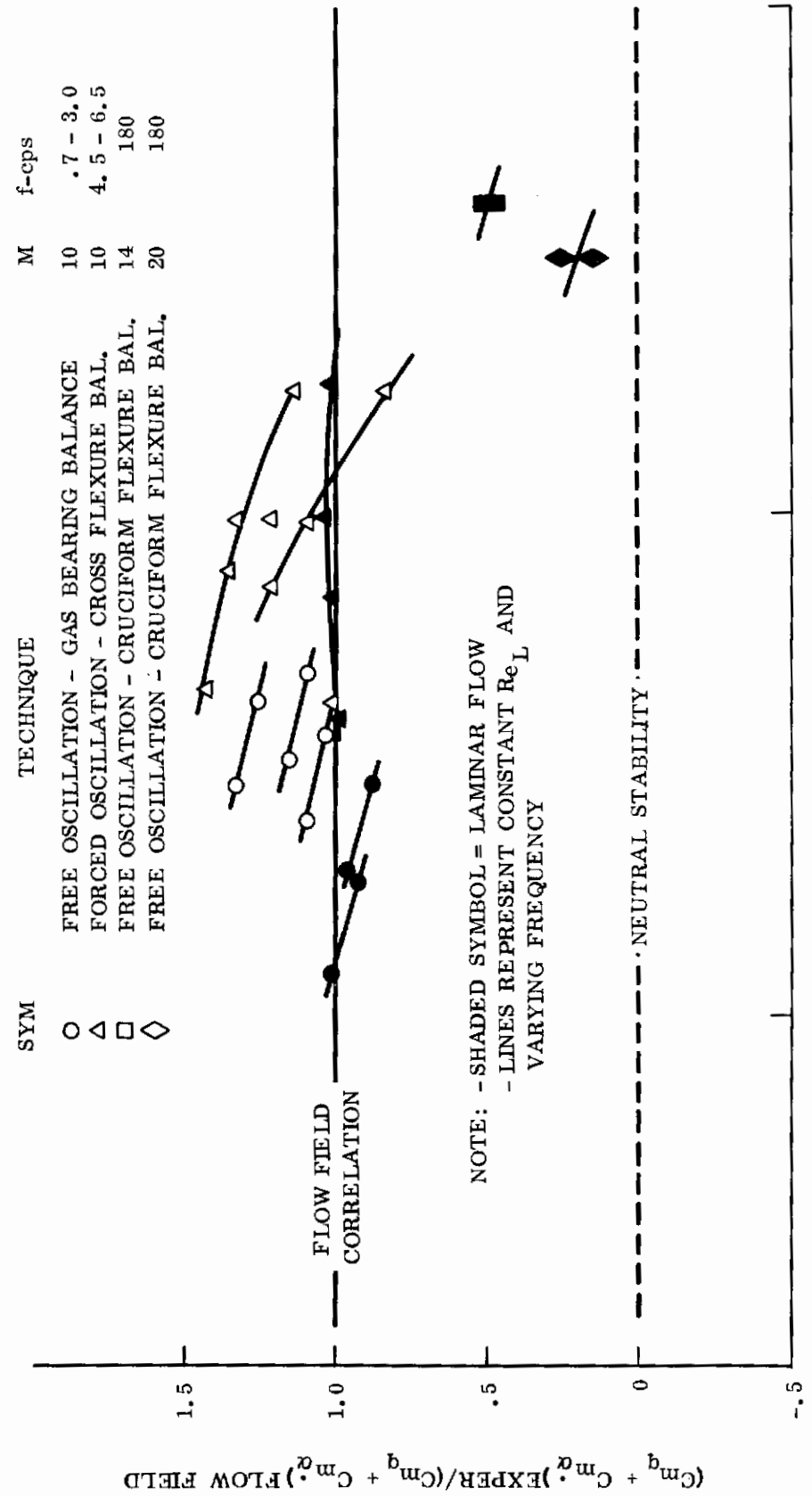

Figure 16. Pitch Damping Variation With Reduced Frequency

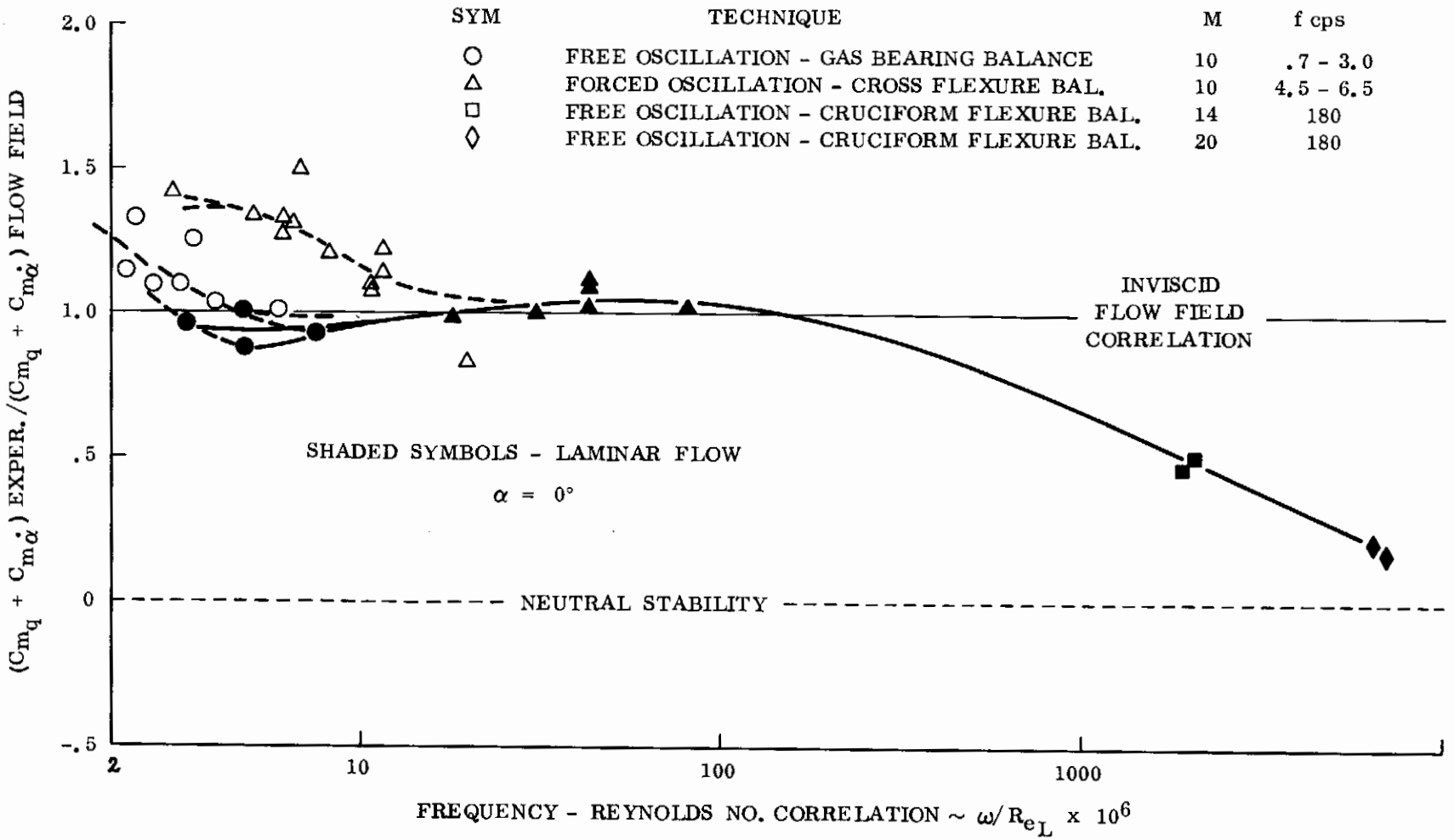

Figure 17. Data Correlation for Dynamic Damping of a 10° Cone

location effects will be eliminated and a direct correlation may be achieved between the AEDC and LTV facilities. It should be kept in mind that by eliminating Mach number in this manner, the Mach number - viscous interaction effect is not necessarily eliminated from the correlation factors.

In order to introduce a viscous effect into the correlation, the effects of frequency as shown in Figure 16 are modified by dividing the frequency term by the Reynolds number at the base of the model. The resulting correlation is a significant change and appears to orient the data in a consistent pattern. This correlation attempt seems to isolate the free and forced oscillation techniques in the transitional Reynolds number range, which could imply an oscillation frequency effect on boundary layer transition. In the laminar high Reynolds number range, (just prior to transition) the damping data is in good agreement with the flow field inviscid solution. The LTV data demonstrates that as frequency and viscous effects increase the damping falls off significantly. As discussed later in Section 8, other data sources confirm that stability is decreased in the low Reynolds number viscous environment and that stability increases during boundary layer transition. It should also be noted that the inviscid flow field solution does not account for these changes in boundary layer characteristics.

7.3 BLUNTNESS EFFECTS

The effects of increasing the nose bluntness on the dynamic damping of a 10-degree cone are shown in Figures 18, 19, and 20. The general trend in the data indicates a decrease in stability with an increase in bluntness. Significant changes in stability occur in the range tested and non-linear variation of stability with bluntness is indicated.

7.4 C.G. EFFECTS

The effects of varying the center of gravity or oscillation pivot location are shown in Figures 18, 19, 20, 21, and 22. The variation in stability with c.g. location is very nearly linear which theory predicts over the relatively small range of c.g. travel. At the high Reynolds number conditions the degree of variation is most significant for the sharp conical body and decreases with the bluntness of the body. This would appear to indicate that the minimum stability point is represented by a more forward c.g. location on blunter bodies, with minimum stability occurring in the range tested for the bluntness ratio of 0.3. At lower Reynolds numbers the trends of the sharper bodies appear to remain unchanged, while the variation of stability with c.g. location for the blunt bodies becomes very significant. These trends indicate probable instability at aft c.g. locations for the blunter shapes at low Reynolds number. The consideration of instabilities of blunt bodies at low Reynolds numbers is therefore highly dependent upon the location of the center of gravity.

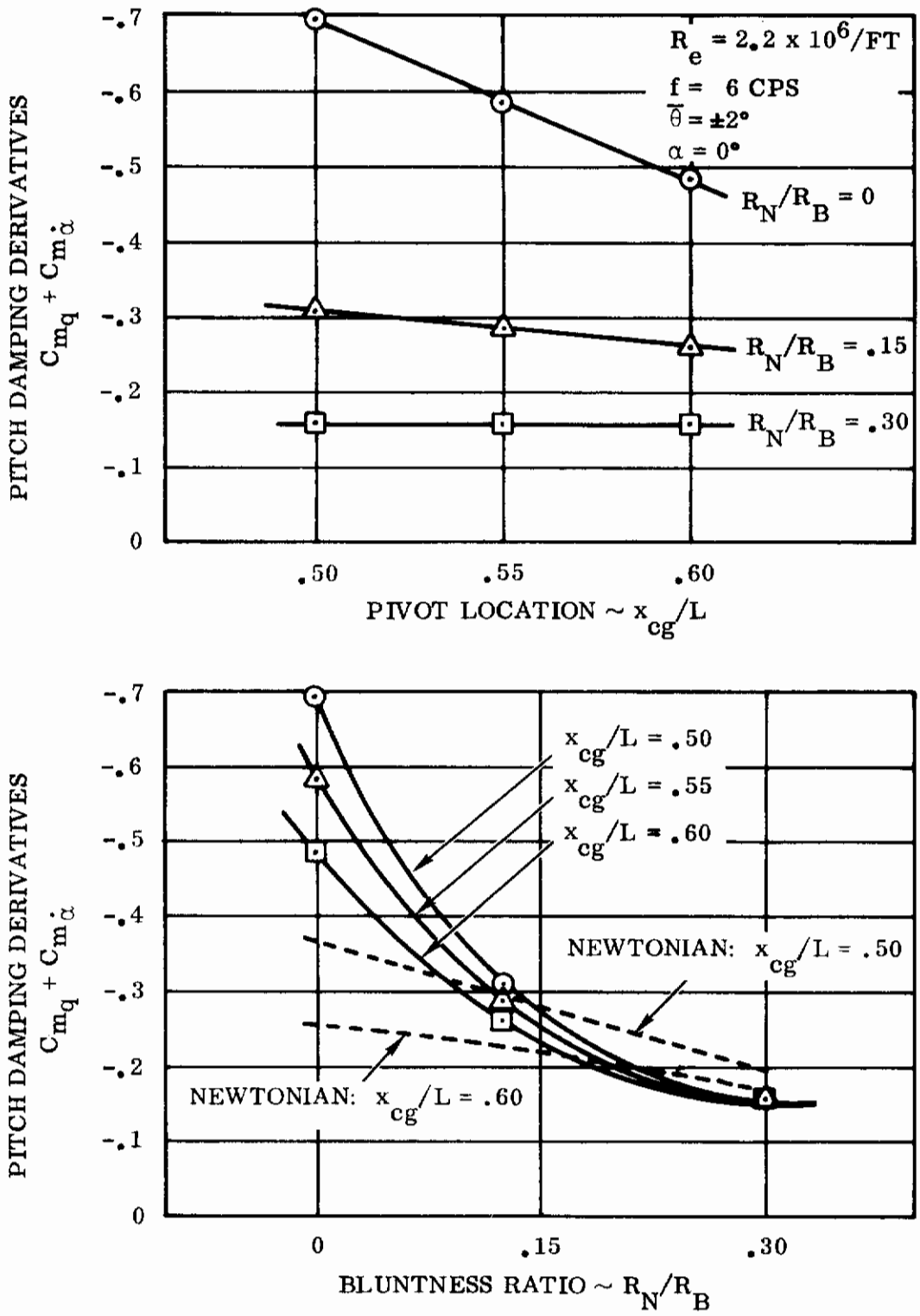

Figure 18. Effects of x_{cg}/L and R_N/R_B

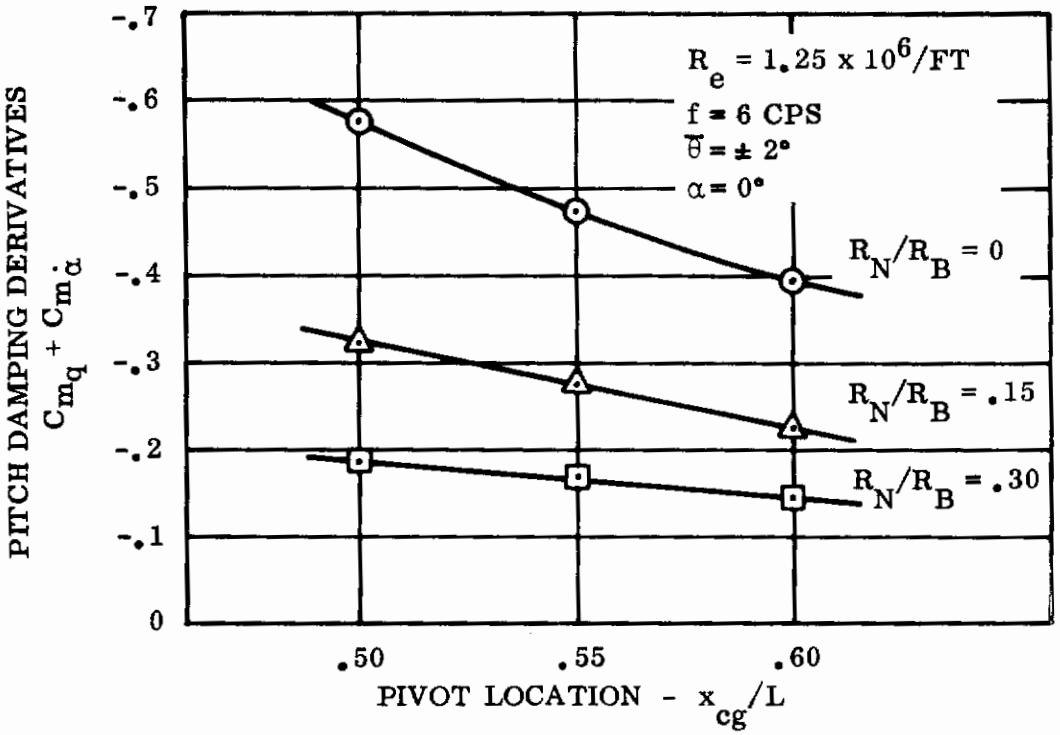

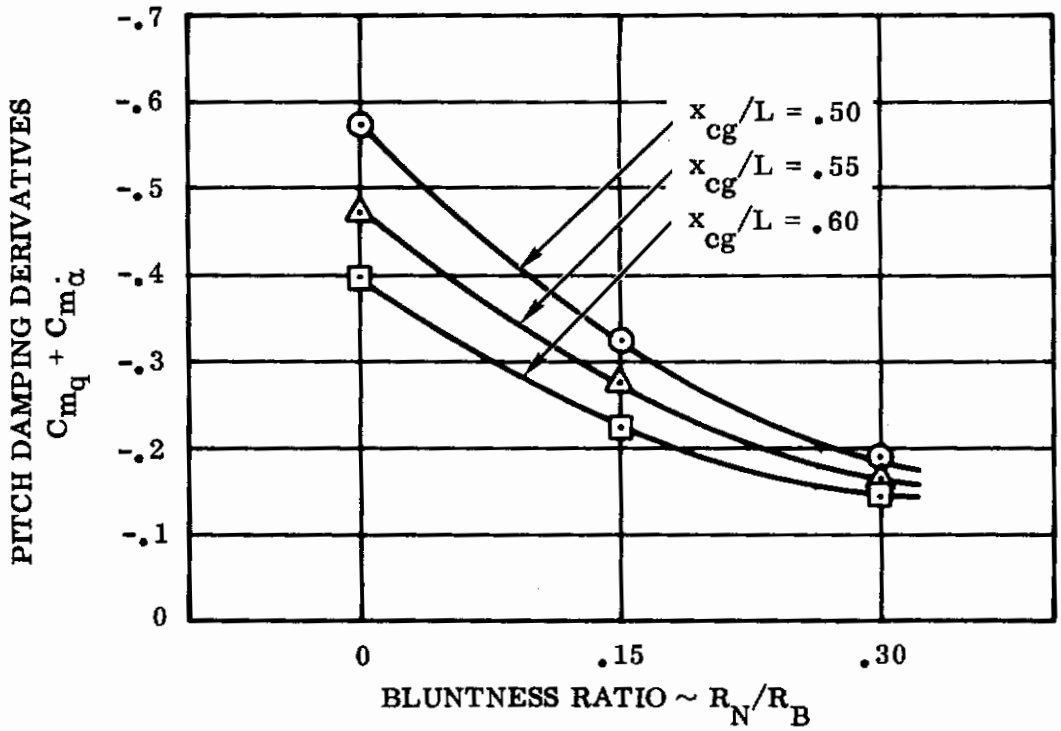

Figure 19. Effects of x_{cg}/L and R_N/R_B

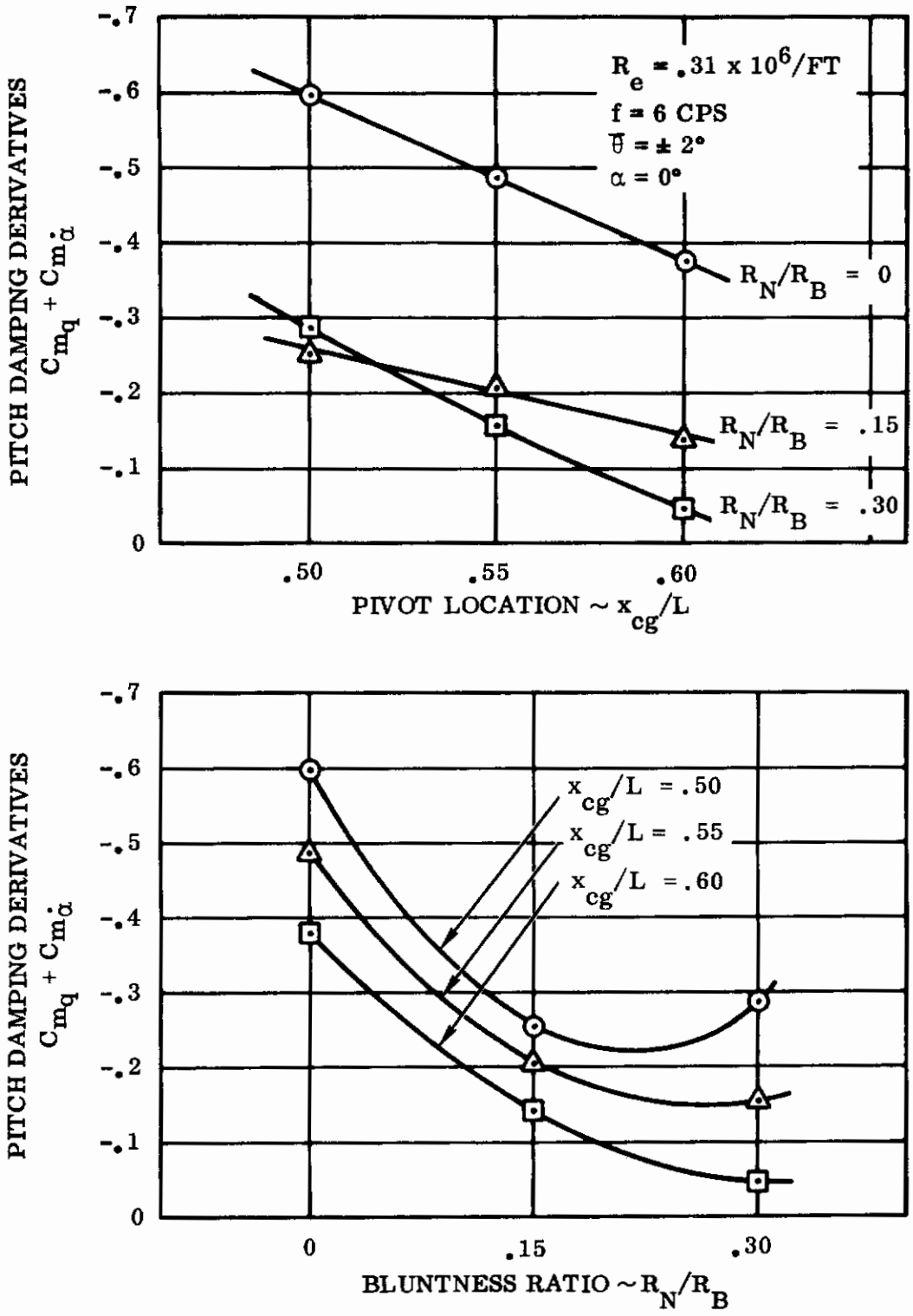

Figure 20. Effects of x_{cg}/L and R_N/R_B

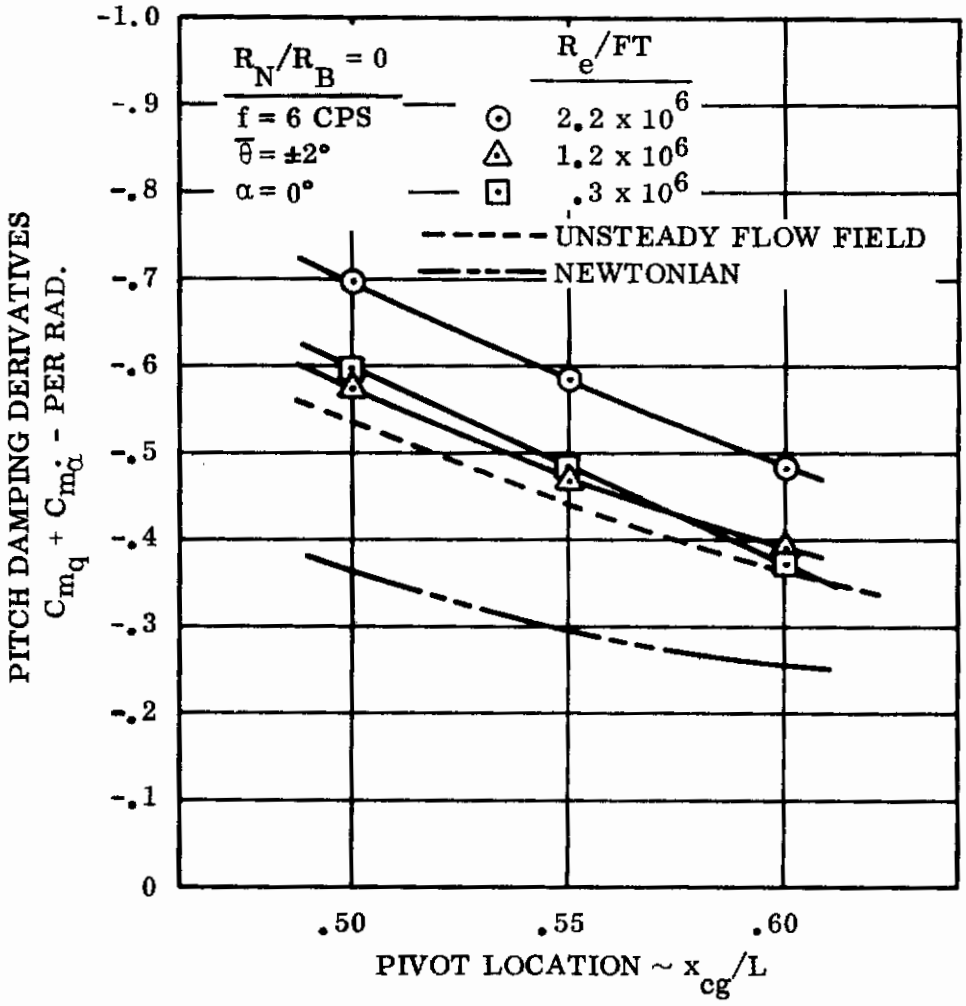

Figure 21. Effects of Reynolds Number on Center of Gravity Variation

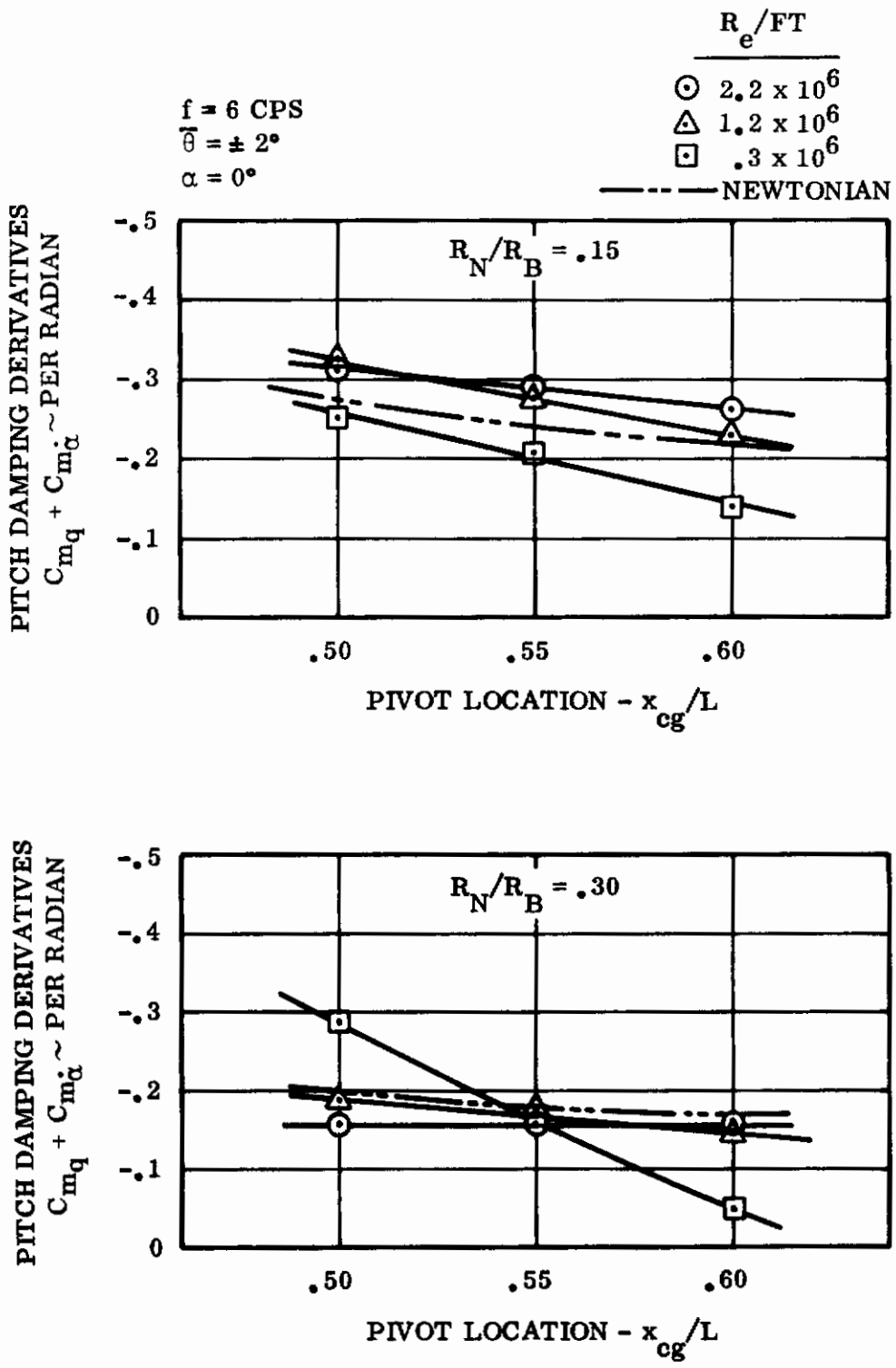

Figure 22. Effects of Reynolds Number of Center of Gravity Variation

Unsteady flow field estimates appear to predict the sharp body damping variation with c.g. location fairly well, neglecting Reynolds number effects, as shown in Figure 18. For the blunter bodies Newtonian estimates predict the variation with c.g. location with the exception of the low Reynolds number case.

7.5 VARIATION WITH ANGLE OF ATTACK

The variation of dynamic damping with angle of attack for a sharp cone is shown in Figures 23, 24, and 25. In the higher Reynolds number ranges this variation appears relatively constant with angle of attack, and neglecting other environmental effects, no significant variation is suggested. Data obtained at very low Reynolds numbers indicate a large increase in damping with increasing angle of attack, which would suggest significant viscous effects on this particular variable. Additional data were obtained for angle of attack for blunter bodies as shown in Figure 26.

7.6 AMPLITUDE EFFECTS

The effects of oscillation amplitude were obtained for the sharp 10° cone using a free oscillation balance with both a sting mount and a transverse rod mount support system. Data were also obtained for bluntness ratios of 0.15 and 0.30 to evaluate the effects of nose bluntness on stability variations with oscillation amplitude. Free oscillation data at five different flow conditions is shown in Figure 6 for the sharp 10° cone. No significant effects of amplitude are evident over the range from ±2 to ±8°.

Figure 27 shows the amplitude effects for a nose bluntness ratio of 0.15 for four flow conditions. A significant reduction in stability is observed as the oscillation amplitude decreases. Comparison with the sharp cone data indicates damping characteristics at oscillation amplitudes above ±8° are relatively the same neglecting Reynolds number and frequency effects. This observation is significant because it implies that bluntness effects on dynamic stability are accentuated by oscillation amplitude. Data obtained on the 10° cone with 0.30 bluntness ratio do not exhibit the same characteristics over the specific amplitude range as shown in Figure 28, but the trends in the data indicate a possible correlation with the other configurations at greater amplitudes. An absence of Reynolds number effects is also observed for the blunter configurations, which is attributed to the elimination of boundary layer transition due to nose bluntness.

Data obtained using the transverse rod support system is shown in Figure 29. The trends in the data appear to agree relatively well with sting mounted data at the high Reynolds number conditions, but seem to be invalid with laminar and transitional

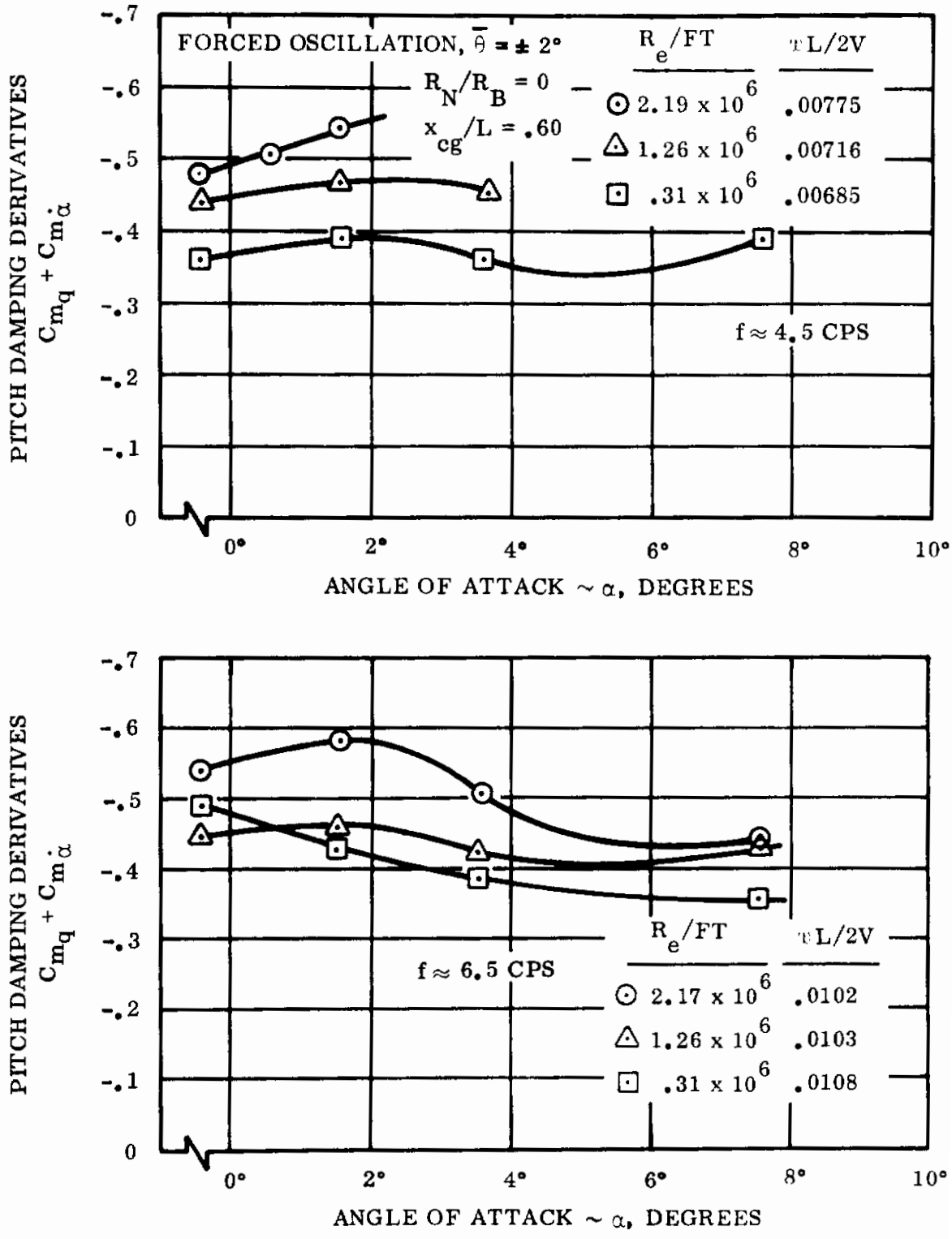

Figure 23. Pitch Damping Variation with Angle of Attack

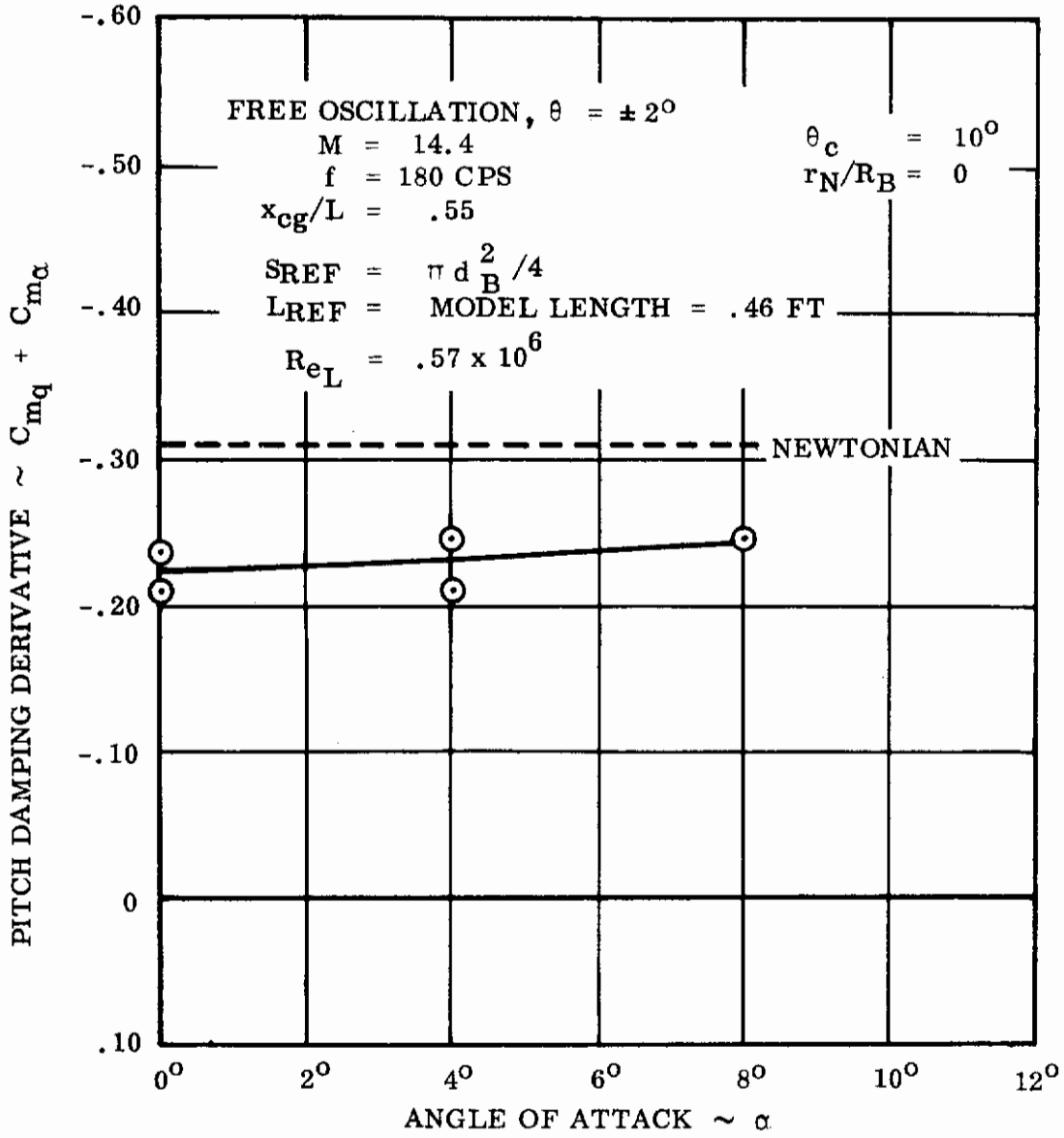

Figure 24. Pitch Damping Derivatives vs Angle of Attack

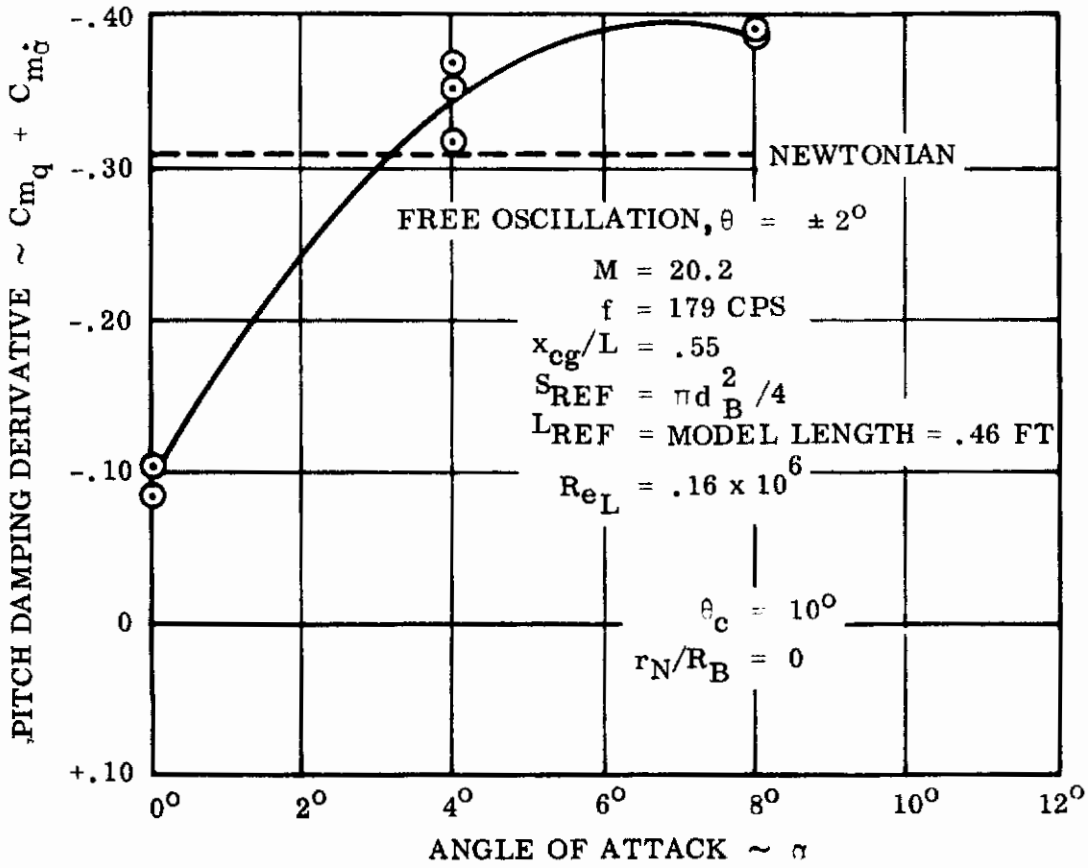

Figure 25. Pitch Damping Derivative vs Angle of Attack

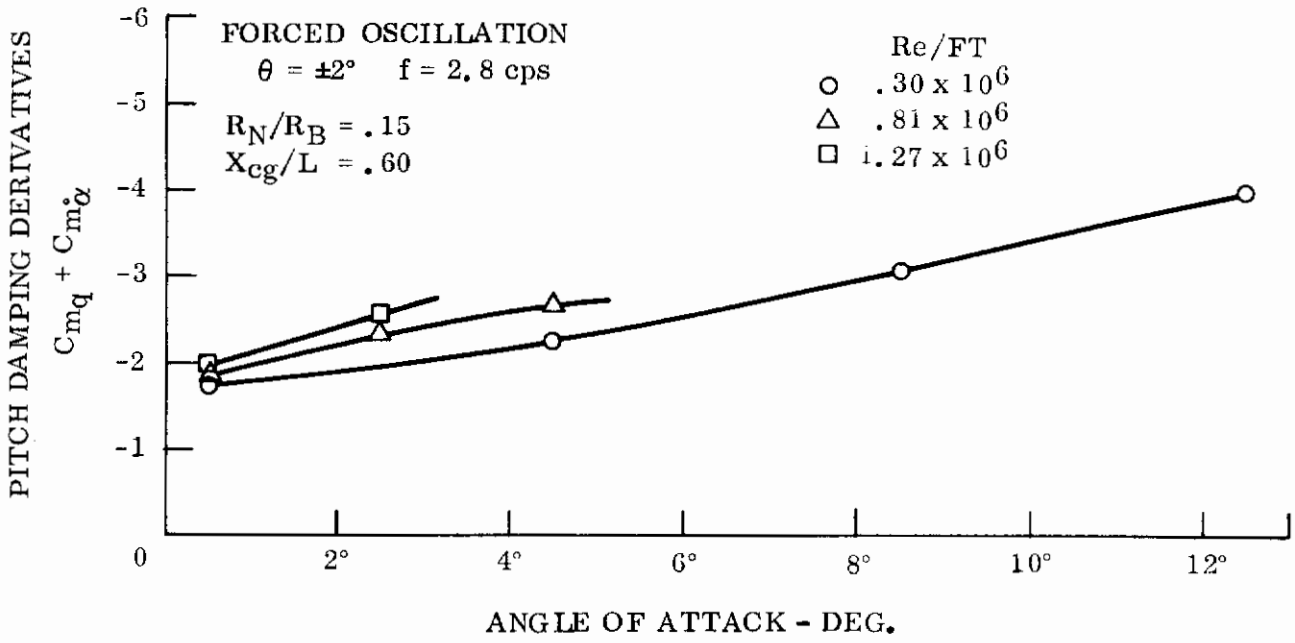

Figure 26. Pitch Damping Variation With Angle of Attack

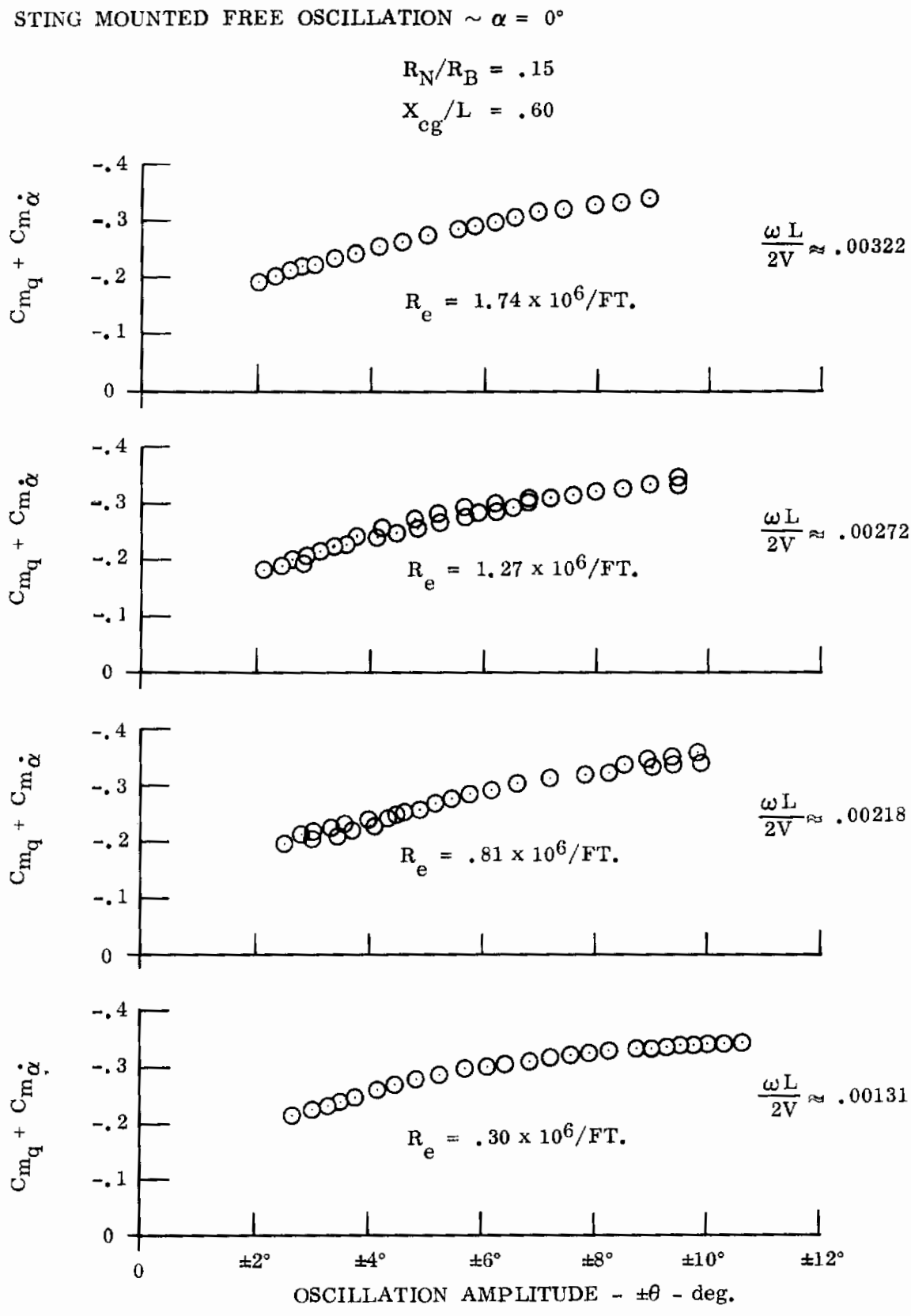

Figure 27. Pitch Damping Variation With Amplitude

STING MOUNTED FREE OSCILLATION

$R_N/R_B = .30$

$X_{c_q}/L = .55$

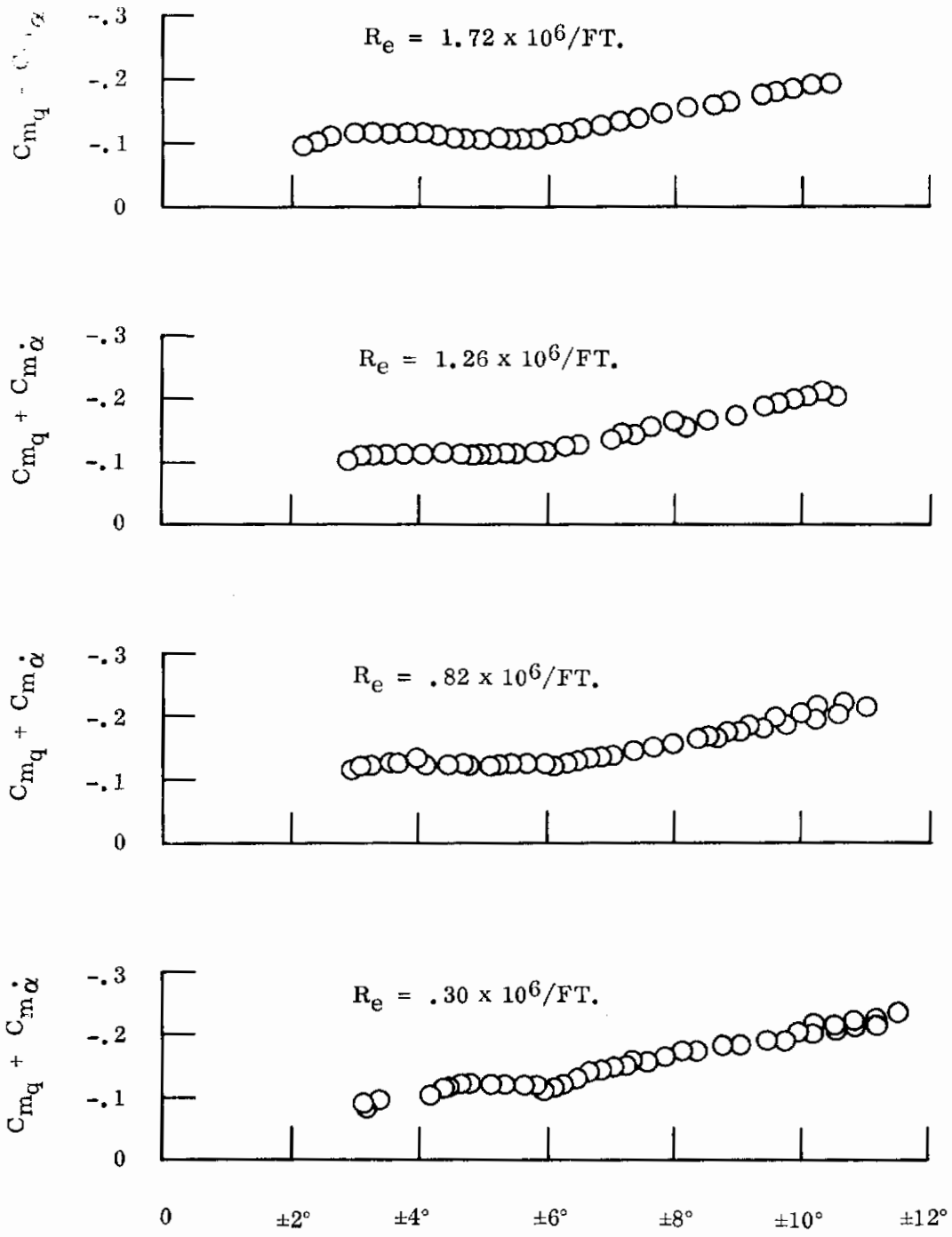

Figure 28. Pitch Damping Variation with Amplitude

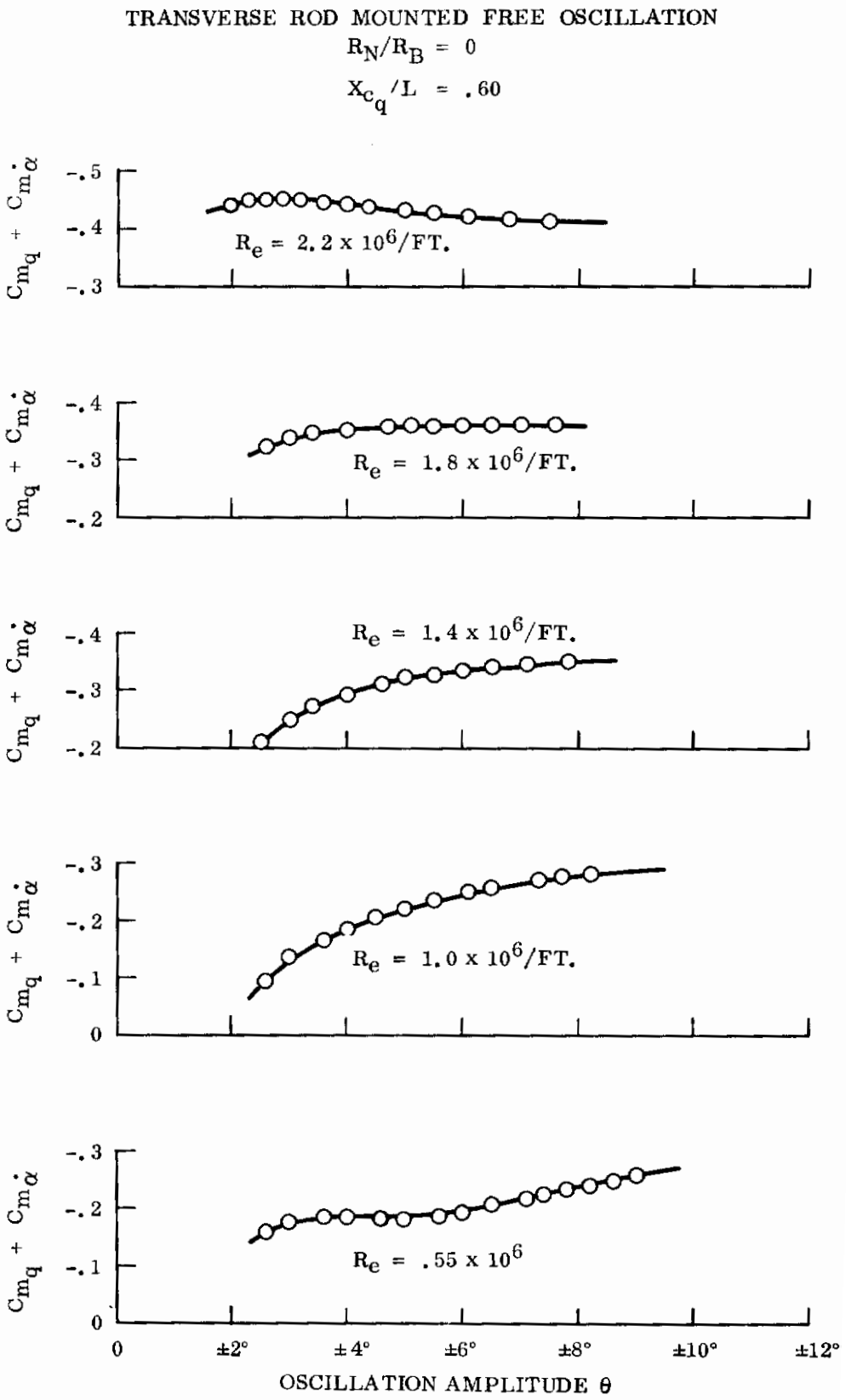

Figure 29. Pitch Damping Variation With Amplitude

flow because of aerodynamic interference effects of the support system. Additional data in Reference 15 indicates that amplitude effects may also be slightly biased by sting interference.

7.7 REYNOLDS NUMBER EFFECTS

The effects of Reynolds number are significant in the analysis of dynamic damping of cones, as shown in Figures 30 and 31. The effects of Reynolds number on the sharp cone pivoted at the 60 percent of length center of gravity location are shown in Figure 25, neglecting the effects of oscillation frequency. A definite trend can be observed which indicates significant changes in stability for transitional and turbulent boundary layer conditions. Shadowgraph flow visualization of the boundary layer on the 10-degree sharp cone supports the interpretation of the boundary layer condition. The results show very repeatable data at low Reynolds numbers, where the data is most difficult to obtain. At the high Reynolds numbers the scatter in the data is most prevalent which might indicate that frequency effects are pronounced in transitional or turbulent boundary layer conditions. The high Reynolds number free oscillation data represent the most accurate and dependable measurements; an abrupt decrease in stability is indicated as the boundary layer goes turbulent. Although the effects of transition are relatively unimportant, the trends of turbulent boundary layer effects could have very significant implications. Speculation is that the trend will level off and approach either flow field or Newtonian estimations at the higher Reynolds numbers.

Variation of the damping characteristics of blunter bodies with Reynolds numbers indicate a general trend of decreased stability at the lower Reynolds numbers, except in the case of extremely forward c.g. locations, as shown in Figures 32 and 33. In this respect, viscous effects appear very much dependent on the c.g. location of blunt bodies.

A decrease in damping measurements on the sharp cone in the Ling-Temco-Vought facility would indicate that viscous effects at the low Reynolds number have a similar effect on cones, neglecting Mach number and frequency effects.

7.8 FREQUENCY EFFECTS

Although Reynolds number effects appear to be the most prominent environmental variable, the effects of frequency are also apparent in all the data to a minor degree. An extremely large increase in frequency is obtained in going from the AEDC tunnel C to the LTV Hot Shot and in relating the two facilities. Free oscillation data in the AEDC tunnel C exhibits a consistent effect of frequency for even a slight variation, which may possibly be attributed to tare calibrations. The reduced frequency parameter,

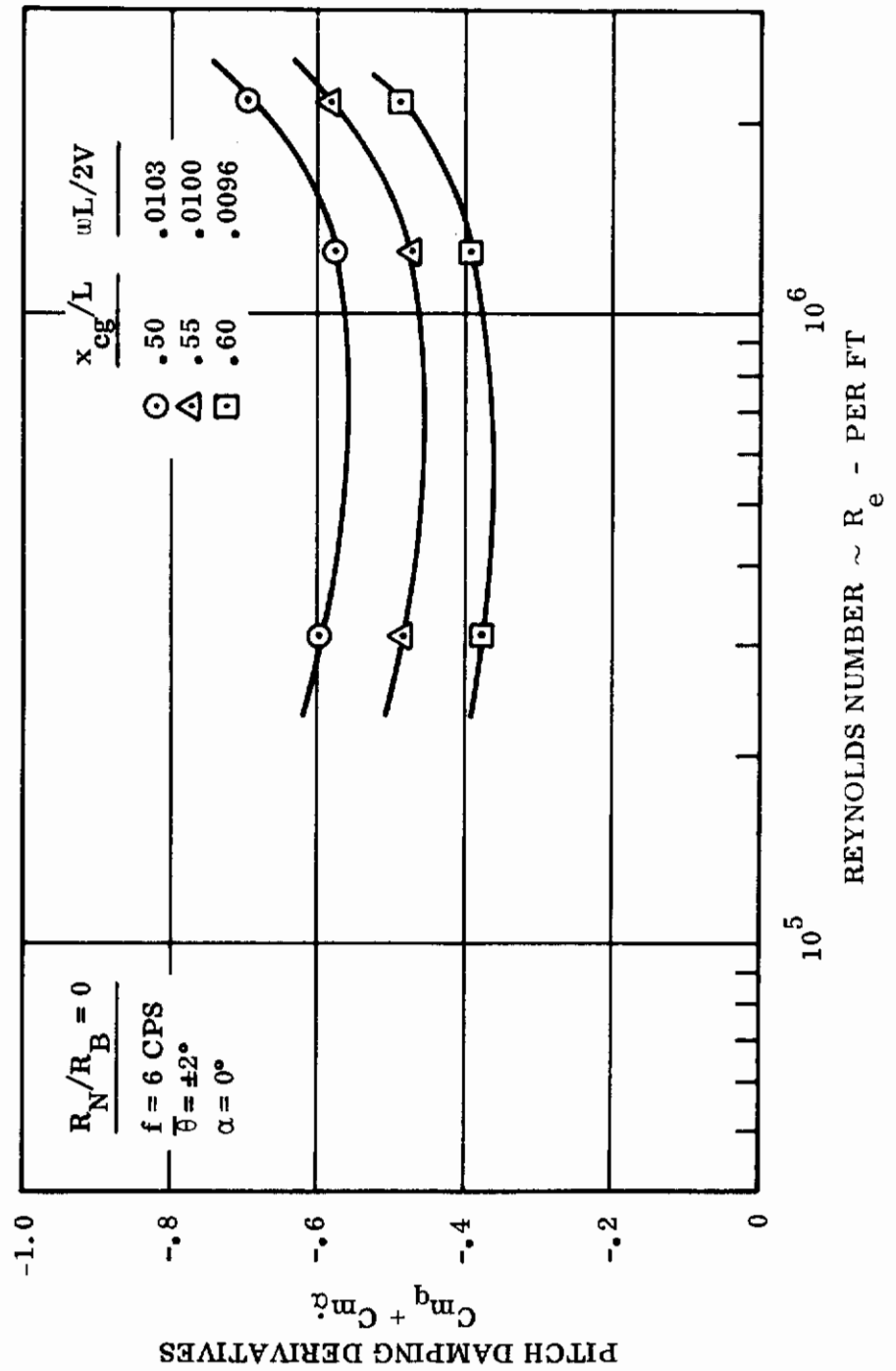

Figure 30. Variation with R_e for Three Pivot Locations

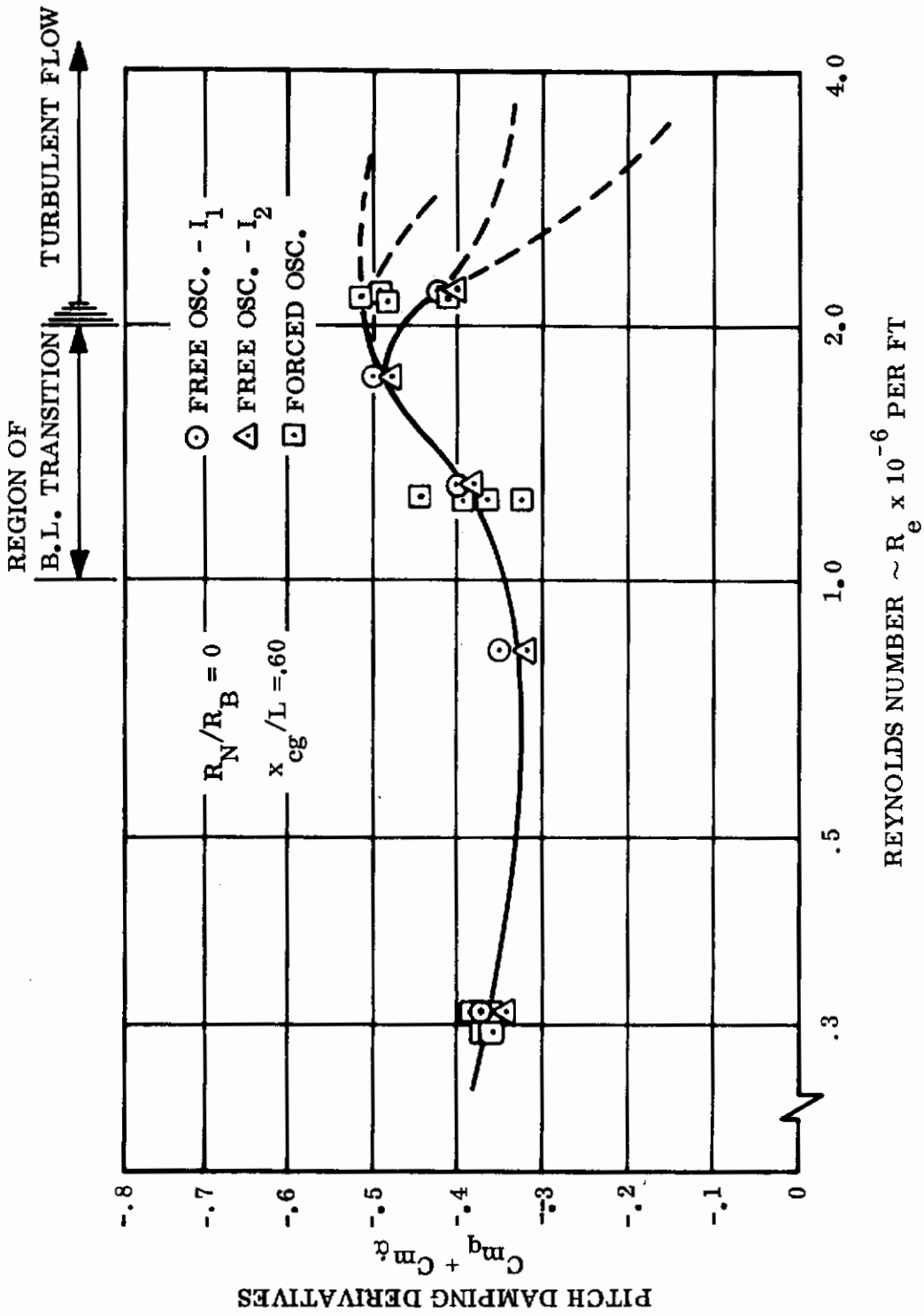

Figure 31. Reynolds Number Effects

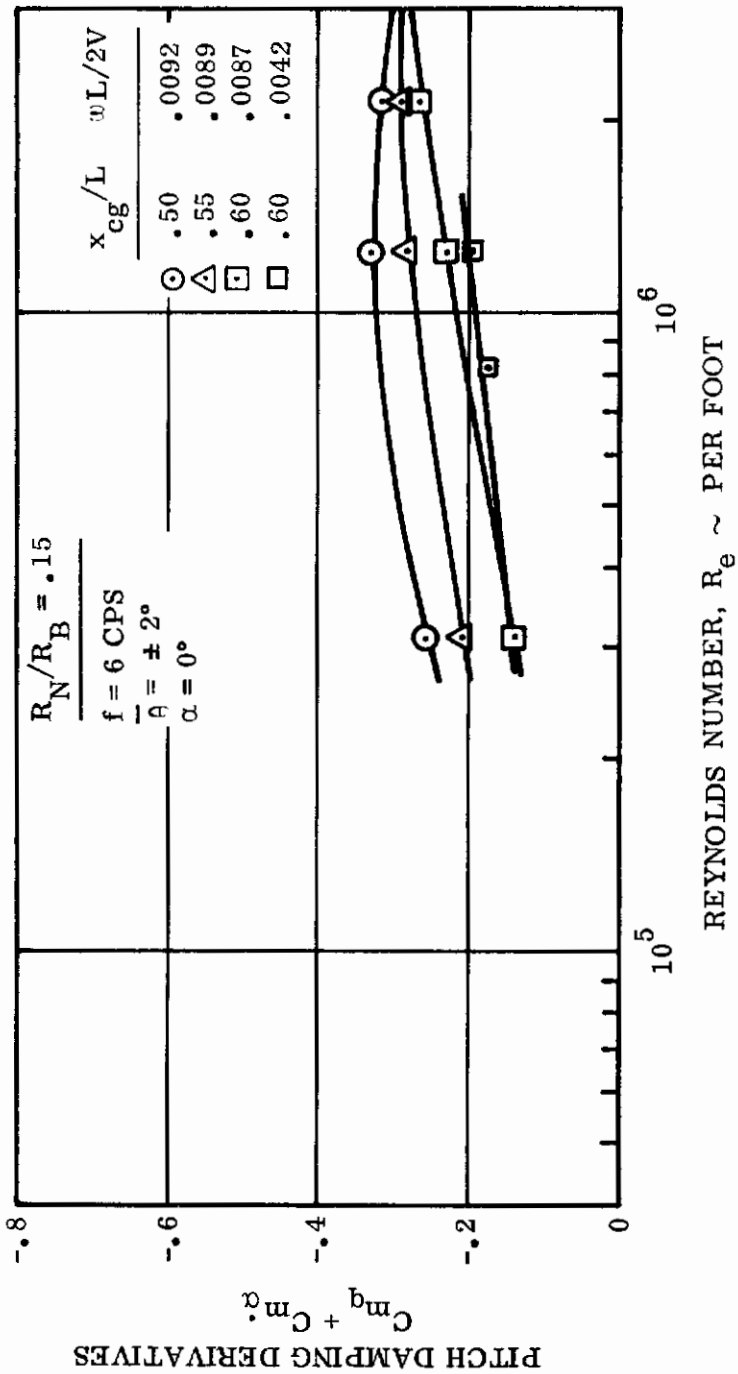

Figure 32. Variation with R_e for Three Pivot Locations

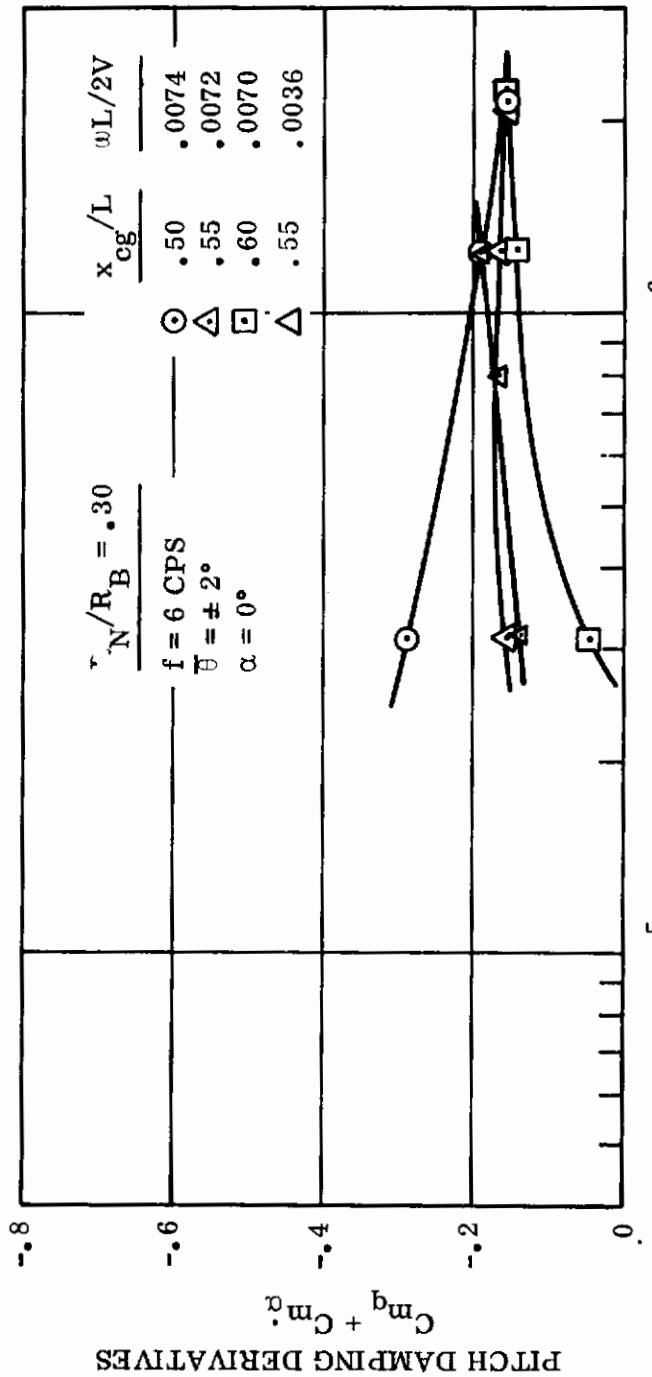

Figure 33. Variation with R_e for Three Pivot Locations

$\omega L/_{2V}$, usually accepted as a standard frequency correlation parameter for dynamic stability, does not appear to provide a good correlation, as shown in Figure 16. The plot does demonstrate a consistent trend, however, of decreasing stability with increasing frequency, but the level appears dependent on Reynolds number effects and the state of the boundary layer.

7.9 STATIC STABILITY DERIVATIVES

In all of the dynamic stability tests, the static stability derivatives may be generated from the data as shown in Section 4. The significance of these data is that they may be compared with established aerodynamic criteria in determining the validity and a level of reliability of the damping data. In most cases the comparison of the static stability derivatives with flow field estimates demonstrate excellent agreement as shown in Figures 7 and 34.

7.10 ANALYSIS OF FLOW VISUALIZATION

A limited amount of flow visualization was obtained from the tests conducted in this experimental program. Shadowgraphs of the boundary layer on portions of the model surface were obtained under static conditions in the AEDC tunnel C. These shadowgraphs were utilized primarily to define the state of the boundary layer. In the LTV Hypervelocity tunnel, Schlieren fastax motion picture coverage provided time histories of the model oscillation and visual motion studies of the flow field during the run. Flow densities at M = 14 and at a Reynolds number of about 1.2×10^6/FT were sufficiently great to obtain relatively accurate measurements of the boundary layer and shock layer thicknesses at the base of the 10-degree cone model. The thickness varies with the angle of the model surface with the flow as shown in Figure 35. The curve represents the fairing of a mass of data accumulated and plotted in Reference 14. Figures 36, 37, and 39 show the variations in boundary layer thickness and shock layer thickness with time and therefore with amplitude. These data demonstrate that there is no appreciable lag in the response of the boundary layer and shock layer to model motion. This conclusion is particularly surprising, considering the extremely high oscillation frequency. The motion of the leeward boundary layer and shock layer at angle of attack is shown to be exactly 180-degrees out of phase, that is moving in the opposite direction relative to the base of the model. This effect constitutes the thickness variation at leeward angles. As the model surface passes from leeward to windward, the boundary layer and shock layer move in phase, or in the same direction, with the model surface, and there is no variation in thickness.

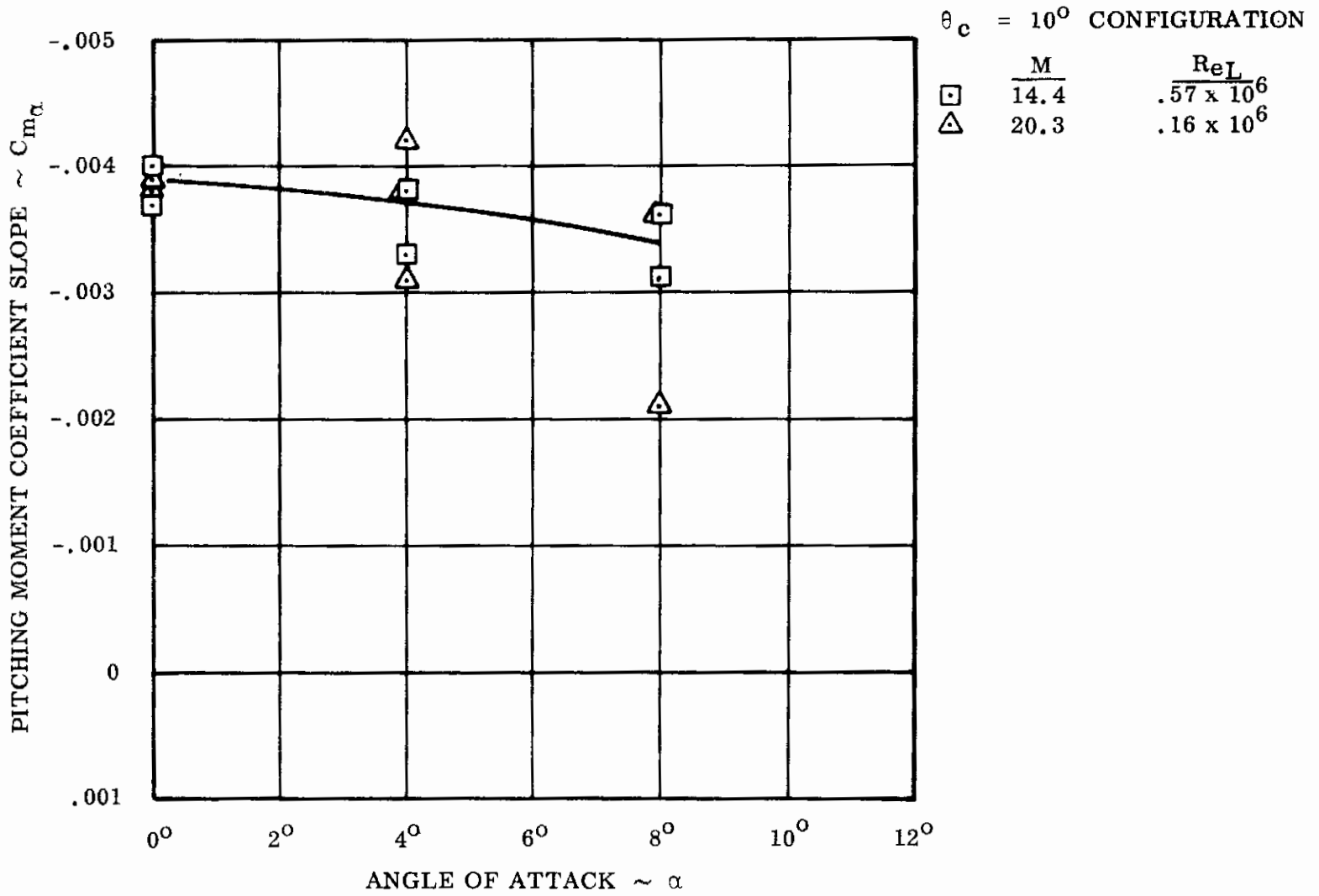

Figure 34. Pitching Moment Coefficient Slope vs Angle of Attack

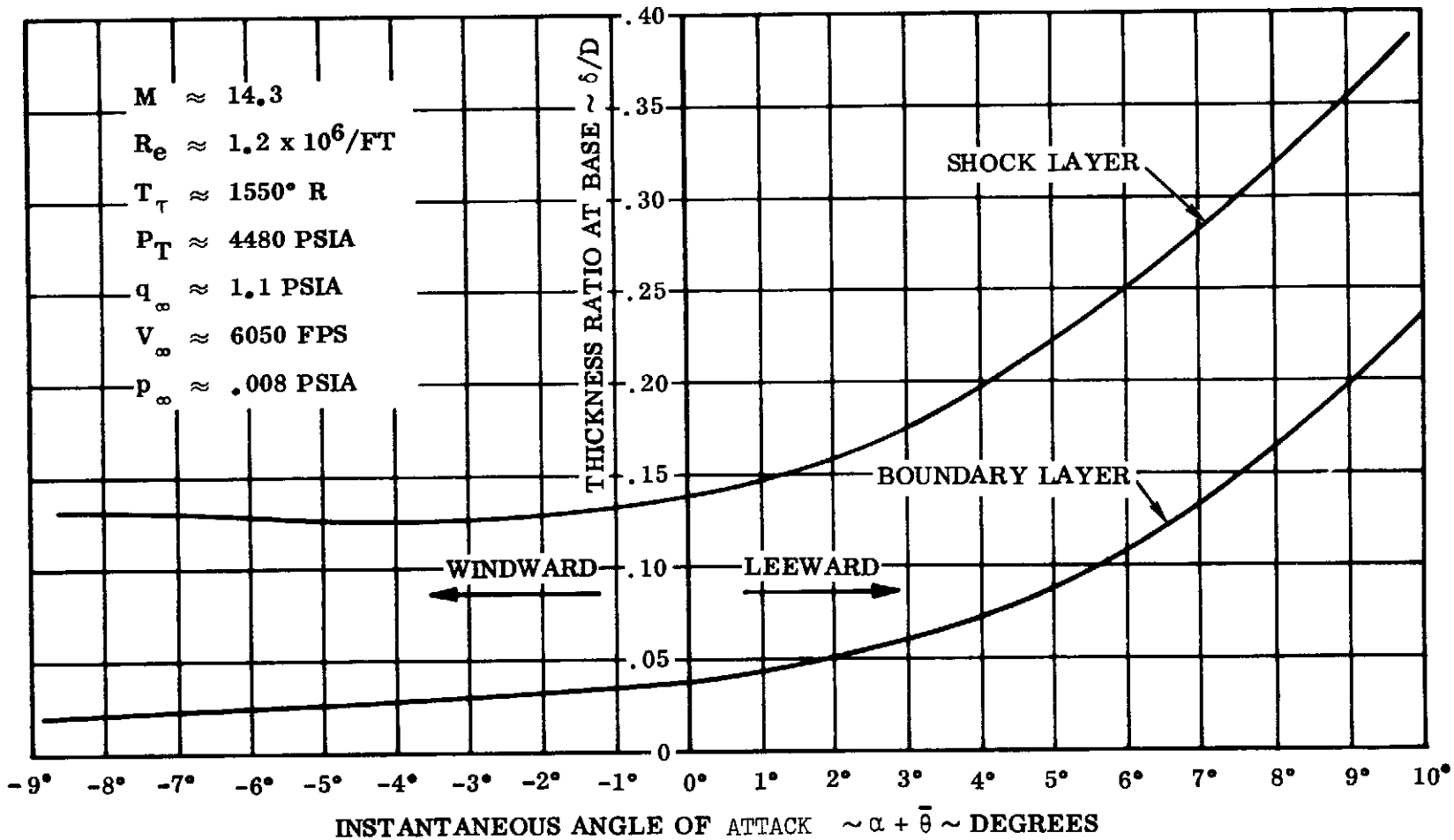

Figure 35. Boundary Layer and Shock Layer Thickness Variation with Angular Displacement at the Base of a 10-Degree Cone in a Hypersonic Flow Field

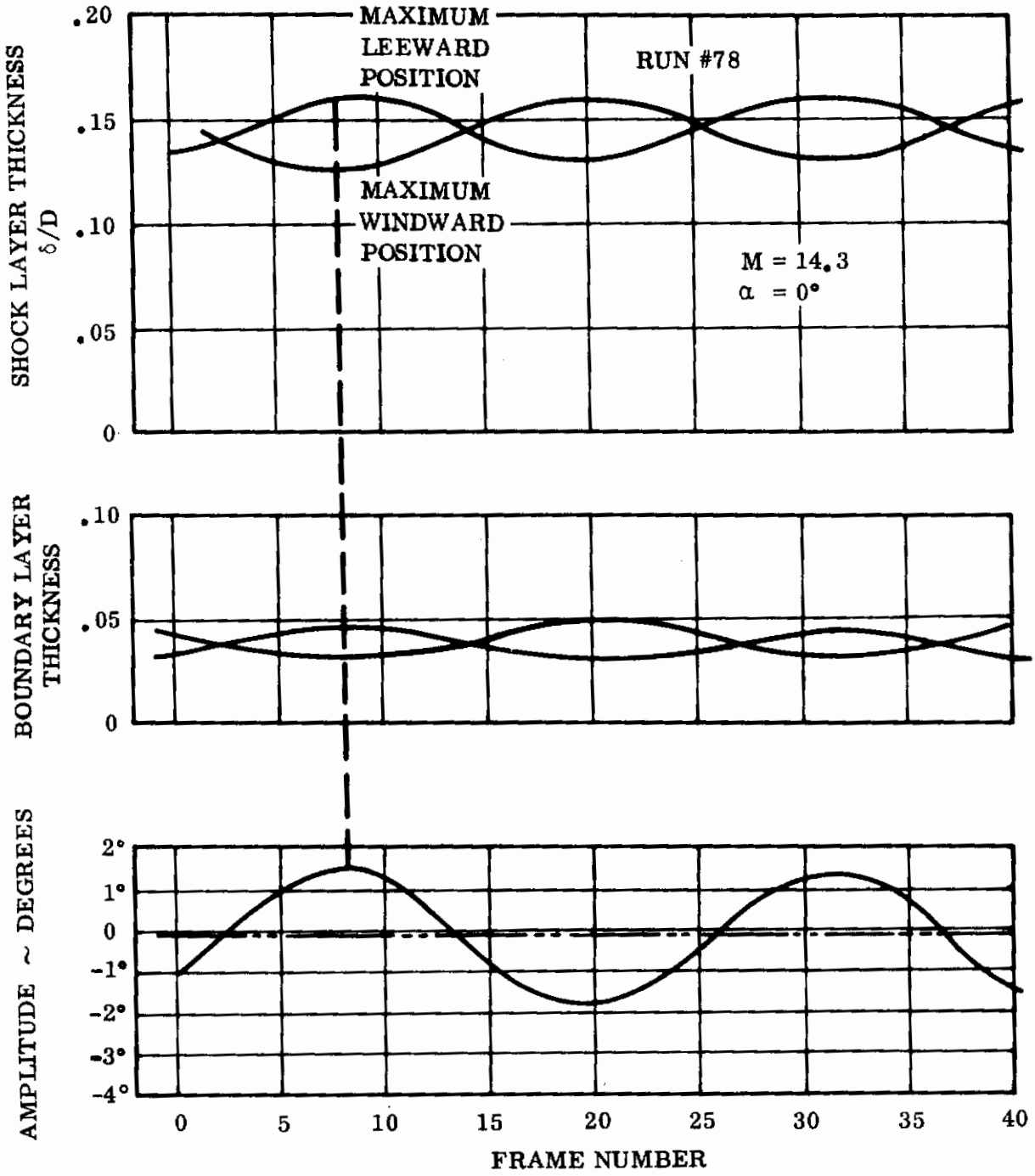

Figure 36. Schlieren ~ Fastax Analysis of Motion and Flow Field Time Histories of an Oscillating 10-Degree Cone

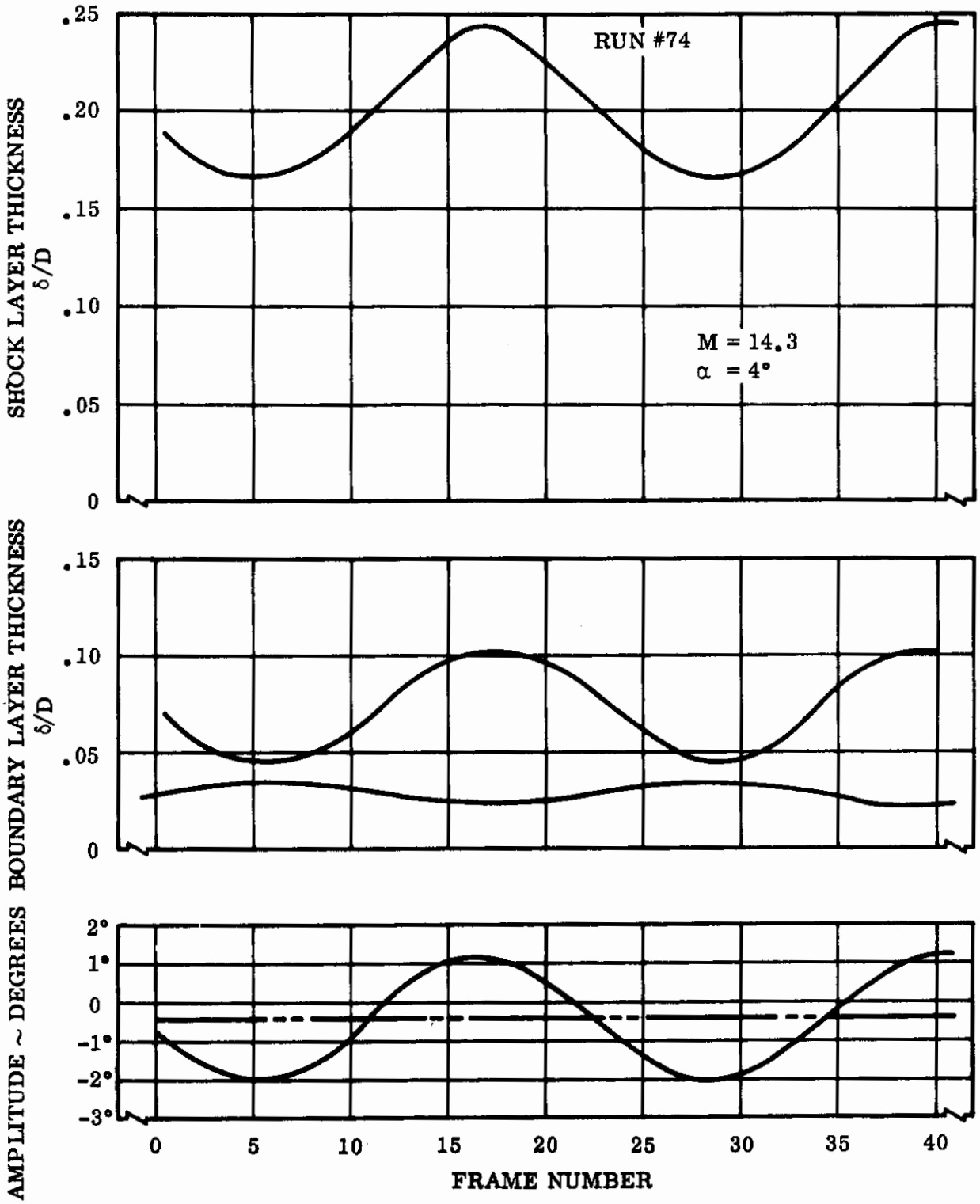

Figure 37. Schlieren ~ Fastax Analysis of Motion and Flow Field Time Histories of an Oscillating 10-Degree Cone

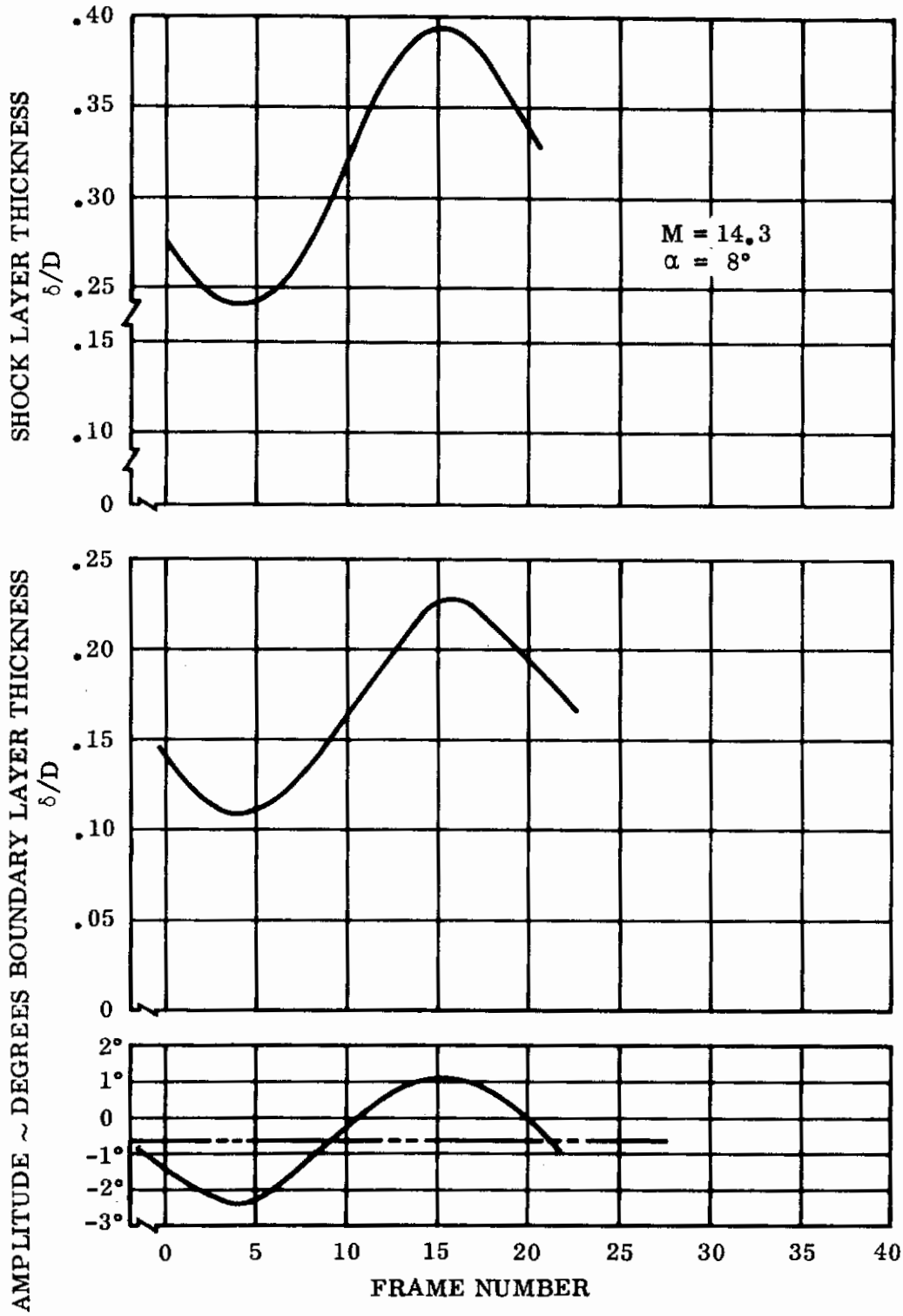

Figure 38. Schlieren ~ Fastax Analysis of Motion and Flow Field Time Histories of an Oscillating 10-Degree Cone

8. SURVEY OF LITERATURE

8.1 INTRODUCTION

A limited amount of data and applicable information is available from published sources which will augment the experimental studies of this program. Most of these data sources are oriented to evaluate the effects of cone angle, nose bluntness, Reynolds number, and oscillation frequency, but additional influences on dynamic stability which have been observed experimentally are included. A cursory survey of all the available data demonstrates that there are many independent variables which affect the aerodynamic damping characteristics of cones. Major unclassified data sources are the Transactions of the Second Technical Workshop in Dynamic Stability Testing and the STA committee reports on dynamic stability. These references illustrate various theoretical techniques and many data sources, which summarize the present state-of-the-art in pre-flight dynamic stability analysis.

8.2 DATA CORRELATIONS

A survey of available literature does not appear to add significantly to the empirical correlation of dynamic stability data, but it certainly does tend to support many trends which have been observed in this experimental program. Data obtained at high hypersonic Mach numbers and low Reynolds numbers in Reference 16 demonstrate that the stability of a 10° cone is greatly reduced under these conditions. This effect, presumably viscous, was consistently observed in the LTV Hot Shot facility. The ARL-AEDC data in Reference 16 were obtained in a different type facility using an entirely different testing technique, and was a significant check on the Chance Vought results. The ARL test results were obtained at frequencies considerably lower than were required in the Hot Shot tests. This fact illustrates that there is a consistent trend of reduced stability which may be attributed primarily to viscous effects at low Reynolds numbers.

The ARL data indicates a good correlation of the data with reduced frequency as shown in Reference 16, but the LTV data does not substantiate this correlation. The best correlation between the two facilities appears to be a function of Reynolds number and frequency as shown in Figure 39.

Substantiation of the effect of increased stability during boundary layer transition was obtained in Reference 12. These tests were conducted in other AEDC facilities at lower Mach numbers and high pressure as a result of the observations made in this experimental program. The results demonstrate conclusively the association of increased damping with boundary layer transition and a reduction in base pressure, but it is highly probable that this effect may be attributed to support interference effects.

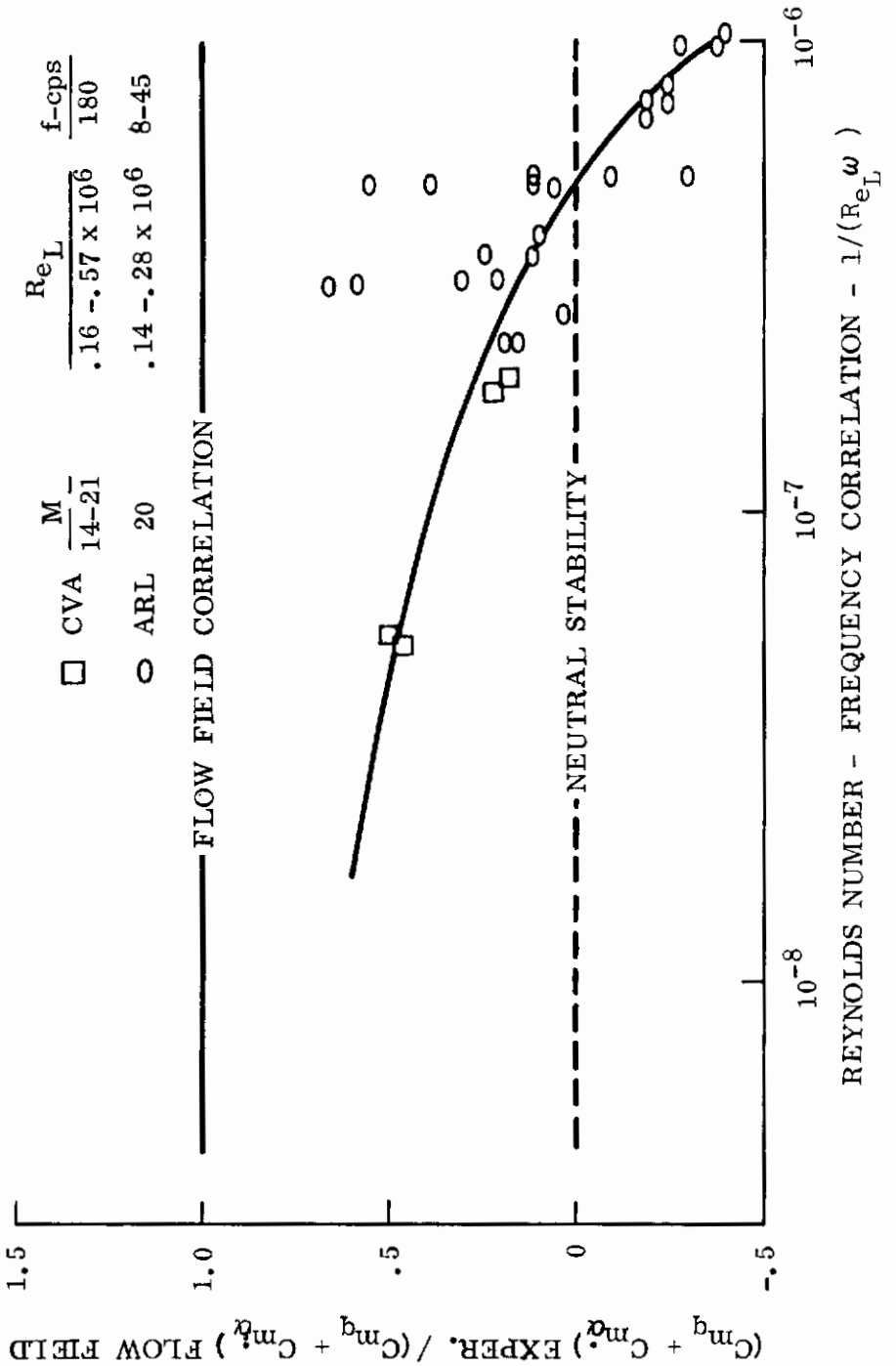

Figure 39. Low Density Data Correlation For A 10° Cone

8.3 BLUNTNESS EFFECTS

The effects of nose bluntness of conical configurations on dynamic stability have been demonstrated in a number of experimental studies. All the data show a similar trend of decreased stability with increased bluntness at all Mach numbers. References 17 and 18 illustrate bluntness effects on a 10° cone at supersonic Mach number in free flight. A correlation of bluntness effects for sphere cone configurations are shown in Reference 19, which demonstates that bluntness effects are also dependent on cone angle effects.

Most theoretical studies to date have dealt primarily with sharp cones. The flow field results demonstrate the same trends of decreased stability with increasing bluntness, but do not appear to predict wind tunnel data at the larger bluntness ratios as well as Newtonian theory. Improvements in the theoretical techniques and in data correlations for blunter bodies would appear to be a problem area for future development.

8.4 CONE ANGLE EFFECTS

A geometric variable which has not been researched in this particular area is the semi-vertex angle of conical configurations. Data extracted from several references for sharp cones are shown in Figure 40. These data indicate a slight increase in damping as the cone angle increases at Mach 10. Free flight data cone angle effects are also shown in Reference 17 at lower Mach numbers, which indicate identical trends with proper data reference conversion. In general, cone angle effects are predictable by theoretical techniques for sharp bodies. The cone angle - nose bluntness correlations previously expressed in Reference 19, suggest that cone angle effects may be significantly altered with blunter configurations.

Other geometric variables which have not been covered in this program are investigated in other literature sources. Of particular interest is the effect of afterbody shape on the damping characteristics of cones. The effects of dome radius are shown in Figure 40 at Mach 10 which implies a drastic reduction in dynamic stability at the higher radius ratios. In Reference 20, the effects of a hemispherical dome at the base of a conical configuration are not evident in free flight at supersonic Mach numbers, and the dome effects are attributed to support system interference effects. This inference is questionable in that there are several classified references which demonstrate a very significant dome effect in transonic of low supersonic free flight tests in ballistic range facilities.

8.5 REYNOLDS NUMBER EFFECTS

Reynolds number effects, which are demonstrated throughout this program, have been investigated in several data sources. In particular, the variations in damping data through the transitional boundary layer regime at various supersonic

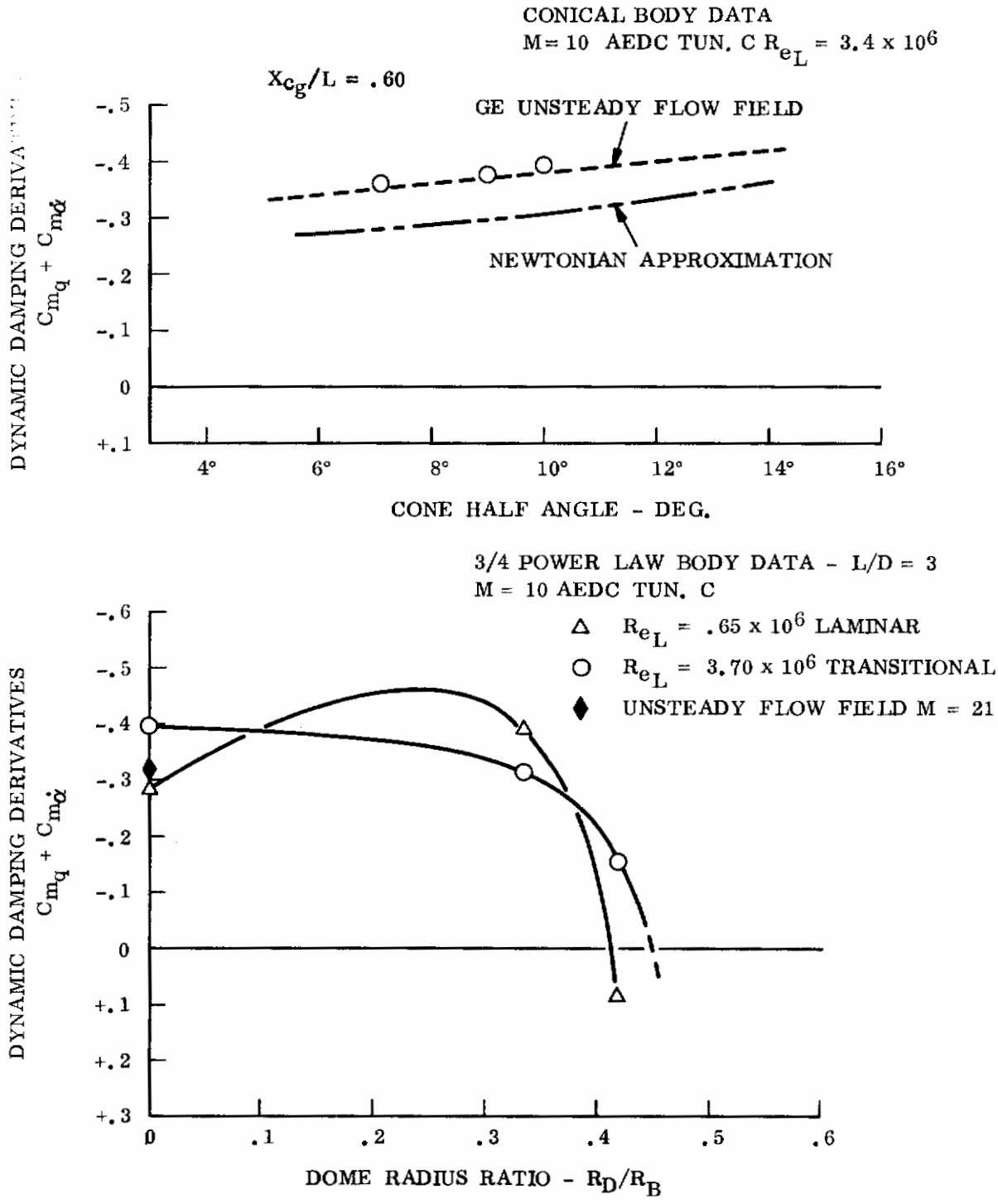

Figure 40. Cone Angle and Afterbody Effects

and hypersonic Mach numbers are found in References 12 and 21. The trends of increased stability with boundary layer transition as observed in this program is confirmed by data obtained in other facilities at lower Mach numbers. The data also indicates that with turbulent flow the damping decreases and approaches the theoretical inviscid value.

The low Reynolds number effects remain undefined at present, but the available data implies that damping decreases with increased viscous effects. Additional data is needed to define these low Reynolds numbers effects and provide sources for the data correlations of viscous effects.

8.6 FREQUENCY EFFECTS

One of the most confusing of the environmental variables is oscillation frequency. Intuitively any effect of frequency on aerodynamic damping must be derived from the boundary layer and pressure response to the rate of change in attitude. Frequency effects are observed in the data, and the inconsistency of these effects throughout various data sources is misleading. In addition to the data obtained in this program, frequency effects were also evaluated in References 16 and 19. The effects of frequency under different Reynolds number conditions, under different balance loading conditions, and at different Mach number conditions should be carefully evaluated to determine if in fact these effects are attributed to environmental condition or to balance calibrations.

The effects of other variables such as oscillation amplitude, angle of attack, and Mach number are also shown in many data references; but the trends are generally consistent and not significant enough to discuss in detail. The effects of mass addition on dynamic stability are substantial and are discussed extensively in classified literature. A survey of mass addition effects on dynamic stability may be found in Reference 7.

9. CONCLUSIONS

9.1 INTRODUCTION

The objectives of the experimental program were to provide ground test data in support of theoretical studies and to investigate and correlate the effects of major simulation variables. By demonstrating the validity of inviscid flow field theory and its capability to define the effects of geometric variables on dynamic stability, a significant design technique would be established. With successful evaluations and correlations for the effects of environmental variables, it would be possible to extrapolate inviscid theory to flight conditions and predict the dynamic behavior of a vehicle during re-entry.

The results of the program have demonstrated that hypersonic dynamic stability derivatives are difficult to predict due to the many complex phenomena involved. Although the test results do indicate that flow field theory is an adequate inviscid estimate of dynamic damping characteristics, viscous effects have a pronounced influence on the results. The lack of data correlation has been surprising but demonstrates the need for continued research in unsteady boundary layer analysis and the development of improved test techniques.

The available data provides a solid foundation for extended research on the isolation and correlation of significant variables, such as oscillation frequency, oscillation amplitude, angle of attack, Reynolds number, and Mach number. These variables and their effects on trends in the stability data are discussed in this section. Recommendations are made for the use of these data, for continued experimental research, and for the research and development of testing techniques and equipment.

9.2 DATA CORRELATIONS

The data correlations shown in the previous sections demonstrate trends rather than actual correlations of results. The susceptibility of the trends in the data to correlation is generally poor and indicate that the correlations, as well as the data, may be biased by the effects of environmental variables or factors such as support interference and balance calibrations. This concept is particularly evident in the AEDC results, in which a consistent decrease in stability is indicated for an increase in frequency. Because of the fact that the data does not correlate in terms of frequency, it is possible that frequency is affecting the balance calibration and not the actual damping.

Correlations may also be affected by an interdependency among several environmental variables. The obvious case has been demonstrated wherein the effects of oscillation frequency are entirely different under various Reynolds number conditions. It is also reasonable to assume that Reynolds number and frequency effects will vary

with oscillation amplitude. This interdependency among so many environmental variables also make correlations of the data extremely difficult.

9.3 SIGNIFICANT VARIABLES

The data do demonstrate which variables are significant. The effects of geometric variables are shown to be highly predictable by flow field theory and indicate that both nose bluntness and center of gravity locations have a significant influence or aerodynamic damping characteristics. Other geometric considerations which were not evaluated in this program are cone angle and afterbody shape. Some of the effects of these variables were obtained from the literature survey and are shown in Figure 40. The effects of a dome radius at the base of a vehicle are shown to be a critical geometric variable for dynamic stability at relatively large dome to base radius ratios. The effect is attributed to flow expansion and separation at the base. Adverse dome effects on dynamic stability have also been observed at transonic speeds and present a significant design problem for advanced re-entry systems. Cone angle effects demonstrate a good agreement with inviscid flow field theory. An additional geometric variable which may be very significant and which has not been evaluated is a c.g. offset. An offset in center of gravity may be attributed to manufacturing tolerances, in-flight ablation asymmetries, or design specifications. The effects of this variable depends on the degree of offset, the mass moment of inertia of the vehicle and the roll rate, and the aerodynamic response to the induced dynamics should be defined.

The significant simulation variables for cone and sphere cone shapes appear to be frequency, Reynolds number, and oscillation amplitude. More intensive research on frequency effects, in hypersonic flow, may demonstrate that these effects can be attributed to data measuring and reduction techniques. Other variables, which were not evaluated in this program, but are considered very significant from the literature survey are ablative mass addition, dynamic pressure gradients, and six degree of freedom motion.

9.4 SIGNIFICANT TRENDS

The most significant and most consistent trends in the damping data are obtained with variations in the geometric variables. A reduction in dynamic damping is observed as the bluntness increases, as the cone angle decreases, and as the static margin decreases in the range tested. An interesting note on the trend in damping with cone angle is that the reference length used to evaluate the damping coefficient can change the trends in the data because of a varying length to diameter ratio. With diameter as the reference length, the effects of cone angle show a significant increase in damping as the cone angle decreases. Therefore, in the particular case of cone angle effects, the trends in the data can be misleading when different reference dimensions are used.

In all cases of geometric variables, trends in the data are highly predictable by flow field theory. In this respect the significance of an agreement in the data with theory is that the inviscid prediction of dynamic damping is adequate.

From the data obtained in this program, trends are observed with Reynolds number, oscillation frequency and oscillation amplitude. These trends show an increase in damping for a transitional boundary layer conditions and a decrease in damping with the viscous effects of low Reynolds number flow. A decrease in damping is also observed for increases in oscillation frequency, but from the literature survey, this trend is shown to be inconsistent and requires further investigation. The effects of oscillation amplitude exhibit a consistent trend, which shows a slight reduction in damping as the amplitude decreases, but these effects also appear to be a function of other geometric and environmental variables.

The trends that are observed in the data for all the geometric and environmental variables illustrate the complexities of dynamic stability simulation. The trends show that many variables are significant and that environmental variables in particular will require considerable research before the effects may be totally defined.

9.5 RECOMMENDATIONS FOR DATA APPLICATIONS

Application of the ground test data for flight predictions must be tempered with considerable engineering judgement, primarily because all of the significant flight variables are not simulated. There are important applications of ground test data for improving theoretical techniques, for developing empirical correlations, and for achieving a greater technological understanding of aerodynamic damping in general. These applications will eventually provide a capability in the ground test simulation of dynamic stability, which is not available at this time.

9.6 RECOMMENDATIONS FOR EXPERIMENTAL STUDIES

Since the formulation of the test program plan, many important simulation techniques have been developed. Also additional information has been generated on other important considerations in flight simulation. Three major fields for experimental studies, which are associated with hypersonic dynamic stability and flight motion are: (1) three degree of freedom testing, with considerations for roll resonance coupling, off-set c.g. locations, and magnus effect with mass addition; (2) Mass addition testing with considerations for ablation asymmetries, ablation rates, ablation phase lags, ablation molecular weights, and vehicle c.g. locations; (3) extended research testing of environmental variables with the emphasis placed on the boundary layer - frequency interaction. The two latter fields of study with and without mass addition, should be concentrated on defining the viscous effects on damping and should include studies on the effects of boundary layer displacement, boundary layer separation, boundary layer transition, vortex shedding and separation, wall temperature and wake expansion - base pressure characteristics. All of these consideration are

significantly altered by mass addition and reflect the environmental causes for apparent changes in aerodynamic damping.

9.7 RECOMMENDATIONS OF TEST TECHNIQUES

Two of the major problems associated with dynamic stability testing appear to be support interference effects and structural or mechanical damping contributions. Ideally the development of free flight techniques in ground test facilities would eliminate these problems and would be the most suitable method to evalutate an actual level in damping. Free flight techniques have been used successfully in both range and wind tunnel facilities, but also introduce other problems which make data measurement and reduction exceedingly complex. Regardless, the development of a free flight technique would appear to have distinct advantages over other methods of obtaining dynamic stability data.

With a model support system, it is recommended that support interference effects be thoroughly evaluated. Data has shown that transverse support systems have a considerable effect of the aerodynamic damping data. Therefore, a sting support system is generally recommended over a transverse support system. With a sting support system the effects of sting diameter and length must be evaluated, and the data must be corrected accordingly. It is recommended that facilities develop standard techniques for evaluating support interference and develop equipment which will keep support interference to a minimum.

In both free and forced oscillation testing, the accuracy of the data depends primarily on the ratio of structural damping to aerodynamic damping and the ability to accurately measure the tares. In using a balance measurement technique, it is recommended that very exact and very comprehensive balance calibrations be made.

9.8 RECOMMENDATIONS FOR FACILITY NEEDS

In terms of future requirements for dynamic stability testing, it is recommended that facilities develop a free flight or three degree of freedom technique for the more advanced studies of oscillating motion, with capabilities of measuring roll damping and non-planar amplitude decay as well as pitch damping. Advanced techniques for dynamic stability testing with mass addition is also a major consideration for advanced studies. The ability to control and regulate mass addition rates, distributions, and phase lags in dynamic stability tests will be an important future requirement for environmental testing. To incorporate this capability into a three degree of freedom testing technique would provide the optimum simulation for dynamic stability and vehicle motion studies.

REFERENCES

1. R. B. Hobbs, "Proposed Wind Tunnel Testing to Support the GE-ASD Hypersonic Dynamic Stability Evaluation," GE PIR 8152-74, May 1963

2. "AEDC Test Facilities Handbook," July 1963

3. Stalmach, Jr., T. C. Pope, and J. L. Lindsey, "Chance Vought Hypervelocity Wind Tunnel Test Techniques and Sample Data," LTV Report No. 2-59740/3R444, Feb. 1963

4. R. J. Berman, "Maneuvering Re-entry Vehicle," GE PIR AT8152-385, May 1964

5. C. H. Murphy, "An Erroneous Concept Concerning Nonlinear Aerodynamic Damping," AIAA Technical Note, AIAA Journal, p. 1418, June 1963

6. R. B. Hobbs, and L. A. Marshall, "Aerodynamic Simulation of Re-entry Flight Dynamic Stability Characteristics With and Without the Effects of Mass Addition," GE TIS 65SD5278, Feb. 1965

7. R. B. Hobbs, "Data Survey for Mass Addition Effects on Re-entry Aerodynamics," GE ATDM 1:99, June 1965

8. R. S. Davis, "Remarks Concerning the Evaluation of Aerodynamic Dynamic Coefficients from Test Data with Varying Aerodynamic Properties," GE-AFM-151, Aug. 1962

9. A. E. Hodapp, Jr., "Evaluation of a Gas Bearing Pivot for a High Amplitude Dynamic Stability Balance," AEDC TDR-62-211, Dec. 1962

10. C. J. Welch, and L. K. Ward, "Structural Damping in Dynamic Stability Testing," AEDC TR-59-5, Feb. 1959

11. R. E. Decker, "Effects of Ablation on the Hypersonic Dynamic Stability Characteristics of the Mark 12 R/V," GE ATDM 1:72, Jan. 1965

12. C. J. Schueler, "Dynamic Stability Results for a 10-Deg. Cone at Mach Numbers 0.8 to 20," AEDC TDR 64-226, Dec. 1964

13. Bain Dayman, Jr., "Summary of Model - Support Interference Problems," Paper presented at the First Technical Workshop on Dynamic Stability Testing, Valley Forge, Pa., July 1965

14. R. B. Hobbs, "Results of an Experimental Study of Hypersonic Dynamic Stability Characteristics for Axisymmetric and Non-Axisymmetric Bodies of Revolution, GE ATDM 1:33, March 1964

15. P. T. Gaskins, "Results of the Transverse Rod Stability Tests in the AEDC Tunnel C," GE ATDM 65-18, Nov. 1965

16. R. H. Urban and R. J. Shanahan, "Dynamic Stability Characteristics of a 10-Deg. Cone at Mach Number 20, " AEDC TR-65-80, April 1965

17. Bain Dayman, Jr., "Free Flight Cone Dynamic Stability Testing at High Amplitudes of Oscillation," Vol II, Proceedings of the Second Technical Workshop on Dynamic Stability Testing, Tullahoma, Tenn., April 1965

18. R. H. Prislin, "Dynamic Stability Testing Techniques at the JPL Laboratory," Vol. II, Proceeding of the Second Technical Workshop on Dynamic Stability Testing, Tullahoma, Tenn., April 1965

19. J. T. Clay and O. Walchner, "Nose Bluntness Effects on Stability Derivatives of Cones in Hypersonic Flow," Vol. I, Proceedings of the Second Technical Workshop on Dynamic Stability Testing, Tullahoma, Tenn., April 1965

20. Bain Dayman, Jr., "Effects of a Hemispherical Afterbody on the Dynamic Stability of a Slender Cone/Wind Tunnel Free Flight Technique," Vol. II, Proceedings of the Second Technical Workshop on Dynamic Stability Testing, Tullahoma, Tenn., April 1965.

21. L. K. Ward, "Influence of Boundary Layer Transition on Dynamic Stability at Hypersonic Speeds, Vol. II, Proceedings of the Second Technical Workshop on Dynamic Stability Testing, Tullahoma, Tenn., April 1965

BIBLIOGRAPHY

1. Berman, R. J., Maneuvering Re-entry Vehicle, GE-PIR-AT-8152-385, May 1964.

2. Birnbaum, A., Sortie, GE-PIR-AT-8152-438, July 1964.

3. Brong, E. A., The Flow Field About a Pointed Cone in Unsteady Motion in a Supersonic Stream, GE-ATFM To Be Published.

4. Davis, R. S., Remarks Concerning the Evaluation of Aerodynamic 'Dynamic' Coefficients from Test Data with Varying Aerodynamic Properties, GE-AFM-151, August 1962.

5. Dayman, B., Jr., et. al, The Influence of Shape on Aerodynamic Damping of Oscillatory Motion During Mars Atmosphere Entry and Measurements of Pitch Damping at Large Oscillation Amplitudes, JPL. RPT. No. 32-380, February 1963.

6. Dayman, B., Jr., Simplified Free Flight Testing in a Conventional Wind Tunnel, JPL. RPT. No. 32-346, October 1962.

7. Hobbs, R. B., Results of an Experimental Study of Hypersonic Dynamic Stability Characteristics for Axisymmetric and Non-Axisymmetric Bodies of Revolution, GE-ATDM 1:33, March 1964.

8. Hobbs, R. B., Results of Experimental Studies on the Hypersonic Dynamic Stability Characteristics of a 10° Cone at M=10, GE ATDM 1:37, May 1964

9. Hobbs, R. B., Results of Experimental Studies on the Hypersonic Dynamic Stability Characteristics of the Basic Sortie Configuration at M-10, GE ATDM 1:43, August 1964.

10. Hobbs, R. B., Proposed Wind Tunnel Testing to Support the GE-ASD Hypersonic Dynamic Stability Evaluation, GE-PIR 8152-74, May 1963.

11. Hobbs, R. B., Pretest Instructions to Obtain Hypersonic Dynamic Stability Data at M=10 in the AEDC Tunnel C, GE-ATPR 16-63, November 1963.

12. Hodapp, A. E., Jr., Uselton, B. L., and Burt. G. E., Dynamic Stability Characteristics of a 10-degree Cone at Mach Number 10, AEDC-TDR-64-98, May 1964.

13. Hodapp, A. E., Jr., Evaluation of a Gas Bearing Pivot for a High Amplitude Dynamic Stability Balance, AEDC TDR-62-221, December 1962.

14. Jaffe, P., Obtaining Free Flight Dynamic Damping of an Axially Symmetric Body (at All Angles of Attack) in a Conventional Wind Tunnel, JPL. RPT. No. 32-544, January 1964.

15. Lindsey, J. L., LTV Hypervelocity Wind Tunnel Dynamic Stability Test of the Sortie Configuration and a Basic 10° Cone, LTV HVWT 23, March 1964.

16. McMenamin, D., Dynamic Derivatives for Cones Derived from Hybrid Theory, GE-AIM-51, September 1962.

17. Orlik-Rückermann, K. J., Wind Tunnel Measurements of Dynamic Derivatives National Aeronautical Establishment (Canada), RPT. No. HG2-11, August 1962.

18. Pope, Alan, Wind Tunnel Testing, John Wiley & Sons, 1954

19. Pope, T. C., and Stalmach, C. J., Jr., Status of Dynamic Stability Testing in the Chance Vought Hypervelocity Wind Tunnel, LTV-2-59740/3R50145, July 1963.

20. Rittenhouse, C. M., and Birnbaum, A., Newtonian Dynamic Damping Coefficients for Sphere Cones at Angle of Attack, GE-ADM-1:12, April 1963.

21. Schiff, Jr., Pretest Instructions to Obtain Hypersonic Dynamic Stability Data at M=14, 17 and 20 in the CVA Hypervelocity Wind Tunnel, GE-ATPR 12-63, September 1963.

22. Stalmach, C. J., Jr., Pope, T. C., and Lindsey, J. L., Chance Vought Hypervelocity Wind Tunnel Test Techniques and Sample Data, LTV 2-59740/3R444, February 1963.

23. Sullivan, P. V., and Onspaugh, C. M., Analytical and Experimental Investigation of Hypersonic Lifting Re-entry Vehicles, ASD-TDR-62-789, Part I, Vol. 3 May 1963.

24. Tobak, M., and Wehrend, W. R., Jr., Stability Derivates of Cones at Supersonic Speeds, NASA-TN-3788, September 1956.

25. Truitt, R. W., Hypersonic Aerodynamics, Ronald Press Co., 1959.

26. Wehrend, W. R., Jr., An Experimental Evaluation of Aerodynamic Damping Moments of Cones with Different Centers of Rotation, NASA-TN-D-1768, March 1963.

27. Welch, C. J., Ledford, R. L., Ward, L. K., and Rhudy, J. P., Dynamic Stability Tests in Hypersonic Tunnels and at Large Model Amplitudes, AEDC-TR-59-24, December 1959.

28. Welch, C. J., and Ward, L. K., Structural Damping in Dynamic Stability Testing, AEDC TR-59-5, February 1959.

29. Welch, C. J., Hance, Q. P., and Ward, L. K., A Forced Oscillation Balance System for the Von Karman Gas Dynamics Facility 40-by-40 inch Supersonic Tunnel, AEDC TDR-61-63, May 1961.

30. AEDC Test Facilities Handbook, July 1963.

31. Proceedings of the Second Technical Workshop on Dynamic Stability Testing, Arnold Air Force Station, Tenn., April 1965

32. Schueller, C. J. Dynamic Stability Results for a 10-Deg. Cone at Mach Numbers 0.8 to 20, AEDC TDR 64-226, December 1964

33. Hobbs, R. B. and Marshall, L. A., Aerodynamic Simulation of Re-Entry Flight Dynamic Stability Characteristics With and Without the Effects of Mass Addition, GE TIS 65 SD5278, February 1965

34. Hobbs, R. B., Data Survey for Mass Addition Effects on Re-Entry Aerodynamics, GE ATDM 1:99, June 1965

35. Gaskins, P. T., Results of the Transverse Rod Stability Tests in the AEDC Tunnel C., GE ATDM 65-18, November 1965

36. Murphy, C. H., An Erroneous Concept Concerning Non-Linear Aerodynamics Damping, AIAA Technical Note, AIAA Journal, p. 1418, June 1963

37. Urban, R. H. and Shanahan, R. J., Dynamic Stability Tests of Several Models of the Advanced Mk. 6 Re-Entry Vehicle at Mach 10, AEDC TRD 62-198, October 1962

38. Decker, R. E., Effects of Ablation on the Hypersonic Dynamic Stability Characteristics of the Mk. 12 R/V, GE ATDM 1:72, Jan 1965

UNCLASSIFIED
Security Classification

DOCUMENT CONTROL DATA - R&D

(Security classification of title, body of abstract and indexing annotation must be entered when the overall report is classified)

1. ORIGINATING ACTIVITY (Corporate author) General Electric Company P.O. Box 8555, Philadelphia, Pa. 19101	2a. REPORT SECURITY CLASSIFICATION Unclassified 2b. GROUP NA

3. REPORT TITLE

Hypersonic Dynamic Stability, Pt II Conical Body Experimental Program

4. DESCRIPTIVE NOTES (Type of report and inclusive dates)

Final Report - May 1963 - October 1965

5. AUTHOR(S) (Last name, first name, initial)

Hobbs Jr., R. B.

6. REPORT DATE	7a. TOTAL NO. OF PAGES	7b. NO. OF REFS
January 1967	113	21

8a. CONTRACT OR GRANT NO. AF33(657)-11411 b. PROJECT NO. 8219 c. Task No 821902 d.	9a. ORIGINATOR'S REPORT NUMBER(S) FDL TDR 64-149 Part II 9b. OTHER REPORT NO(S) (Any other numbers that may be assigned this report) None

10. AVAILABILITY/LIMITATION NOTICES

Distribution of this report is unlimited

11. SUPPLEMENTARY NOTES	12. SPONSORING MILITARY ACTIVITY
NA	AFFDL (FDCC) Wright-Patterson AFB, Ohio

13. ABSTRACT

Wind Tunnel Tests were conducted in the AEDC Tunnel C at M = 10 and in the Ling Temco Vought Hypervelocity Tunnel at M = 14 and 20 to obtain experimental data on the hypersonic dynamic stability characteristics of a 10-degree half-angle cone. These data were generated to support dynamic stability studies and to evaluate the effects of many geometric and environmental variables, which influence the oscillatory motion of re-entry vehicles.

The state-of-the-art of experimental ground testing in hypersonic dynamic stability is reviewed in detail with respect to simulation and data measuring capabilities. Data correlations were obtained to compare facilities and to evaluate the degree of consistency of results using different techniques in measuring and reducing the data. The confidence level for the data is established by means of these correlations, and conclusive interpretations of the data for application in flight estimates can only be made when the significance of these correlations are fully realized. The data correlations do bring out definite inconsistencies in test results and demonstrate the more obvious shortcomings of ground test simulation in this type of experiment research.

Test results indicate that the 10-degree cone configuration is dynamically stable over the entire scope of matrix variables covered in this experimental program. Dynamic instabilities observed in flight remain unconfirmed by these ground test results. Logically, these instabilities are induced by some other influence, such as ablation, and require more advanced, sophisticated studies to define the causes and effects in entirety.

DD FORM 1 JAN 64 1473

UNCLASSIFIED
Security Classification

14. KEY WORDS	LINK A		LINK B		LINK C	
	ROLE	WT	ROLE	WT	ROLE	WT
Hypersonic unsteady testing Dynamic damping Conical reentry vehicles						

INSTRUCTIONS

1. ORIGINATING ACTIVITY: Enter the name and address of the contractor, subcontractor, grantee, Department of Defense activity or other organization *(corporate author)* issuing the report.

2*a*. REPORT SECURITY CLASSIFICATION: Enter the overall security classification of the report. Indicate whether "Restricted Data" is included. Marking is to be in accordance with appropriate security regulations.

2*b*. GROUP: Automatic downgrading is specified in DoD Directive 5200.10 and Armed Forces Industrial Manual. Enter the group number. Also, when applicable, show that optional markings have been used for Group 3 and Group 4 as authorized.

3. REPORT TITLE: Enter the complete report title in all capital letters. Titles in all cases should be unclassified. If a meaningful title cannot be selected without classification, show title classification in all capitals in parenthesis immediately following the title.

4. DESCRIPTIVE NOTES: If appropriate, enter the type of report, e.g., interim, progress, summary, annual, or final. Give the inclusive dates when a specific reporting period is covered.

5. AUTHOR(S): Enter the name(s) of author(s) as shown on or in the report. Enter last name, first name, middle initial. If military, show rank and branch of service. The name of the principal author is an absolute minimum requirement.

6. REPORT DATE: Enter the date of the report as day, month, year; or month, year. If more than one date appears on the report, use date of publication.

7*a*. TOTAL NUMBER OF PAGES: The total page count should follow normal pagination procedures, i.e., enter the number of pages containing information.

7*b*. NUMBER OF REFERENCES: Enter the total number of references cited in the report.

8*a*. CONTRACT OR GRANT NUMBER: If appropriate, enter the applicable number of the contract or grant under which the report was written.

8*b*, 8*c*, & 8*d*. PROJECT NUMBER: Enter the appropriate military department identification, such as project number, subproject number, system numbers, task number, etc.

9*a*. ORIGINATOR'S REPORT NUMBER(S): Enter the official report number by which the document will be identified and controlled by the originating activity. This number must be unique to this report.

9*b*. OTHER REPORT NUMBER(S): If the report has been assigned any other report numbers *(either by the originator or by the sponsor)*, also enter this number(s).

10. AVAILABILITY/LIMITATION NOTICES: Enter any limitations on further dissemination of the report, other than those imposed by security classification, using standard statements such as:

(1) "Qualified requesters may obtain copies of this report from DDC."

(2) "Foreign announcement and dissemination of this report by DDC is not authorized."

(3) "U. S. Government agencies may obtain copies of this report directly from DDC. Other qualified DDC users shall request through _____."

(4) "U. S. military agencies may obtain copies of this report directly from DDC. Other qualified users shall request through _____."

(5) "All distribution of this report is controlled. Qualified DDC users shall request through _____."

If the report has been furnished to the Office of Technical Services, Department of Commerce, for sale to the public, indicate this fact and enter the price, if known.

11. SUPPLEMENTARY NOTES: Use for additional explanatory notes.

12. SPONSORING MILITARY ACTIVITY: Enter the name of the departmental project office or laboratory sponsoring *(paying for)* the research and development. Include address.

13. ABSTRACT: Enter an abstract giving a brief and factual summary of the document indicative of the report, even though it may also appear elsewhere in the body of the technical report. If additional space is required, a continuation sheet shall be attached.

It is highly desirable that the abstract of classified reports be unclassified. Each paragraph of the abstract shall end with an indication of the military security classification of the information in the paragraph, represented as *(TS)*, *(S)*, *(C)*, or *(U)*.

There is no limitation on the length of the abstract. However, the suggested length is from 150 to 225 words.

14. KEY WORDS: Key words are technically meaningful terms or short phrases that characterize a report and may be used as index entries for cataloging the report. Key words must be selected so that no security classification is required. Identifiers, such as equipment model designation, trade name, military project code name, geographic location, may be used as key words but will be followed by an indication of technical context. The assignment of links, rules, and weights is optional.